



UNIVERSITAT  
POLITÈCNICA  
DE VALÈNCIA

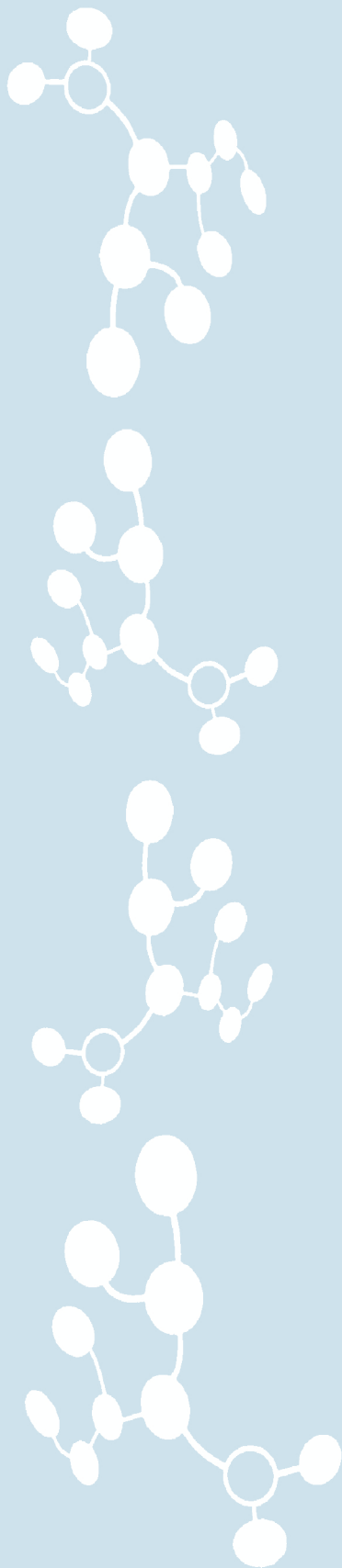
# NEW MECHANISMS OF DELLA PROTEIN REGULATION AND ACTIVITY IN ARABIDOPSIS

PhD THESIS  
Noel Blanco Tourián

ADVISORS  
Dr. David Alabadí Diego  
Dr. Miguel Ángel Blázquez Rodríguez



Valencia, May 2020













UNIVERSITAT  
POLITÈCNICA  
DE VALÈNCIA

PhD IN BIOTECHNOLOGY

**NEW MECHANISMS OF DELLA PROTEIN  
REGULATION AND ACTIVITY IN ARABIDOPSIS**

NOEL BLANCO TOURIÑÁN

ADVISORS:

Dr. DAVID ALABADÍ DIEGO

Dr. MIGUEL Á. BLÁZQUEZ RODRÍGUEZ


VALENCIA, MAY 2020



El **Dr. David Pablo Alabadí Diego**, Científico Titular del CSIC, y el **Dr. Miguel Ángel Blázquez Rodríguez**, Profesor de Investigación del CSIC, ambos pertenecientes al Instituto de Biología Molecular y Celular de Plantas (IBMCP, UPV-CSIC) de Valencia,

CERTIFICAN que Noel Blanco Touriñán, ha realizado bajo su dirección en el Instituto de Biología Molecular y Celular de Plantas, el trabajo titulado «**New mechanisms of DELLA protein regulation and activity in Arabidopsis**», y que autorizan su presentación para optar al grado de Doctor en Biotecnología de la Universidad Politécnica de Valencia.

Y para que así conste, firman el presente certificado en Valencia a 25 de mayo de 2020.



Dr. David Pablo Alabadí Diego



Dr. Miguel Á. Blázquez Rodríguez



**A mis padres**



# AGRADECIMIENTOS

Sorprendentemente (o no tanto), éste ha sido el apartado que más me ha costado empezar a escribir. La principal razón es que soy muy despistado y estoy seguro de que se me olvidará dedicar unas líneas de reconocimiento a algunas personas que me han acompañado en este camino de tanto enriquecimiento personal. De manera general, me gustaría agradecer a todos y todas las que contribuís diariamente al ambiente tan familiar y profesional del IBMCP, de verdad que lo hacéis todo más fácil.

En primer lugar, me gustaría agradecer a mis directores de tesis, Miguel y David. David, voy a empezar a rellenar este párrafo con alabanzas, ¡estás a tiempo de parar de leer! Si no lees los agradecimientos como dices, ¡seguro que te lo cuenta Miguel, así que ahí va! Os admiro tanto a nivel profesional como personal, de verdad que sois un ejemplo a seguir y no me imagino unos mejores directores de tesis. Muchas gracias por guiarme estos años de máster y doctorado, por transmitirme esa pasión que tenéis por la ciencia y por haberme enseñado prácticamente todo lo que sé. Ha sido un placer compartir estos años con vosotros (¡más de 6 años y medio!), excepto cuando David apagaba el aire acondicionado... ¡el mayor sufrimiento de la tesis! David, echarás de menos la expresión: “David, tenemos un problema...”.

A mis compañeros de los laboratorios 2.07 y 2.08 (y también a los de antes 4 labos). ¡Qué barbaridad de gente y qué ambiente de trabajo tan bueno creáis! Os pido disculpas de antemano porque no menciono explícitamente a todos, pero me gustaría destacar que, de alguna manera u otra, todos me habéis ayudado y siempre os estaré agradecido. Javi Agustí, gracias por confiar en mí y contar conmigo en alguno de tus trabajos. Jorge, Asier y Pepi... Cuando pienso en vosotros, inevitablemente me vienen a la cabeza las risas en el 2.07. Jorge, gracias también por la ayuda en la estética de la tesis. Ah, y va siendo hora de separarnos, ¿no? En el fondo sabemos que no pasará. Cris Marí, gracias por tu confianza y las eternas conversaciones, las echaré mucho de menos. Eugenio, gracias por estar siempre dispuesto a ayudarme y por ser la gran persona que eres. Esteve, creo que eres y siempre serás mi pareja científica. Eres de las mejores personas que he conocido y sin duda me siento afortunado de poder haber trabajado contigo y teneros como amigos a Isa y a ti. Antonio, gracias por confiar en mí e implicarme en tus trabajos. Aunque hayas llegado más tarde, has conseguido que no solo te admire a nivel científico, sino que también te vea como una pieza fundamental en el laboratorio. ¡Y por supuesto, te has convertido en un gran amigo! También extrañaré los cafés mañaneros con Balanzá y contigo. A mis amigos del “Supricio

team”: Alberto, Yaiza, Anna y Laura. ¡Cuántas cosas hemos hecho en tan poco tiempo! Gracias por todos los viajes (Granada, Oporto, Camino de Santiago, Oviedo, Sant Sadurn y Japón) y por todo lo que nos queda por vivir juntos. Cris Úrbez, Mari Ángeles, Juan, MD y Daniela, vuestras sonrisas me alegraban el día incluso en días malos. Úrbez, se me caen las lágrimas solo de pensar que no te veré cada día, eres una persona muy muy especial. Joan, Flor y Marco, ¡que grandes personas sois y como os echo de menos! Finalmente, no puedo olvidarme de Ángela, Pako y de todos los estudiantes que han pasado por el laboratorio: Julián, Claudio, Nerea, Rosa y Celia. Celia, ¡cómo extraño tenerte cerca en Valencia! ¡Chicos, echaré mucho de menos los “coffees” con vosotros y las cervezas fuera del lab!

También dentro del IBMCP, gracias a todo el personal de los Servicios de Microscopía (Mari Sol), Secuenciación (Eugenio y Ana), Cuantificación de hormonas vegetales (Esther Carrera), Bioinformática (Javier Forment), Genómica (Lorena), Proteómica (Susana) e Invernadero (Victoria). Javier, tu ayuda ha sido clave para los análisis de este y otros trabajos. No me puedo olvidar del personal de administración, destacando la continua ayuda de Patricia, Juni y María Ortiz. También quiero agradecer a Mapi y Puri por permitirme participar en sus clases y así adquirir experiencia docente. Sin duda, ¡sois increíbles!

Fuera del IBMCP. Miguel de Lucas, gracias por recibirme en tu laboratorio y por todo el positivismo que transmites. ¡Ha sido un auténtico placer estar en tu laboratorio, repetiría esa experiencia una y otra vez! María Eugenia Blázquez, gracias por el diseño de la portada y la contraportada de esta tesis. ¡Lo que me agobiaba y lo rápido que lo has hecho! A Rodrigo García, por estar siempre dispuesto a ayudarme. ¡Espero verte pronto! Fredy et Clara, merci de m'avoir accueilli dans votre laboratoire et pour votre excellente supervision. Une partie du mérite de cette thèse est à vous et à Ouardia. Merci également à Moussa Benhamed et David Latrasse, pour votre aide avec le RNAPII ChIP-seq. Muchas gracias también al equipo de Jorge Casal y resto de colaboradores por hacer posible sacar adelante el trabajo de COP1. Antía Rodríguez, gracias por aceptarme en tu grupo como posdoc sin ni tan siquiera haber defendido. No me quiero olvidar de Belén Picó. Me gustaría agradecerte toda tu inestimable ayuda, creo que tu papel es clave en todo el proceso burocrático para la presentación de la tesis doctoral. De verdad que muchas gracias por toda esa ayuda tan desinteresada.

Elisa, Sergio, Elba y Menno... La verdad es que he tenido mucha suerte de conoceros en mi estancia en Durham. ¡Sois geniales! Espero que podamos hacer muchos más viajes juntos como los de Snowdonia y las Highlands. Sabela, Mariajo, Andrés, Sergio (Galindo), Maite,



David (COMAV), Raquel y Tamara, también habéis formado parte de muchos momentos durante esta etapa. ¡Ya sabéis lo que os echo de menos!

Félix, ¡cómo me has cambiado la vida! Te he conocido hace tan solo 7 meses, y desde entonces no has parado de apoyarme en estos momentos tan difíciles de escritura y confinamiento. Gracias por tu ayuda y paciencia infinitas. ¡Estoy deseando que podamos empezar a viajar! También gracias por compartir a Baldo conmigo, no imaginaba que una gata me pudiese querer tanto, sin duda nos ha hecho el confinamiento más ameno con sus locuras y mimos.

Finalmente, gustaría agradecer a mi familia polo sei apoio, non é fácil que esteades tan lonxe e aínda así fagades todo tan fácil. Especialmente a meus avós, a meu irmán e a miña cuñada, o meu sobriño Naím e a meus pais. A Naím, o meu ollíño dereito: grazas por recibirme sempre como se o tempo non pasara. A meus pais: grazas por transmitirme que con esforzo e constancia se pode chegar a onde queiramos. Sen ningunha dúbida, é grazas a vos que cheguei a onde estou. Esta tese doutoral vai dedicada a volos dous.

---

La realización de esta Tesis Doctoral ha sido posible gracias a un contrato predoctoral para la formación de doctores (BES-2014-068868) y a la ayuda a la movilidad predoctoral para la realización de estancias breves (EEBB-I-16-11070) del Ministerio de Economía y Competitividad, y a una beca EMBO Short-Term (number 8047). Igual de importante ha sido la contribución de materiales (semillas y reactivos) de distintos laboratorios (especificados en la sección de agradecimientos del capítulo correspondiente) y la ayuda experimental y/o intelectual de todos los autores recogidos en la portada de cada capítulo.

---



## SUMMARY

DELLA proteins are plant-specific transcriptional regulators known to relay environmental information to the transcriptional networks to modulate growth and development accordingly. The view of DELLAs as signalling hubs is justified by two characteristics: first, they control the activity of a large number of transcriptional factors (TFs) and other transcriptional regulators through physical interaction; and, second, they are degraded by the 26S proteasome in response to the phytohormone gibberellin (GA), whose metabolism is very sensitive to environmental stimuli (e.g. light, temperature, salt stress). However, at least two observations indicate that this mechanistic framework is still incomplete: (i) warm temperature destabilizes the GA-insensitive DELLA *rga-Δ17*, indicating that DELLAs cannot be destabilized only by changes in GA levels; and (ii) when found at the chromatin, DELLAs are localized not only in gene promoters, but also in gene bodies, suggesting that DELLAs may regulate transcription through interactions with proteins other than TFs. In this Thesis, we provide evidence that shows how a different E3 ubiquitin ligase controls the stability of DELLAs in a GA-independent manner, and how DELLAs regulate gene expression by directly interacting with the basal transcriptional machinery. In the first chapter, using a combination of genetic, physiological, and molecular approaches we demonstrate that DELLAs are targeted to proteolytic degradation by the E3 ubiquitin ligase CONSTITUTIVELY PHOTOMORPHOGENIC 1 (COP1). We show that COP1 interacts with the DELLAs GAI and RGA *in vitro* and *in vivo*, and that it promotes their polyubiquitination. We propose that COP1 represents a major pathway to degrade DELLAs in response to shade or to warm temperature. In the second chapter, we describe the interaction between DELLAs and the transcription elongation complex Polymerase-Associated Factor 1 (Paf1c). We show that Paf1c is required for the genome-wide deposition of monoubiquitinated H2B (H2Bub), a mark necessary for the progression of RNA polymerase II (RNAPII), and that this function is largely dependent on the presence of DELLAs. Likewise, impaired Paf1c or DELLA function results in a similar alteration in the accumulation and distribution of RNAPII in the Paf1c-target genes. We propose that DELLAs would exert this action by modulating the recruitment of Paf1c to the chromatin. These two new mechanisms underscore the importance of DELLAs as a central node in the environmental signalling network and should be considered in any potential application of DELLAs as biotechnological targets.



# RESUMEN

Las proteínas DELLA son reguladores transcripcionales específicos de plantas que transmiten información ambiental a las redes transcripcionales que modulan el crecimiento y el desarrollo. La propuesta de que las DELLAs actúan como “hubs” en redes de señalización se justifica por dos razones: primero, controlan la actividad de un gran número de factores de transcripción (FTs) y otros reguladores transcripcionales mediante interacción física; y segundo, son degradadas por el proteosoma 26S en respuesta a la fitohormona giberelina (GA), cuyo metabolismo es muy sensible a los estímulos ambientales (p. ej. luz, temperatura, estrés salino). Sin embargo, al menos dos observaciones sugieren que la información relativa a estos mecanismos no es completa: (i) las temperaturas altas desestabilizan incluso a *rga-Δ17*, una versión de DELLA insensible a GAs, lo que indica que la estabilidad de las DELLAs no depende sólo de cambios en los niveles de GAs; y (ii) cuando se encuentran en la cromatina, las DELLAs no solo se posicionan en los promotores, sino también a lo largo de las regiones codificantes, lo que sugiere que las DELLAs podrían regular la transcripción mediante interacciones con otras proteínas diferentes a FTs. En esta Tesis, proporcionamos evidencia sobre una nueva E3 ubiquitina ligasa que controla la estabilidad de las DELLAs de una manera independiente a las GAs, y cómo las DELLA regulan la expresión génica interaccionando directamente con la maquinaria de transcripción basal. En el primer capítulo, usando una combinación de aproximaciones genéticas, fisiológicas y moleculares, demostramos que las DELLAs son marcadas para su degradación proteolítica por la E3 ubiquitina ligasa CONSTITUTIVELY PHOTOMORPHOGENIC 1 (COP1). Mostramos que COP1 interacciona al menos con las DELLAs GAI y RGA *in vitro* e *in vivo*, y que promueve su poliubiquitinación. Proponemos que COP1 representa una vía importante de degradación de DELLAs en respuesta a sombra y temperaturas altas. En el segundo capítulo, describimos la interacción entre las DELLAs y el complejo de elongación transcripcional Polymerase-Associated Factor 1 (Paf1c). Mostramos que, como en animales, Paf1c se requiere para la deposición a nivel genómico de la H2B monoubiquitinada (H2Bub), una marca necesaria para la progresión de la RNA polimerasa II (RNAPII), y que esta función depende en gran medida de la presencia de DELLAs. Asimismo, la reducción de la función de las DELLAs provoca defectos equivalentes a los de la pérdida de función de Paf1c en cuanto a la acumulación y distribución de la RNAPII en los genes diana de Paf1c. Proponemos que las DELLAs podrían por tanto regular la transcripción modulando el reclutamiento de Paf1c a la cromatina.

Estos nuevos mecanismos inciden en la importancia de las DELLAs como nodos centrales en las redes de señalización al ambiente y podrían ser considerados como dianas biotecnológicas en aproximaciones futuras.

# RESUM

Les proteïnes DELLA són reguladors transcripcionals específics de les plantes conegudes per transmetre informació mediambiental a les xarxes transcripcionals per modular el creixement i desenvolupament. La visió actual de DELLAs com a “hubs” de senyalització es justifica per dues característiques: en primer lloc, controlen l'activitat d'un gran nombre de factors transcripcionals (FTs) i d'altres reguladors transcripcionals mitjançant la interacció física; i, en segon lloc, es degraden pel proteosoma 26S en resposta a la fitohormona giberel·lina (GA), el metabolisme de la qual és molt sensible als estímuls ambientals (per exemple, la llum, la temperatura, l'estrès salí). No obstant això, almenys dues observacions indiquen que aquest marc mecanicista encara és incomplet: (i) la temperatura càlida desestabilitza la DELLA *rga-Δ17*, que és insensible a GAs, indicant que les DELLA no es desestabilitzen només per canvis en els nivells d'aquesta fitohormona; i (ii) quan es troben a la cromatina, les DELLA no només es localitzen en els promotors dels gens, sinó també a la regió que es transcriu, cosa que suggereix que poden regular la transcripció mitjançant interaccions amb proteïnes diferents de FTs. En aquesta tesi, proporcionem evidències que mostren com una ubiquitina E3 lligasa diferent controla l'estabilitat de les proteïnes DELLA de manera independent de GAs, i com les DELLA regulen l'expressió gènica interactuant directament amb la maquinària transcripcional basal. En el primer capítol, mitjançant una combinació d'enfocaments genètics, fisiològics i moleculars, demostrem que les DELLA s'envien a la degradació proteolítica mitjançant la ubiquitina E3 lligasa CONSTITUTIVELY PHOTOMORPHOGENIC 1 (COP1). Mostrem que la COP1 interacciona amb els DELLA GAI i RGA *in vitro* i *in vivo*, i que afavoreix la seva poliubiquitinació. Proposem que COP1 representa la via principal per degradar les DELLA en resposta a l'ombra o a la temperatura càlida. Al segon capítol, es descriu la interacció entre les DELLA i el complex d'allargament de transcripció Polymerase Associated Factor 1 (Paf1c). Mostrem que Paf1c es requereix per a la deposició a tot el genoma de H2B monoubiquitinada (H2Bub), una marca necessària per a la progressió de l'ARN Polimerasa II (RNAPII), i que aquesta funció depèn en gran part de la presència de DELLA. De la mateixa manera, quan la funció Paf1c o DELLA està deteriorada, es produeix una alteració similar en l'acumulació i distribució de RNAPII als gens diana de Paf1c. Proposem que les DELLA realitzen aquesta acció modulant el reclutament de Paf1c a la cromatina.

Aquests dos nous mecanismes posen de manifest la importància de les proteïnes DELLA com a node central de la xarxa de senyalització ambiental i haurien de ser considerats en qualsevol aplicació potencial de DELLA com a objectius biotecnològics.



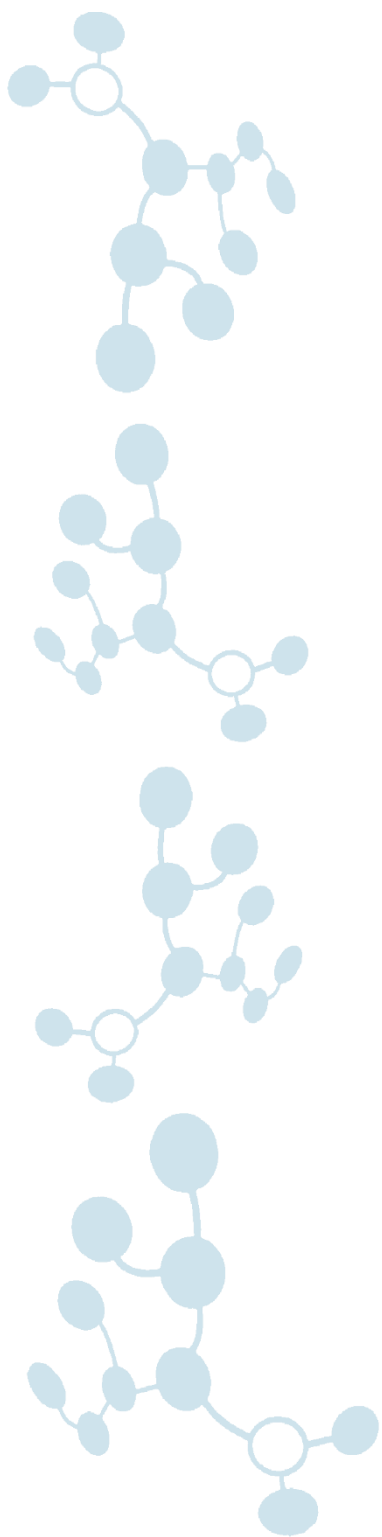
# TABLE OF CONTENTS

<b>INTRODUCTION</b> .....	1
1. Gibberellin signalling: DELLA proteins as master regulators .....	3
2. Post-translational modifications of DELLA proteins.....	5
3. Molecular mechanisms of DELLA action .....	8
4. References .....	12
<b>OBJECTIVES</b> .....	17
<b>CHAPTER 1</b> .....	21
0. Abstract .....	22
1. Introduction.....	23
2. Results.....	24
Warm temperature or shade decrease the abundance of a GA-insensitive DELLA protein.....	24
COP1 affects RGA levels in response to shade and warmth.....	24
Changes in RGA abundance precede changes in GA .....	26
Relative contribution of each pathway .....	26
COP1 promotes degradation of a GA-insensitive DELLA protein.....	27
COP1 interacts physically with GAI and RGA in yeast .....	27
COP1 interacts with GAI and RGA in planta.....	29
COP1/SPA1 forms a ternary complex with DELLA.....	29
COP1 ubiquitinates GAI and RGA <i>in vitro</i> .....	31
COP1 controls hypocotyl elongation in a DELLA-dependent manner .....	31
3. Discussion .....	34
4. Material and methods .....	35
Plant material.....	35
Confocal microscopy in Arabidopsis .....	36
Western analysis of GFP-RGA and GFP-(rga- $\Delta$ 17).....	37
Real-time qPCR .....	37
Gibberellin quantification .....	37
Degradation assays in <i>Nicotiana benthamiana</i> .....	38
Yeast two-hybrid assays .....	39
Co-immunoprecipitation.....	39
Co-localization assays in <i>N.benthamiana</i> .....	40
Bimolecular fluorescence complementation .....	40

Co-localization assays in mammalian cells .....	41
Analysis of confocal images of mammalian cells .....	41
Pull-down assays with p62-beads .....	42
<i>In vitro</i> ubiquitination assay .....	42
Growth assays .....	42
Acknowledgements .....	43
<b>5. Supplemental information .....</b>	<b>44</b>
<b>6. References .....</b>	<b>50</b>
<b>CHAPTER 2 .....</b>	<b>55</b>
<b>0. Abstract .....</b>	<b>56</b>
<b>1. Introduction .....</b>	<b>57</b>
<b>2. Results .....</b>	<b>58</b>
DELLAs interact with the Paf1c subunit ELF7 .....	58
DELLAs are part of a gene regulatory network with Paf1c .....	60
Both DELLAs and ELF7 influence H2Bub general abundance and distribution ..	63
DELLAs are required for the recruitment of Paf1c to the chromatin .....	65
RNAPII occupancy and distribution is dependent on DELLAs and ELF7 .....	67
<b>3. Discussion .....</b>	<b>69</b>
<b>4. Material and methods .....</b>	<b>72</b>
Plant material .....	72
Growth conditions and treatments .....	73
Yeast two-hybrid assays .....	73
Bimolecular fluorescence complementation assay .....	74
Co-immunoprecipitation assays .....	74
Gene expression analysis .....	74
ChIP experiments .....	75
ChIP-seq bioinformatics .....	76
Subcellular fractionation .....	77
Immunoblot analysis .....	78
Acknowledgements .....	78
<b>5. Supplemental information .....</b>	<b>79</b>
<b>6. References .....</b>	<b>90</b>
<b>GENERAL DISCUSSION .....</b>	<b>95</b>
<b>1. Relative importance of the different mechanisms .....</b>	<b>98</b>
<b>2. Evolutionary implications .....</b>	<b>99</b>

3. Biotechnological implications .....	101
4. References .....	103
<b>CONCLUSIONS .....</b>	<b>107</b>





# Introduction



The plant hormones gibberellins (GA) are a class of diterpenoid acids that control major aspects of plant growth and development, including seed dormancy and germination, root and stem elongation, the induction of flowering, fruit development and pollen maturation (Achard and Genschik, 2009; Davière and Achard, 2013). The analysis of plants defective in GA biosynthesis or perception revealed an additional role for GA in the response to both abiotic and biotic stresses (Colebrook et al., 2014). Importantly, research of the last two decades provides us with a good understanding of GA metabolism and signalling (Hedden and Sponsel, 2015). In this section, we provide an overview of the GA signalling pathway, focusing on the molecular function and the regulation of DELLA proteins, the major negative regulators of the signalling pathway.

## 1. Gibberellin signalling: DELLA proteins as master regulators

The key elements of the GA signalling pathway have been identified through the isolation and characterization of dwarf, GA-insensitive mutants in *Arabidopsis* and rice (Davière and Achard, 2013; Minguet et al., 2014). The receptor GA-INSENSITIVE DWARF1 (GID1), the DELLA proteins and the F-box proteins GID2 in rice and SLEEPY1 (SLY) and SNEEZY (SNZ) in *Arabidopsis* constitute the core of the GA signalling cascade (Davière and Achard, 2013).

DELLAs are the master negative elements in the GA signalling pathway in vascular plants (Dill and Sun, 2001a; Itoh et al., 2002). These proteins belong to the plant-specific GRAS family and act as transcriptional regulators (Silverstone et al., 2001). DELLAs are defined by the N-terminal DELLA regulatory domain, which includes the DELLA (aspartic acid-glutamic acid-leucine-leucine-alanine) (hence their name), the TVHYNP and the Poly serine/threonine/valine (Poly S/T/V) conserved motifs (Fig. 1). As we will explain later, the DELLA and TVHYNP motifs are involved in the interaction with the GA-loaded GID1 receptor, and the Poly S/T/V motif participates in the regulation of DELLAs by post-translational modifications. The two-third C-terminal end of the protein corresponds to the GRAS domain, which is present in all GRAS proteins and contains several conserved motifs involved in protein-protein interactions (Fig. 1) (Vera-Sirera et al., 2016). GIBBERELLIC ACID INSENSITIVE (GAI) was the first DELLA member cloned in *Arabidopsis* and its role in GA signalling cascade was demonstrated by the characterization of the dwarf GA insensitive-1 (*gai-1*) mutant (Koorneef et al., 1985; Peng et al., 1997). Although in some species (e.g. rice, tomato or barley) there is only a single DELLA gene, *Arabidopsis* has five (GAI, REPRESSOR of *ga* 1-3 [RGA], RGA-LIKE 1 [RGL1], RGL2 and RGL3) (Ikeda et al., 2001;

Chandler et al., 2002; Jasinski et al., 2008). Interestingly, the phenotypic analysis of *Arabidopsis* loss-of-function mutants in *DELLA* genes revealed that they are partially redundant; for instance, *GAI* and *RGA* jointly control shoot or root growth (Dill and Sun, 2001a; King et al., 2001). Moreover, promoter-swapping experiments showed that the biochemical activity of the different DELLAs in *Arabidopsis* is mostly conserved and that the differences in the processes that they regulate is rather due to their differential expression patterns (Gallego-Bartolomé et al., 2010).

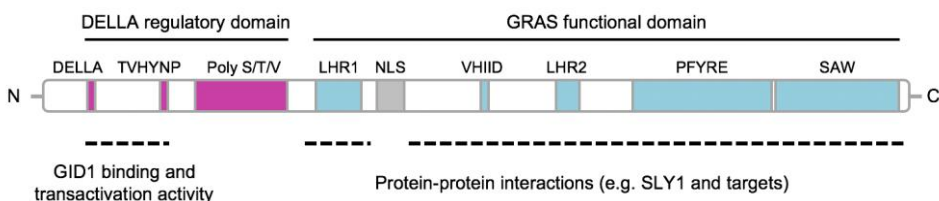


**Fig. 1. Domain structure of DELLAs.** Diagram showing both DELLA major domains: DELLA regulatory and GRAS functional domains. The motifs contained in each domain and their functions are indicated.

The GA signalling cascade begins with the perception of GA hormone by *GID1* (Fig. 2) (Ueguchi-Tanaka et al., 2005; Murase et al., 2008; Shimada et al., 2008). Interestingly, while there is a single *GID1* gene in rice, there are three orthologs in *Arabidopsis* (*GID1A*, *GID1B* and *GID1C*) that have partially overlapping functions (Nakajima et al., 2006). The binding of GA triggers an allosteric change in the N-terminal lid of the receptor that (i) blocks the GA molecule in its position, and (ii) allows the interaction of the lid with the DELLA and TVHYNP motifs of the DELLA protein (Fig. 2) (Ueguchi-Tanaka et al., 2007; Willige et al., 2007; Murase et al., 2008; Shimada et al., 2008). The formation of GA-*GID1*-DELLA complex leads to conformational changes in the GRAS domain of DELLA that allow the recognition and subsequent interaction between the VHIID and LHR2 motifs of DELLA and the F-box protein encoded by *GID2* in rice and *SLY1* in *Arabidopsis* (Hirano et al., 2010; Ariizumi et al., 2011; see Minguet et al., 2014 for a detailed review). The F-box protein is part of the SCF (*SKP1*, *CULLIN*, *RBX*) E3 ubiquitin-ligase complex that ubiquitinates DELLA to be degraded by the 26S proteasome (Fig. 2) (McGinnis et al., 2003; Sasaki et al., 2003; Dill et al., 2004; Fu et al., 2004). Importantly, deletion or mutation of the DELLA motif renders a DELLA protein unable to interact with the GA-loaded *GID1*, resulting in a constitutively active version that is insensitive to GA-induced degradation (Dill et al., 2001b; Willige et al., 2007).



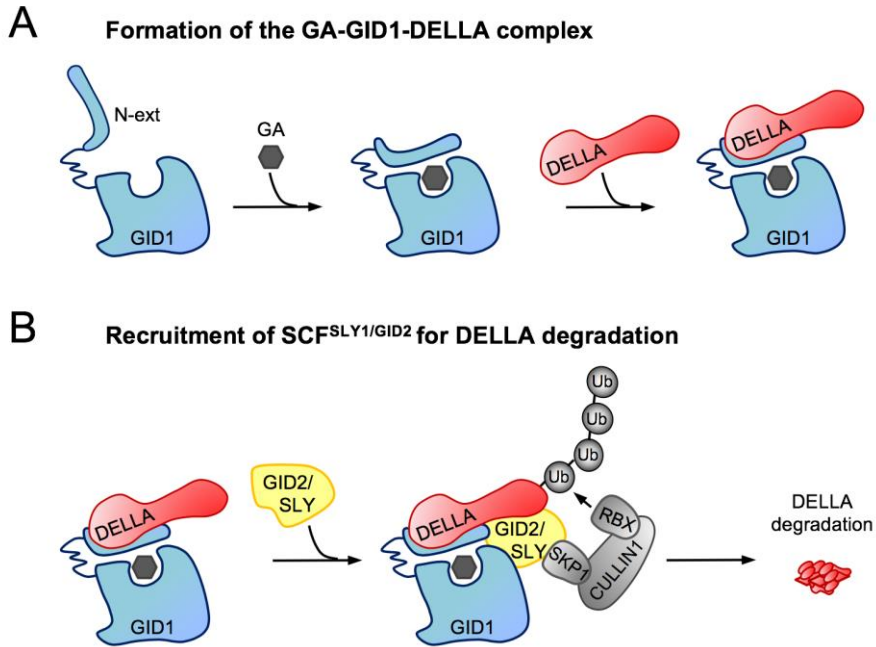


**Fig. 2. GA signalling mediates DELLAs degradation.** This model illustrates the formation of the GA-GID1-DELLA complex (A) and the subsequent recruitment of SCF<sup>SLY1/GID2</sup> E3 ubiquitin complex for DELLA degradation (B).

## 2. Post-translational modifications of DELLA proteins

In addition to the GA-stimulated degradation via ubiquitin-proteasome pathway, DELLA activity or stability can be also regulated by other post-translational modifications (PTM) (Camut et al., 2017). Indeed, it has been proposed that some of these PTM might modulate DELLA activity more dynamically than proteolysis in response to environmental cues (Conti et al., 2014; Zentella et al., 2016, 2017; Camut et al., 2017).

**Phosphorylation** was the first PTM discovered for DELLAs although its relevance remains still poorly understood (Sasaki et al., 2003; Fu et al., 2004; Gomi et al., 2004; Itoh et al., 2005). Recent studies show that phosphorylation stabilizes DELLAs and is required for their activity. The characterization of the rice mutant *early flowering 1 (el1)* indicated that EL1 is a serine/threonine protein kinase that phosphorylates SLR1 (the rice DELLA protein) *in vitro* in both the N- and C-terminus. Although the molecular mechanism is unclear, a hypothetical model of EL1 function proposes that the phosphorylation at the C-terminal sustains SLR1

activity, whereas the N-terminal phosphorylated form blocks the GA-mediated degradation (Fig. 3A). Phenotypic analysis of *EL1* loss-of-function mutant plants showed that *el1* mutation suppresses the dwarf phenotype of *SLR1* over-expression, supporting the negative function of EL1 in GA signalling pathway (Dai and Xue, 2010). On the other hand, although it had been previously proposed that the degradation of DELLAs requires Ser/Thr dephosphorylation activity (Wang et al., 2009), it was not until recently when a phosphatase involved in GA signalling pathway was identified. Specifically, Qin et al. (2014) found that the phosphatase TOPP4, one of the Arabidopsis orthologs of the mammalian phosphatase PP1, promotes the GA-induced degradation of DELLAs by dephosphorylating these proteins (Fig. 3A). In agreement, the dwarf phenotype of *topp4* mutant plants is associated with higher levels of DELLA proteins.

Recent work by Tai-ping Sun's laboratory (Duke University, USA) showed that DELLA proteins can also be modified by **O-fucosylation** or **O-GlcNAcylation** (Zentella et al., 2016, 2017). The O-fucosylation of DELLA is mediated by the O-fucosyltransferase SPINDLY (SPY), whereas the O-GlcNAcylation is carried out by the O-linked N-acetylglucosamine transferase SECRET AGENT (SEC) (Fig. 3B). Interestingly, the DELLA O-GlcNAcylated or O-fucosylated peptides identified by mass spectrometry are clustered in the same regions at the N-terminus, including the Poly S/T/V motif. Genetic and biochemical analysis allowed the authors to propose a model in which SEC-dependent O-GlcNAcylation and SPY-dependent O-fucosylation of DELLA play opposite roles. O-GlcNAcylation by SEC might modify DELLA conformation into a closed conformation that prevents the binding of DELLA to its partners (e.g. BZR1, PIFs) and, therefore, their inactivation. In contrast, O-fucosylation promotes an open conformation that it is more active, thereby enhancing the binding of DELLA to their interacting proteins (Fig. 3B).

The **conjugation of DELLAs by the ubiquitin-like protein SUMO** (Small Ubiquitin-like Modifier) was reported as a novel GA-independent mechanism to control their levels (Conti et al., 2014). Conti and colleagues found that SUMO-conjugated DELLA binds to GID1 receptor in a GA-independent manner, thereby blocking the GID1 access to non-SUMOylated DELLAs (Fig. 3C). This mechanism reduces DELLA degradation and seems to be particularly relevant under stress conditions, since it would allow an accumulation of non-SUMOylated DELLAs able to start restraining growth even before the reduction of GA levels.

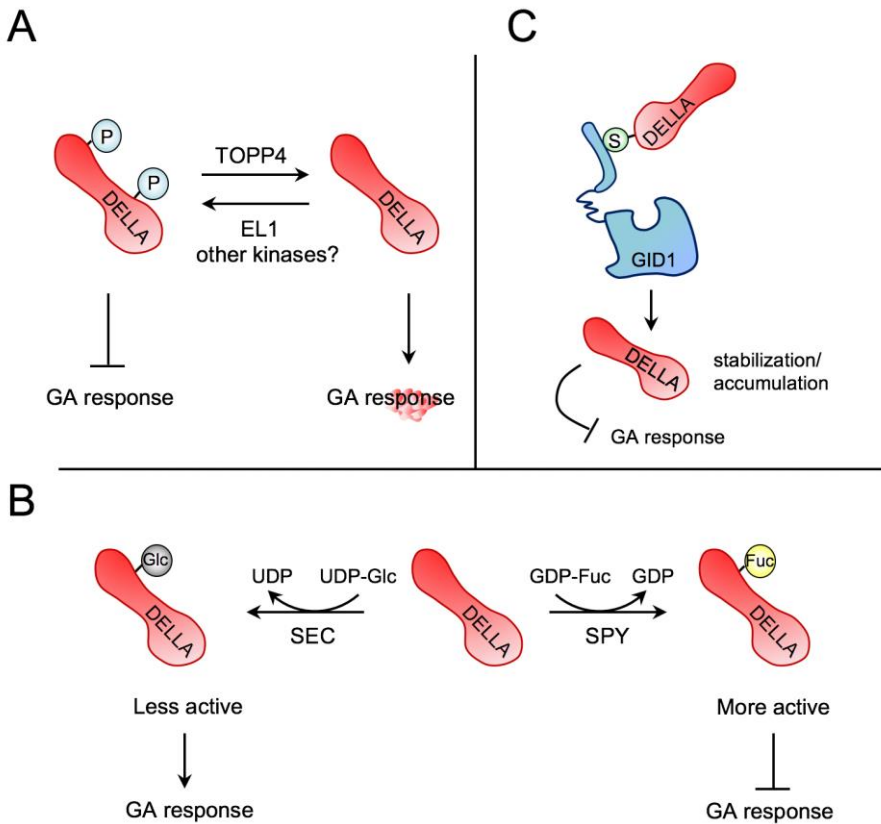


**Fig. 3. DELLAs regulation by other PTM.** (A) The EL1/TOPP4 model. The phosphorylation mediated by EL1 (and other kinases?) stabilizes DELLAs, whereas TOPP4-mediated dephosphorylation leads to DELLAs degradation. (B) The SPY/SEC model. SEC-dependent O-GlcNAcylation inhibits DELLA activity whereas SPY-dependent O-fucosylation represses GA responses by stimulating DELLA function. (C) SUMO modification. SUMO-conjugated DELLAs bind to GID1 receptor in a GA-independent manner, thereby avoiding the degradation of non-sumoylated DELLAs by the GA-GID1 signalling pathway. P refers to phosphorylation, Glc to O-GlcNAcylation, Fuc to O-fucosylation and S to sumoylation.

Unpublished results from our laboratory, as well as results published by other labs, suggest that DELLAs could be destabilized by a mechanism independent on GAs. First, a GA-insensitive, truncated version of RGA lacking the DELLA and VHYNP motifs is destabilized in cell-free degradation assays (Wang et al., 2009). Second, warm temperature caused a reduction in levels of the GA-insensitive *rga-Δ17* protein in the *Arabidopsis* hypocotyl, while no effect on its transcript levels was observed (Alabadí and Blázquez, unpublished). And third, the DELLA from *Marchantia polymorpha* (MpDELLA) is stabilized by the MG132 proteasome inhibitor (Hernández-García and Blázquez, unpublished), although active GAs

and *GID1* receptors seem to be missing in this species (Bowman et al., 2017; Blázquez et al., 2020). In **Chapter 1** of this Thesis, we show that the E3 ubiquitin ligase *CONSTITUTIVELY PHOTOMORPHOGENIC1* (*COP1*) defines this novel mechanism controlling *DELLA* stability and that it is relevant for the plant to respond to warm temperature and shade.

### 3. Molecular mechanisms of *DELLA* action

Current research on *GA* action is focused on the molecular mechanisms through which *DELLAs* regulate transcription. These mechanisms are just beginning to be understood and, in this section, we describe what is known so far.

The identification of *PHYTOCHROME INTERACTING FACTORS* (*PIFs*), *PIF3* and *PIF4*, as *DELLA* interactors represented a breakthrough in the field since it explained how *DELLAs* can regulate transcription (De Lucas et al., 2008; Feng et al., 2008). This work showed by chromatin immunoprecipitation (*ChIP*) and transactivation assays that the DNA binding ability of these transcription factors (*TFs*) was blocked upon interaction with the *DELLA* proteins (Fig. 4A). Since then, an ever-increasing number of *TFs* that are inhibited upon interaction with *DELLA* has been identified, indicating that this **sequestration mechanism** is quite extended (see Davière and Achard, 2016; Vera-Sirera et al., 2016 and Thomas et al., 2018 for detailed reviews). For instance, this is the case of the interaction with the brassinosteroids signalling element *BRASSINAZOLE-RESISTANTE1* (*BZR1*) (Gallego-Bartolomé et al., 2012; Bai et al., 2012; Li et al., 2012), with the positive regulators of the ethylene-signalling pathway *ETHYLENE INSENSITIVE3* (*EIN3*) and *EIN3-LIKE1* (*EIL1*) (An et al., 2012), with the trichome regulators *GLABRA1* (*GL1*), *GLABRA3* (*GL3*) and *ENHANCER of GLABRA3* (*EGL3*) (Qi et al., 2014), with the cell cycle regulators *TCP14/15* (Davière et al., 2014; Resentini et al., 2015) or with the positive regulator of vascular development *KNAT1/BREVIPEDICELLUS* (*BP*) (Felipo-Benavent et al., 2018).

This role of *DELLAs* regulating transcription while staying away from the chromatin is also manifested through interactions with non-DNA-binding transcriptional regulators that indirectly influence *TFs* activity, or with components of the chromatin remodelling machinery. For instance, *DELLAs* interact with and inhibit the negative regulator of jasmonic acid (*JA*) signalling *JASMONATE-ZIM-DOMAIN1* (*JAZ1*). *DELLA-JAZ1* binding releases the bHLH *TF* *MYC2*, promoting *JA* signalling (Fig. 4B) (Hou et al., 2010). Regarding chromatin remodelling machinery, it was reported that *DELLAs* interact with *SWITCH SUBUNIT3C*

(SWI3C) to regulate GA biosynthesis (Sarnowska et al., 2013) and PICKLE (PKL) to control skotomorphogenesis (Zhang et al., 2014). The latter interaction inhibits the PKL-PIF3 binding, reducing the repressive histone mark H3K27me3 on cell elongation-related genes (Fig. 4C).

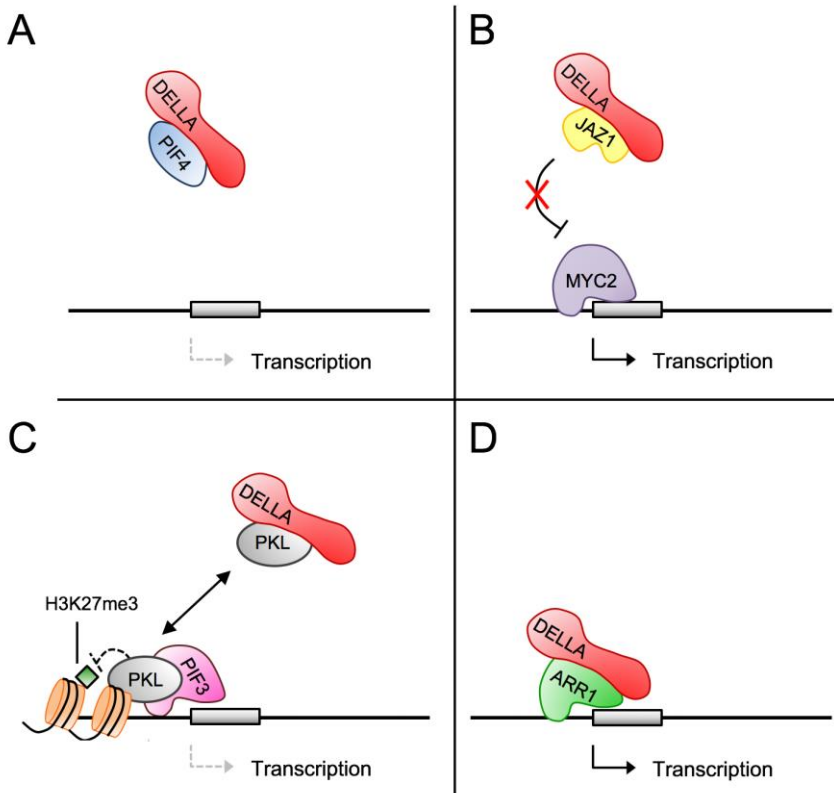


**Fig. 4. Molecular mechanisms of DELLA activity.** (A) DELLAs block the DNA binding activity of TFs (e.g. PIF4). (B) DELLAs sequester a repressor of a TF. For example, DELLA-JAZ1 interaction facilitates the activity of MYC2 TF. (C) DELLAs prevent the recruitment of the chromatin remodeler PKL to the promoter of its target genes. DELLA-PKL interaction avoids the decrease of the repressive mark H3K27me3 mediated by PKL and subsequently the expression of genes promoting cell elongation. (D) DELLAs act as co-activators at the target loci. In all cases, the effect of DELLAs in transcription is indicated.

Further insight into the mechanisms of DELLA action has been gained from recent studies characterising the interactions between DELLAs and GAI-ASSOCIATED FACTOR 1(GAF1)/IDD2, ABSCISIC ACID INSENSITIVE 3 (ABI3)/ABI5 and ARABIDOPSIS type B RESPONSE REGULATOR1 (ARR1) (Lim et al., 2013; Fukazawa et al., 2014; Marín-de la Rosa et al., 2015). In all these cases, DELLAs are recruited to the target promoters to act

as transcriptional co-activators (Fig. 4D). Thus, DELLA-GAF1, ABI3/5 and ARR1 are physiological relevant to control the expression of genes involved in GA biosynthesis, germination and root growth and de-etiolation processes, respectively. Importantly, this **transactivation mechanism** is not a marginal mechanism of DELLAs action since ChIP-seq analyses have demonstrated that RGA sits in the promoters of more than 2.800 genes (Marín-de la Rosa et al., 2015; Serrano-Mislata et al., 2017). Interestingly, the transactivation activity resides at the N-terminal DELLA domain and seems to be conserved in nonvascular land plants (Hirano et al., 2012; Hernández-García et al., 2019).

Both sequestration and transactivation mechanisms involve genome-wide transcriptional control. However, our laboratory uncovered a **non-genomic role** for DELLA in the regulation of cortical microtubule organization (Fig. 5) (Locascio et al., 2013). Specifically, Locascio and colleagues reported that DELLAs physically interact with the prefoldin complex (PFDC) in the nucleus. The localization of PFDC in the nucleus compromises its role as co-chaperone of the main cytosolic chaperone, CTT, in the folding of actins and tubulins (Vainberg et al., 1998). Consequently, the availability of tubulin is reduced in the absence of GA, affecting microtubule organization and therefore preventing anisotropic cell elongation.

The DELLA-dependent localization of PFDC in the nucleus opens the intriguing possibility that DELLAs regulate gene expression also through a mechanism that is different to the interaction with DNA-binding TFs. This possibility is based on the observation that the PFDC subunit PFD4 performs a role in the nucleus in the regulation of cold acclimation by promoting nuclear proteasome-mediated ELONGATED HYPOCOTYL 5 (HY5) degradation that is fully dependent on DELLAs (Perea-Resa et al., 2017). It is worth mentioning that ongoing projects in our laboratory are challenging the hypothesis of DELLA-PFDC working together in the control of (i) chromatin remodeling through modulating the activity of SWR1 complex that changes the canonical histone 2A (H2A) by the variant H2A.Z (Kumar and Wigge, 2010; Marí-Carmona et al, unpublished) and, (ii) pre-mRNA splicing by maintaining the proper levels of the Sm-like protein LSM8 (Esteve-Bruna et al, unpublished).

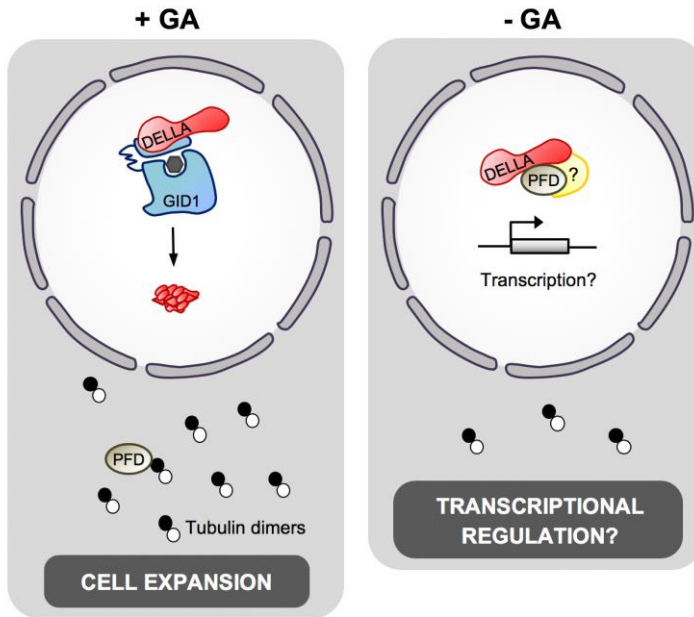


**Fig. 5. A non-genomic role of DELLAs.** DELLAs directly interact and hold the PFD complex in the nucleus in the absence of GA. Higher GA levels provoke the destruction of DELLAs, so that PFD functions as co-chaperone in the cytosol to produce active tubulin dimers that are necessary for cell expansion. PFD in the nucleus might also mediate genomic effects of DELLAs through a novel mechanism different to those shown in Fig. 4.

Are these the only mechanisms through which DELLAs regulate gene expression? Two observations lead us to the hypothesis that DELLAs regulate transcription elongation: (1) the presence of DELLAs not only in the promoters, but also in gene bodies (Marín-de la Rosa et al., 2015; Serrano-Mislata et al., 2017); and (2) the identification of ELF7, a member of the transcription elongation complex Polymerase-Associated Factor 1 (Paf1c), as DELLA interactor. Results presented in **Chapter 2** indicate that DELLAs regulate the recruitment of ELF7 to the chromatin to control transcriptional regulation mediated by RNAPII.

## 4. References

- Achard, P. and Genschik, P.** (2009). Releasing the brakes of plant growth: How GAs shutdown DELLA proteins. *J. Exp. Bot.* **60**: 1085–1092.
- An, F., Zhang, X., Zhu, Z., Ji, Y., He, W., Jiang, Z., Li, M., and Guo, H.** (2012). Coordinated regulation of apical hook development by gibberellins and ethylene in etiolated *Arabidopsis* seedlings. *Cell Res.* **22**: 915–927.
- Ariizumi, T., Lawrence, P.K., and Steber, C.M.** (2011). The role of two F-box proteins, SLEEPY1 and SNEEZY, in *Arabidopsis* gibberellin signaling. *Plant Physiol.* **155**: 765–775.
- Bai, M.Y., Shang, J.X., Oh, E., Fan, M., Bai, Y., Zentella, R., Sun, T.P., and Wang, Z.Y.** (2012). Brassinosteroid, gibberellin and phytochrome impinge on a common transcription module in *Arabidopsis*. *Nat. Cell Biol.* **14**: 810–817.
- Blázquez, M.A., Nelson, D.C., and Weijers, D.** (2020). Evolution of Plant Hormone Response Pathways. *Annu. Rev. Plant Biol.* **71**: annurev-arplant-050718-100309.
- Bowman, J.L. et al.** (2017). Insights into Land Plant Evolution Garnered from the *Marchantia polymorpha* Genome. *Cell.* **171**: 287–304.e15.
- Camut, L., Davière, J.M., and Achard, P.** (2017). Dynamic Regulation of DELLA Protein Activity: SPINDLY and SECRET AGENT Unmasked! *Mol. Plant.* **10**: 785–787.
- Chandler, P.M., Marion-Poll, A., Ellis, M., and Gubler, F.** (2002). Mutants at the Slender1 locus of barley cv himalaya. Molecular and physiological characterization. *Plant Physiol.* **129**: 181–190.
- Colebrook, E.H., Thomas, S.G., Phillips, A.L., and Hedden, P.** (2014). The role of gibberellin signalling in plant responses to abiotic stress. *J. Exp. Biol.* **217**: 67–75.
- Conti, L., Nelis, S., Zhang, C., Woodcock, A., Swarup, R., Galbiati, M., Tonelli, C., Napier, R., Hedden, P., Bennett, M., and Sadanandom, A.** (2014). Small Ubiquitin-like Modifier Protein SUMO Enables Plants to Control Growth Independently of the Phytohormone Gibberellin. *Dev. Cell.* **28**: 102–110.
- Dai, C. and Xue, H.W.** (2010). Rice early flowering1, a CKI, phosphorylates DELLA protein SLR1 to negatively regulate gibberellin signalling. *EMBO J.* **29**: 1916–1927.
- Davière, J.M. and Achard, P.** (2016). A Pivotal Role of DELLAs in Regulating Multiple Hormone Signals. *Mol. Plant.* **9**: 10–20.
- Davière, J.M., Wild, M., Regnault, T., Baumberger, N., Eisler, H., Genschik, P., and Achard, P.** (2014). Class I TCP-DELLA interactions in inflorescence shoot apex determine plant height. *Curr. Biol.* **24**: 1923–1928.
- Davière, J.M. and Achard, P.** (2013). Gibberellin signaling in plants. *Dev.* **140**: 1147–1151.
- De Lucas, M., Davière, J.M., Rodríguez-Falcón, M., Pontin, M., Iglesias-Pedraz, J.M., Lorrain, S., Fankhauser, C., Blázquez, M.A., Titarenko, E., and Prat, S.** (2008). A molecular framework for light and gibberellin control of cell elongation. *Nature.* **451**: 480–484.
- Dill, A., Thomas, S.G., Hu, J., Steber, C.M., and Sun, T.P.** (2004). The *Arabidopsis* F-box protein SLEEPY1 targets gibberellin signaling repressors for gibberellin-induced degradation. *Plant Cell.* **16**: 1392–1405.
- Dill, A., and Sun, T.P.** (2001a). Synergistic derepression of gibberellin signaling by removing RGA and GAI function in *Arabidopsis thaliana*. *Genetics.* **159**: 777–785.



- Dill, A., Jung, H.S., and Sun, T.P.** (2001b). The DELLA motif is essential for gibberellin-induced degradation of RGA. *Proc. Natl. Acad. Sci. U. S. A.* **98**: 14162–14167.
- Felipo-Benavent, A., Úrbez, C., Blanco-Touriñán, N., Serrano-Mislata, A., Baumberger, N., Achard, P., Agusti, J., Blázquez, M.A., and Alabadi, D.** (2018). Regulation of xylem fiber differentiation by gibberellins through DELLA-KNAT1 interaction. *Dev.* **145**: 1–7.
- Feng, S. et al.** (2008). Coordinated regulation of *Arabidopsis thaliana* development by light and gibberellins. *Nature.* **451**: 475–479.
- Fu, X., Richards, D.E., Fleck, B., Xie, D., Burton, N., and Harberd, N.P.** (2004). The *Arabidopsis* mutant *sleepy1gar2-1* protein promotes plant growth by increasing the affinity of the SCFSLY1 E3 ubiquitin ligase for DELLA protein substrates. *Plant Cell.* **16**: 1406–1418.
- Fukazawa, J., Teramura, H., Murakoshi, S., Nasuno, K., Nishida, N., Ito, T., Yoshida, M., Kamiya, Y., Yamaguchi, S., and Takahashi, Y.** (2014). DELLAs function as coactivators of GAI-ASSOCIATED FACTOR1 in regulation of gibberellin homeostasis and signaling in *Arabidopsis*. *Plant Cell.* **26**: 2920–2938.
- Gallego-Bartolomé, J., Minguet, E.G., Grau-Enguix, F., Abbas, M., Locascio, A., Thomas, S.G., Alabadi, D., and Blázquez, M.A.** (2012). Molecular mechanism for the interaction between gibberellin and brassinosteroid signaling pathways in *Arabidopsis*. *Proc. Natl. Acad. Sci. U. S. A.* **109**: 13446–13451.
- Gallego-Bartolomé, J., Minguet, E.G., Marín, J.A., Prat, S., Blázquez, M.A., and Alabadi, D.** (2010). Transcriptional diversification and functional conservation between DELLA proteins in *Arabidopsis*. *Mol. Biol. Evol.* **27**: 1247–1256.
- Gomi, K., Sasaki, A., Itoh, H., Ueguchi-Tanaka, M., Ashikari, M., Kitano, H., and Matsuoka, M.** (2004). *GID2*, an F-box subunit of the SCF E3 complex, specifically interacts with phosphorylated SLR1 protein and regulates the gibberellin-dependent degradation of SLR1 in rice. *Plant J.* **37**: 626–634.
- Hedden, P. and Sponsel, V.** (2015). A Century of Gibberellin Research. *J. Plant Growth Regul.* **34**: 740–760.
- Hernández-García, J., Briones-Moreno, A., Dumas, R., and Blázquez, M.A.** (2019). Origin of Gibberellin-Dependent Transcriptional Regulation by Molecular Exploitation of a Transactivation Domain in DELLA Proteins. *Mol. Biol. Evol.* **36**: 908–918.
- Hirano, K., Kouketu, E., Katoh, H., Aya, K., Ueguchi-Tanaka, M., and Matsuoka, M.** (2012). The suppressive function of the rice DELLA protein SLR1 is dependent on its transcriptional activation activity. *Plant J.* **71**: 443–453.
- Hirano, K., Asano, K., Tsuji, H., Kawamura, M., Mori, H., Kitano, H., Ueguchi-Tanaka, M., and Matsuoka, M.** (2010). Characterization of the molecular mechanism underlying gibberellin perception complex formation in rice. *Plant Cell.* **22**: 2680–2696.
- Hou, X., Lee, L.Y.C., Xia, K., Yan, Y., and Yu, H.** (2010). DELLAs Modulate Jasmonate Signaling via Competitive Binding to JAZs. *Dev. Cell.* **19**: 884–894.
- Ikeda, A., Ueguchi-Tanaka, M., Sonoda, Y., Kitano, H., Koshioka, M., Futsuhara, Y., Matsuoka, M., and Yamaguchi, J.** (2001). Slender rice, a constitutive gibberellin response mutant, is caused by a null mutation of the *SLR1* gene, an ortholog of the height-regulating gene *GAI/RGA/RHT/D8*. *Plant Cell.* **13**: 999–1010.
- Itoh, H., Sasaki, A., Ueguchi-Tanaka, M., Ishiyama, K., Kobayashi, M., Hasegawa, Y., Minami, E., Ashikari, M., and Matsuoka, M.** (2005). Dissection of the phosphorylation of rice DELLA protein, SLENDER RICE1. *Plant Cell Physiol.* **46**: 1392–1399.

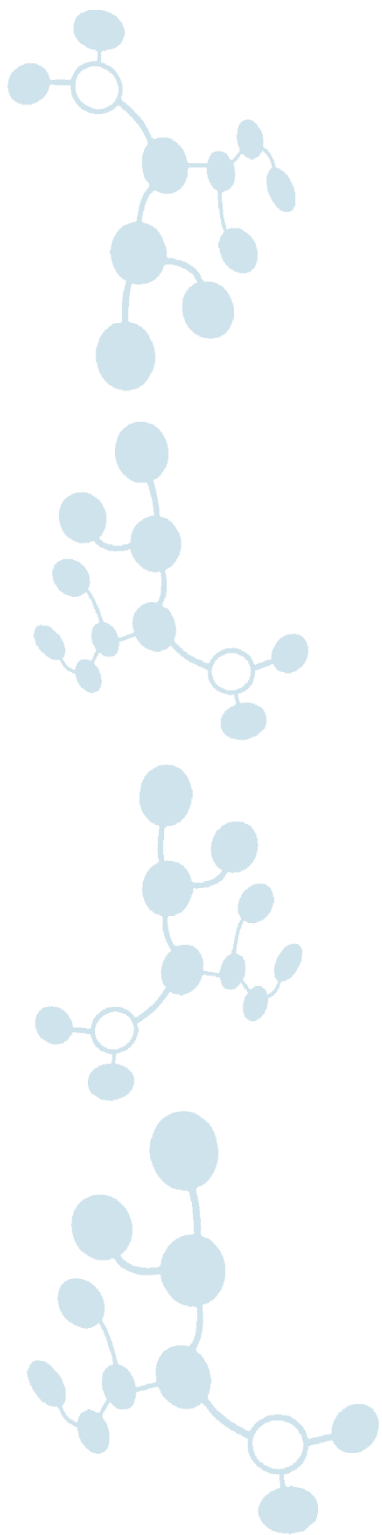
- Itoh, H., Ueguchi-Tanaka, M., Sato, Y., Ashikari, M., and Matsuoka, M.** (2002). The gibberellin signaling pathway is regulated by the appearance and disappearance of slender rice1 in nuclei. *Plant Cell*. **14**: 57–70.
- Jasinski, S., Tattersall, A., Piazza, P., Hay, A., Martinez-Garcia, J.F., Schmitz, G., Theres, K., McCormick, S., and Tsiantis, M.** (2008). PROCERA encodes a DELLA protein that mediates control of dissected leaf form in tomato. *Plant J*. **56**: 603–612.
- King, K.E., Moritz, T., and Harberd, N.P.** (2001). Gibberellins are not required for normal stem growth in *Arabidopsis thaliana* in the absence of GAI and RGA. *Genetics*. **159**: 767–776.
- Koorneef, M., Elgersma, A., Hanhart, C.J., van Loenen-Martinet, E.P., van Rijn, L., and Zeevaart, J.A.D.** (1985). A gibberellin insensitive mutant of *Arabidopsis thaliana*. *Physiol. Plant*. **65**: 33–39.
- Kumar, S.V. and Wigge, P.A.** (2010). H2A.Z-Containing Nucleosomes Mediate the Thermosensory Response in *Arabidopsis*. *Cell*. **140**: 136–147.
- Li, Q.F., Wang, C., Jiang, L., Li, S., Sun, S.S.M., and He, J.X.** (2012). An interaction between BZR1 and DELLAs mediates direct signaling crosstalk between brassinosteroids and gibberellins in *Arabidopsis*. *Sci. Signal*. **5**: ra72.
- Lim, S., Park, J., Lee, N., Jeong, J., Toh, S., Watanabe, A., Kim, J., Kang, H., Kim, D.H., Kawakami, N., and Choi, G.** (2013). ABA-insensitive3, ABA-insensitive5, and DELLAs interact to activate the expression of *SOMNUS* and other high-temperature-inducible genes in imbibed seeds in *Arabidopsis*. *Plant Cell*. **25**: 4863–4878.
- Locascio, A., Blázquez, M.A., and Alabadí, D.** (2013). Dynamic regulation of cortical microtubule organization through prefoldin-DELLA interaction. *Curr. Biol*. **23**: 804–809.
- Marín-de la Rosa, N. et al.** (2015). Genome Wide Binding Site Analysis Reveals Transcriptional Coactivation of Cytokinin-Responsive Genes by DELLA Proteins. *PLoS Genet*. **11**: 1–20.
- McGinnis, K.M., Thomas, S.G., Soule, J.D., Strader, L.C., Zale, J.M., Sun, T.P., and Steber, C.M.** (2003). The *Arabidopsis SLEEPY1* gene encodes a putative F-box subunit of an SCF E3 ubiquitin ligase. *Plant Cell*. **15**: 1120–1130.
- Minguet, E.G., Alabadí, D., and Blázquez, M.A.** (2014). Gibberellin implication in plant growth and stress responses. In *Phytohormones: A Window to Metabolism, Signaling and Biotechnological Applications*. Springer, New York, NY. Tran LS., Pal S. (Eds).
- Murase, K., Hirano, Y., Sun, T.P., and Hakoshima, T.** (2008). Gibberellin-induced DELLA recognition by the gibberellin receptor GID1. *Nature*. **456**: 459–463.
- Nakajima, M. et al.** (2006). Identification and characterization of *Arabidopsis* gibberellin receptors. *Plant J*. **46**: 880–889.
- Peng, J., Carol, P., Richards, D.E., King, K.E., Cowling, R.J., Murphy, G.P., and Harberd, N.P.** (1997). The *Arabidopsis GAI* gene defines a signaling pathway that negatively regulates gibberellin responses. *Genes Dev*. **11**: 3194–3205.
- Perea-Resa, C., Rodríguez-Milla, M.A., Iniesto, E., Rubio, V., and Salinas, J.** (2017). Prefoldins Negatively Regulate Cold Acclimation in *Arabidopsis thaliana* by Promoting Nuclear Proteasome-Mediated HY5 Degradation. *Mol. Plant*. **10**: 791–804.
- Qi, T., Huang, H., Wu, D., Yan, J., Qi, Y., Song, S., and Xie, D.** (2014). *Arabidopsis* DELLA and JAZ proteins bind the WD-Repeat/ bHLH/MYB complex to modulate gibberellin and jasmonate signaling synergy. *Plant Cell*. **26**: 1118–1133.
- Qin, Q., Wang, W., Guo, X., Yue, J., Huang, Y., Xu, X., Li, J., and Hou, S.** (2014). *Arabidopsis*

- DELLA Protein Degradation Is Controlled by a Type-One Protein Phosphatase, TOPP4. *PLoS Genet.* **10**.
- Resentini, F., Felipo-Benavent, A., Colombo, L., Blázquez, M.A., Alabadí, D., and Masiero, S.** (2015). TCP14 and TCP15 mediate the promotion of seed germination by gibberellins in *Arabidopsis thaliana*. *Mol. Plant.* **8**: 482–485.
- Sarnowska, E.A. et al.** (2013). DELLA-interacting SWI3C core subunit of switch/sucrose nonfermenting chromatin remodeling complex modulates gibberellin responses and hormonal cross talk in *Arabidopsis*. *Plant Physiol.* **163**: 305–317.
- Sasaki, A., Itoh, H., Gomi, K., Ueguchi-Tanaka, M., Ishiyama, K., Kobayashi, M., Jeong, D.H., An, G., Kitano, H., Ashikari, M., and Matsuoka, M.** (2003). Accumulation of phosphorylated repressor for Gibberellin signaling in an F-box mutant. *Science.* **299**: 1896–1898.
- Serrano-Mislata, A., Bencivenga, S., Bush, M., Schiessl, K., Boden, S., and Sablowski, R.** (2017). DELLA genes restrict inflorescence meristem function independently of plant height. *Nat. Plants.* **3**: 749–754.
- Shimada, A., Ueguchi-Tanaka, M., Nakatsu, T., Nakajima, M., Naoe, Y., Ohmiya, H., Kato, H., and Matsuoka, M.** (2008). Structural basis for gibberellin recognition by its receptor GID1. *Nature.* **456**: 520–523.
- Silverstone, A.L., Jung, H.-S., Dill, A., Kawaide, H., Kamiya, Y., and Sun, T.** (2001). Repressing a Repressor. *Plant Cell.* **13**: 1555–1566.
- Thomas, S.G., Blázquez, M.A., and Alabadí, D.** (2018). DELLA Proteins: Master Regulators of Gibberellin-Responsive Growth and Development. In *Annual Plant Reviews online*, J.A. Roberts (Ed.).
- Ueguchi-Tanaka, M., Nakajima, M., Katoh, E., Ohmiya, H., Asano, K., Saji, S., Hongyu, X., Ashikari, M., Kitano, H., Yamaguchi, I., and Matsuoka, M.** (2007). Molecular interactions of a soluble gibberellin receptor, GID1, with a rice DELLA protein, SLR1, and gibberellin. *Plant Cell.* **19**: 2140–2155.
- Ueguchi-Tanaka, M., Ashikari, M., Nakajima, M., Itoh, H., Katoh, E., Kobayashi, M., Chow, T.Y., Hsing, Y.I.C., Kitano, H., Yamaguchi, I., and Matsuoka, M.** (2005). *GIBBERELLIN INSENSITIVE DWARF1* encodes a soluble receptor for gibberellin. *Nature.* **437**: 693–698.
- Vainberg, I.E., Lewis, S.A., Rommelaere, H., Ampe, C., Vandekerckhove, J., Klein, H.L., and Cowan, N.J.** (1998). Prefoldin, a chaperone that delivers unfolded proteins to cytosolic chaperonin. *Cell.* **93**: 863–873.
- Vera-Sirera, F., Gomez, M.D., and Perez-Amador, M.A.** (2016). DELLA Proteins, a Group of GRAS Transcription Regulators that Mediate Gibberellin Signaling. In *Plant Transcription Factors: Evolutionary, Structural and Functional Aspects*. D. H. Gonzalez (Ed.).
- Wang, F., Zhu, D., Huang, X., Li, S., Gong, Y., Yao, Q., Fu, X., Fan, L.M., and Deng, X.W.** (2009). Biochemical insights on degradation of *Arabidopsis* DELLA proteins gained from a cell-free assay system. *Plant Cell.* **21**: 2378–2390.
- Willige, B.C., Ghosh, S., Nill, C., Zourelidou, M., Dohmann, E.M.N., Maier, A., and Schwechheimer, C.** (2007). The DELLA domain of GA INSENSITIVE mediates the interaction with the GA INSENSITIVE DWARF1A gibberellin receptor of *Arabidopsis*. *Plant Cell.* **19**: 1209–1220.
- Zentella, R., Sui, N., Barnhill, B., Hsieh, W.P., Hu, J., Shabanowitz, J., Boyce, M., Olszewski, N.E., Zhou, P., Hunt, D.F., and Sun, T.P.** (2017). The *Arabidopsis* O-

fucosyltransferase SPINDLY activates nuclear growth repressor DELLA. *Nat. Chem. Biol.* **13**: 479–485.

**Zentella, R. et al.** (2016). O-GlcNAcylation of master growth repressor DELLA by SECRET AGENT modulates multiple signaling pathways in Arabidopsis. *Genes Dev.* **30**: 164–176.

**Zhang, D., Jing, Y., Jiang, Z., and Lin, R.** (2014). The chromatin-remodeling factor PICKLE integrates brassinosteroid and gibberellin signaling during skotomorphogenic growth in Arabidopsis. *Plant Cell.* **26**: 2472–2485.



# Objectives



Gibberellin(GA)-dependent regulation of DELLA levels and the modulation of transcription factor activity by direct interaction with DELLAs provide a good mechanistic framework to understand how DELLAs mediate environmental regulation of transcriptional programs. However, different observations summarized in the Introduction (e.g., the temperature-dependent changes in the protein levels of GA-insensitive DELLA alleles, and the presence of DELLAs in gene bodies) led us to investigate additional mechanisms of DELLA protein regulation and activity in Arabidopsis. Therefore, the two specific objectives pursued in this Thesis are:

1. **Unveiling the mechanism that destabilizes DELLA independently of GAs.** We hypothesize that DELLA levels might be controlled by the E3 ubiquitin ligase COP1, and that this regulation could be relevant in particular growth conditions.
2. **Identifying the molecular mechanisms by which DELLAs may regulate gene expression beyond the modulation of the transcription factor activity.** We hypothesize that DELLAs regulate the activity of the basal transcriptional machinery and that this mechanism could involve the interaction of DELLAs with the Paf1 complex.







# Chapter 1

## **COP1 destabilizes DELLA proteins in Arabidopsis**

Blanco-Touriñán N, Legris M, Minguet EG, Costigliolo-Rojas C, Nohales MA, Iniesto E, García-León M, Pacín M, Heucken N, Blomeier T, Locascio A, Černý M, Esteve-Bruna D, Díez-Díaz M, Brzobohatý B, Frerigmann H, Zurbriggen MD, Kay SA, Rubio V, Blázquez MA, Casal JJ, Alabadí D (2020). COP1 destabilizes DELLA proteins in Arabidopsis.

**Proc Natl Acad Sci USA**, doi: 10.1073/pnas.190796911

DELLA transcriptional regulators are central components in the control of plant growth responses to the environment. This is considered to be mediated by changes in the metabolism of the hormones gibberellins (GAs), which promote the degradation of DELLAs. However, here we show that warm temperature or shade reduced the stability of a GA-insensitive DELLA allele in *Arabidopsis thaliana*. Furthermore, the degradation of DELLA induced by the warmth preceded changes in GA levels and depended on the E3 ubiquitin ligase CONSTITUTIVELY PHOTOMORPHOGENIC1 (COP1). COP1 enhanced the degradation of normal and GA-insensitive DELLA alleles when co-expressed in *Nicotiana benthamiana*. DELLA proteins physically interacted with COP1 in yeast, mammalian and plant cells. This interaction was enhanced by the COP1 complex partner SUPPRESSOR OF *phyA-105* 1 (SPA1). The level of ubiquitination of DELLA was enhanced by COP1 and COP1 ubiquitinated DELLA proteins *in vitro*. We propose that DELLAs are destabilized not only by the canonical GA-dependent pathway but also by COP1 and that this control is relevant for growth responses to shade and warm temperature.

## 1. Introduction

A plant can adopt markedly different morphologies depending on the environment it has to cope with. This plastic behaviour relies on highly interconnected signalling pathways, which offer multiple points of control (Casal et al., 2004). Light and temperature are among the most influential variables of the environment in plant life. For instance, light cues from neighbouring vegetation as well as elevated ambient temperature (e.g. 28 °C) enhance the growth of the hypocotyl (among other responses) respectively to avoid shade (Casal, 2013) and enhance cooling (Quint et al., 2016).

Several features place DELLA proteins as central elements in environmental responses (Claeys et al., 2014). First, DELLAs are nuclear-localized proteins that interact with multiple transcription factors and modulate their activity (Van De Velde et al., 2017). Second, they are negative elements in the gibberellin (GA) signalling pathway and their stability is severely diminished upon recognition of their N-terminal domain by the GA-activated GIBBERELLIN INSENSITIVE1 (GID1) receptor, which recruits the SCF<sup>SLY/GID2</sup> complex to promote their ubiquitination-dependent degradation by the proteasome (Sun, 2011). Third, GA metabolism is tightly regulated by the environment, for instance, shade and warm temperature induce GA accumulation (Alabadí and Blázquez, 2009; Quint et al., 2016).

DELLA levels increase during seedlings de-etiolation or cold exposure and promote transcriptional changes associated with photomorphogenesis or with the adaptation to low temperatures, respectively (Achard et al., 2007; Alabadí et al., 2008; Lantzouni et al., 2020). On the contrary, they decrease during the night and in response to shade inflicted by neighbour plants or to warm ambient temperature, allowing the promotion of hypocotyl and/or petiole elongation by transcription factors such as PHYTOCHROME INTERACTING FACTOR4 (Djakovic-Petrovic et al., 2007; De Lucas et al., 2008; Stavang et al., 2009; Arana et al., 2011). Interestingly, the role of DELLAs in all these processes is the opposite to that of CONSTITUTIVELY PHOTOMORPHOGENIC1 (COP1), another central regulator of light and temperature responses. COP1 is an E3 ubiquitin ligase that promotes proteasome-dependent degradation of a number of transcription factors involved in light and temperature signalling. COP1 becomes inactivated by light perceived by phytochromes and cryptochromes and by low to moderate temperature (4 °C to 23 °C) (Liu et al., 2011; Lian et al., 2011; Catalá et al., 2011; Lu et al., 2015; Sheerin et al., 2015; Park et al., 2017b) and requires the activity of the SUPPRESSOR OF *phyA-105* proteins (SPA1 to 4 in Arabidopsis) to be active *in vivo* (Hoecker, 2017). Here we show the direct physical

interaction between DELLAs and COP1/SPA1 complex and propose a mechanism of regulation of DELLA stability different from the canonical GA signalling pathway.

## 2. Results

### Warm temperature or shade decrease the abundance of a GA-insensitive DELLA protein.

Warm temperatures (28 °C hereafter) or shade decrease the abundance of the DELLA protein REPRESSOR OF *ga 1-3* (RGA) (Fig. 1A, Fig. S1A) (Djakovic-Petrovic et al., 2007; De Lucas et al., 2008; Stavang et al., 2009; Arana et al., 2011). Two observations indicate that changes in GA cannot fully account for these reductions. First, increasing doses of the GA-inhibitor paclobutrazol (PAC) elevated RGA nuclear abundance observed by confocal microscopy in a *pRGA:GFP-RGA* line (Silverstone et al., 2001), but the reductions caused by shade or warmth persisted even under saturating levels of the inhibitor (Fig. 1A, Fig. S2A). Second, warm temperature or shade reduced the levels of *rga-Δ17*, a mutant version of RGA that is fully insensitive to GA, in the *pRGA:GFP-(rga-Δ17)* line (Fig. 1B and C, Fig. S1A and S2B) (Dill et al., 2001). Changes in RGA transcript levels do not mediate the altered RGA abundance in response to shade (Djakovic-Petrovic et al., 2007) or warm temperature (Fig. S1B). Importantly, treatment with the inhibitor of the 26S proteasome MG132 fully impaired changes in RGA abundance (Fig. 2A). Altogether, these results suggest the existence of a non-canonical pathway of DELLA degradation.

### COP1 affects RGA levels in response to shade and warmth.

RGA levels are elevated in *cop 1-4* seedlings (Cagnola et al., 2018). Compared to light at moderate temperature, darkness, or 2 to 8 h of shade or warm temperature increased the nuclear abundance of COP1 (Pacín et al., 2014, 2013; Park et al., 2017b) in a *35S:YFP-COP1 cop 1-4* line (Oravec et al., 2006), while reducing RGA levels (Djakovic-Petrovic et al., 2007; Achard et al., 2007; Stavang et al., 2009) (Fig. 1D and E). The light-induced increase in RGA showed wild-type kinetics in the *cop 1-4* seedlings (note parallel curves), suggesting that this change is driven by a COP1-independent light-induced down-regulation of GA biosynthesis (Gil and García-Martínez, 2000; Zhao et al., 2007; Achard et al., 2007; Alabadí et al., 2008). Conversely, *cop 1-4* seedlings grown in the light at moderate temperature (20 °C) and transferred either to shade at the same temperature or to light at 28 °C, showed a markedly delayed decrease in GFP-RGA (Fig. 1E).

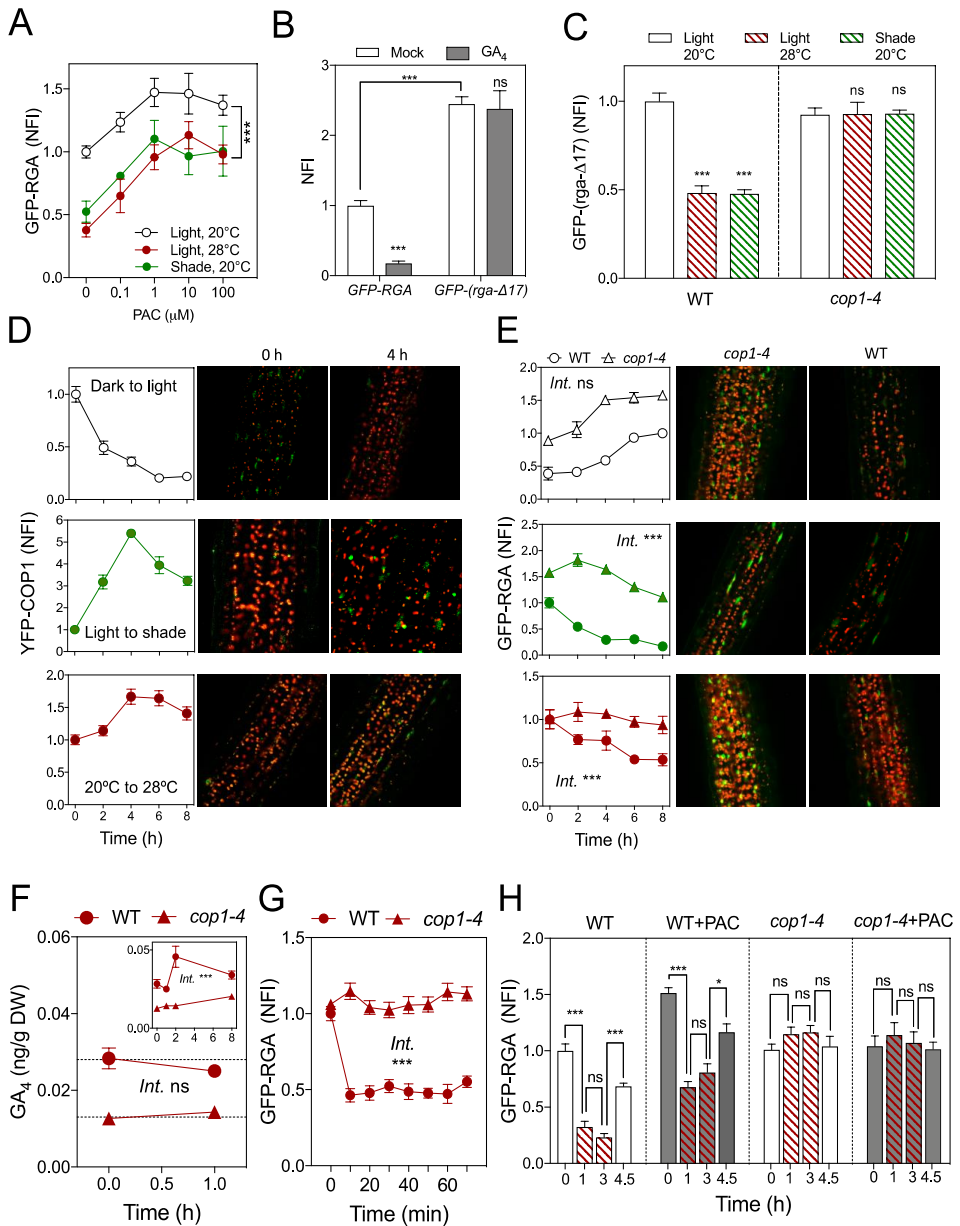


**Fig. 1. COP1 regulates RGA levels in Arabidopsis hypocotyls in response to shade and warmth.** (A) GFP-RGA levels respond to shade and warmth in the absence of GA synthesis. We incubated the seedlings with the indicated doses of PAC for 8 h, before exposure to shade or 28 °C for 4 h. (B) GFP-(*rga-Δ17*) is insensitive to GA-induced degradation. Seedlings of *pRGA:GFP-RGA* and *pRGA:GFP-(rga-Δ17)* lines were mock-treated or treated with 3 μM GA<sub>4</sub> for 4 h. (C) Shade or warmth reduce GFP-(*rga-Δ17*) levels in a COP1-dependent-manner. Seedlings were exposed to the treatment for 3 days. (D-E) Dynamics of nuclear accumulation of YFP-COP1 (D) in the wild-type and of GFP-RGA (E) in the wild-type (circles) and *cop1-4* mutants (triangles) after the transfer from darkness to light (white symbols), light to shade (green symbols), and 20 °C to 28 °C (red symbols). (F) Time course of GA<sub>4</sub> levels in wild-type and *cop1-4* seedlings before (time = 0 h) and after transfer to 28 °C (the inset shows an extended time-course). (G) Time course of nuclear

levels of GFP-RGA in wild-type and *cop1-4* seedlings before (time =0 h) and after transfer to 28 °C. (H) The reduction of GFP-RGA levels in response to 28 °C is reversible, unaffected by a saturating dose of PAC and dependent on COP1. Seedlings of *pRGA:GFP-RGA* in the wild-type and *cop1-4* backgrounds were returned to 20 °C after 3 h-treatment of 28 °C. We incubated the seedlings with PAC for 8 h before exposure to 28 °C. Confocal data (A-E, G and H) show the normalized fluorescence intensity (NFI) in nuclei (NFI= 1 in the wild-type seedling control, and in B in the wild-type RGA control). For representative images, see D-E (8 h time point) and Fig. S2A and B. Confocal microscopy data are means and SE of 5-10 (A), 6-9 (B), 6-14 (C), 18 (D-E), 6-13 (G) and 18 (H) seedlings (a minimum of 10 and up to 50 nuclei were averaged per seedling replicate). GA<sub>4</sub> data are means and SE of three independent biological replicates. In A-C and G, we indicate the significance of the differences with the control condition (B also shows the difference between genotypes) in Student's *t* test or ANOVA followed by Bonferroni tests. In E-G we indicate the significance of the term accounting for the interaction (*int.*) between condition (light, temperature) and genotype (wild type, *cop1*) in multiple regression analysis. In H, we indicate the significance of the comparison with the preceding bar in ANOVA followed by Bonferroni tests. \* *P* < 0.05, \*\* *P* < 0.01, \*\*\* *P* < 0.005; ns, non-significant.

### Changes in RGA abundance precede changes in GA.

GA<sub>4</sub> levels were unaffected by transferring the seedlings from 20 °C to 28 °C for 1 h (Fig. 1F), whilst 10 min of warm temperature were enough to induce significant nuclear accumulation of COP1 (Fig. S2C) and decrease GFP-RGA levels in a COP1-dependent manner (Fig. 1G). These results indicate that rapid warmth-induced degradation of RGA requires COP1 and precedes changes in GA.

### Relative contribution of each pathway.

GA levels did increase after 2 h of warm temperature (Fig. 1F, inset). However, two observations indicate a negligible contribution of these changes in GA levels to the reduced GFP-RGA abundance in response to warmth. First, we observed no significant decreases in GFP-RGA between 1 and 3 h at 28 °C (i.e., concomitantly with the increase in GA) (Fig. 1H), despite the fact that GFP-RGA responds to exogenously applied GA in less than 15 min (Silverstone et al., 2001). Second, application of a saturating dose of PAC to block GA synthesis significantly increased GFP-RGA levels but resulted in a parallel kinetics in response to warm temperature (Fig. 1H). GFP-RGA levels increased rapidly after returning the seedlings from 28 °C to 20 °C, a response also observed in the presence of PAC (Fig. 1H). *cop1-4* showed reduced levels of GA<sub>4</sub> but retained some GA<sub>4</sub> response to temperature (*P* < 0.05, Fig. 1F, inset), which may have contributed to residual GFP-RGA degradation observed in this mutant beyond 4 h of shade or warmth (*P* < 0.05, Fig. 1E). Similarly, the *cop1* mutation lowers GA levels in pea without eliminating their response to light (Weller et al., 2009). Taken together, these observations indicate that changes in GA have no major

direct contribution to the rapid changes in RGA abundance, because when GA levels are elevated, COP1 has already induced RGA decay. However, the canonical GA pathway would make an indirect contribution to the rapid changes, setting basal RGA levels within a range where the system becomes sensitive to COP1. In fact, although shade and warmth did reduce GFP-(*rga-Δ17*) levels (Fig. 1C, Fig. S2B), these effects were not rapid (Fig. S2D and E). Similarly, warm temperature does not provoke rapid changes in RGA levels in the GA-deficient mutant *ga1* (Stavang et al., 2009).

### **COP1 promotes degradation of a GA-insensitive DELLA protein.**

The fact that warm temperature or shade failed to reduce the nuclear abundance of RGA or *rga-Δ17* in the *cop1-4* mutant (Fig. 1C, E, G, H and 2A) and that these changes are dependent on the 26S proteasome (Fig. 2A), suggests that COP1 promotes DELLA degradation. We first tested this possibility in transient expression assays in *Nicotiana benthamiana* leaves. Co-expression of COP1 caused 26S proteasome-dependent decrease of HA-RGA and HA-(*rga-Δ17*) in leaves of long-day grown *N. benthamiana* plants, while it had no impact on levels of the unrelated protein HA-GFP (Fig. 2B and C). Warm temperature decreased HA-(*rga-Δ17*) in a COP1-mediated manner (Fig. S3). This suggests that COP1 mediates the destabilization of RGA by non-canonical mechanisms.

### **COP1 interacts physically with GAI and RGA in yeast.**

To explore if COP1 mediates RGA degradation by non-canonical mechanisms, we investigated whether COP1 physically interacts with DELLA proteins. We performed yeast two-hybrid (Y2H) assays between COP1 and the two DELLAs with a major role in light- and temperature-dependent growth, RGA and GIBBERELLIC ACID INSENSITIVE (GAI) (Alabadí et al., 2004; Stavang et al., 2009; Arana et al., 2011). To avoid the reported strong auto-activation of full-length DELLAs in yeast, we used previously established variants with deletions of the N-terminus named M5GAI and RGA52 (De Lucas et al., 2008; Gallego-Bartolomé et al., 2012). COP1 was able to interact with both (Fig. 3A). SUPPRESSOR OF *phyA-105* 1 (SPA1) and other SPA proteins involved in a functional complex with COP1 (Hoecker and Quail, 2001; Hoecker, 2017) were also able to interact with GAI and RGA in Y2H assays (Fig. 3B).

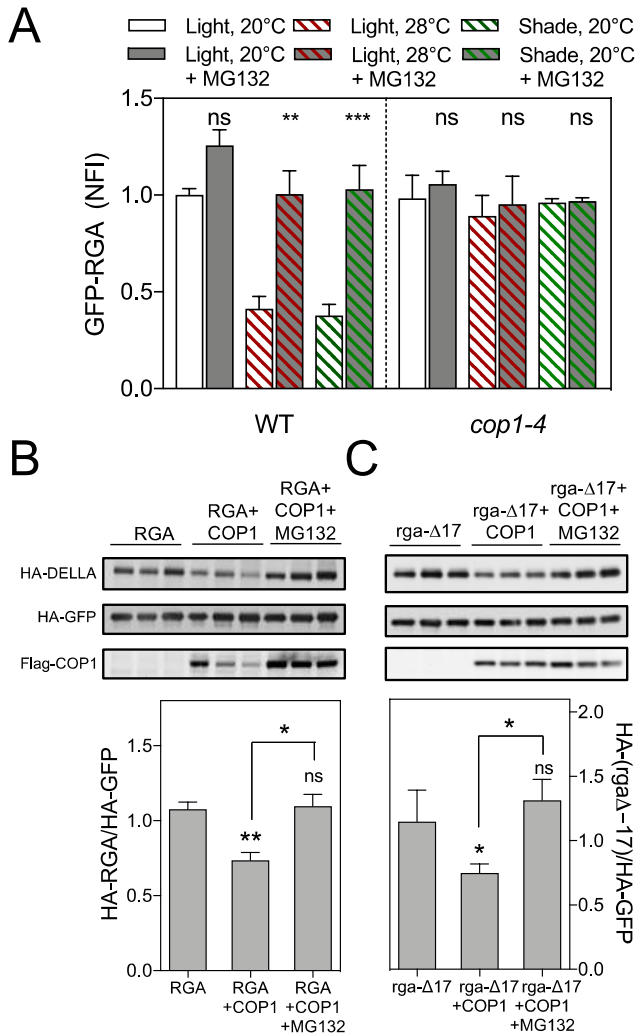


**Fig. 2. COP1 destabilizes DELLAs.** (A) The reduction of GFP-RGA levels by warm temperature or shade requires the 26S proteasome and COP1. Confocal data show the NFI in nuclei (NFI=1 in the wild-type seedling control). NFI data are means and SE of 6-9 seedlings (10-30 nuclei were averaged per seedling replicate). Asterisks indicate that the difference is statistically significant (Student's *t* test, \*  $P < 0.05$  and \*\*\*  $P < 0.001$ ; ns, non-significant). (B-C) COP1 destabilizes RGA (B) and the GA-insensitive *rga-Δ17* (C) in *N. benthamiana* leaves. HA-RGA and HA-(*rga-Δ17*) were transiently expressed alone or with Flag-COP1 in leaves of *N. benthamiana*. For MG132 treatments leaves were infiltrated with a solution of 25  $\mu$ M of the inhibitor 8 h before sampling. HA-GFP was used as control to demonstrate the specificity of COP1 action. Blots show data from three individual infiltrated leaves per mixture. Plots show HA-RGA and HA-(*rga-Δ17*) normalized against HA-GFP. Data are means and SE of 3 leaves from one experiment, repeated twice with similar results. Asterisks indicate that the difference is statistically significant (Student's *t* test, \*  $P < 0.05$  and \*\*  $P < 0.01$ ; ns, non-significant).



### **COP1 interacts with GAI and RGA in planta.**

To investigate whether the interaction between DELLAs and COP1 also occurs in plant cells, we first performed co-immunoprecipitation assays in leaves of *N. benthamiana* co-expressing DsRED-COP1-HA and YFP-M5GAI or YFP-RGA52. While DsRED-COP1-HA was pulled down by anti-GFP antibodies from leaf extracts co-expressing YFP-M5GAI and the interaction appeared to be enhanced in the presence of c-myc-SPA1, the DsRED-COP1-HA and YFP-RGA52 interaction was only observed when the three proteins were co-expressed (Fig. 3C). c-myc-SPA1 was also specifically co-immunoprecipitated with YFP-M5GAI (Fig. 3C). These results suggest that SPA1 enhances the interaction between COP1 and DELLA proteins. Consistent with this idea, we observed re-localization of YFP-GAI, YFP-RGA, and RGA52-YFP to nuclear bodies co-occupied by DsRED-COP1-HA in the presence of c-myc-SPA1 (Fig. 3D, Fig. S4A).

### **COP1/SPA1 forms a ternary complex with DELLA.**

The formation of a ternary complex was evidenced by bimolecular fluorescence complementation (BiFC) assays in leaves of *N. benthamiana*, in which the co-localization of signals from mRFP-SPA1 and the reconstituted YFP, due to the interaction between YFC-DELLAs and YFN-COP1, was evident in nuclear bodies (Fig. 3E, Fig. S4B). Similarly, YFP signal in nuclear bodies was observed by co-expressing c-myc-SPA1 (Fig. S4C). However, no YFP fluorescence was detected in the absence of SPA1 or when YFC was fused to Del2GAI, a truncated version of GAI that does not interact with SPA1 (Fig. 3E, Fig. S4B-E). As expected, mRFP-SPA1 was recruited to nuclear bodies when co-expressed with YFN-COP1 (Fig. 3E, Fig. S4B) (Seo et al., 2003).

To quantify the interaction between GAI or RGA and the COP1-SPA1 complex we expressed these proteins tagged to fluorescent reporters in mammalian cells. This orthogonal system allows to perform such studies with the components of interest, in the absence of other plant proteins that might interfere with the evaluation. The fluorescence from DELLA-mCherry fusions in the cytosol and nucleus was relatively homogeneous when either GAI or RGA were expressed alone (Fig. 3F; note the ratio of fluorescence between different nuclear regions close to 1 in Fig. 3G). However, the ratio between DELLA fluorescence inside / outside the speckle-like structures formed in the nucleus by the COP1-

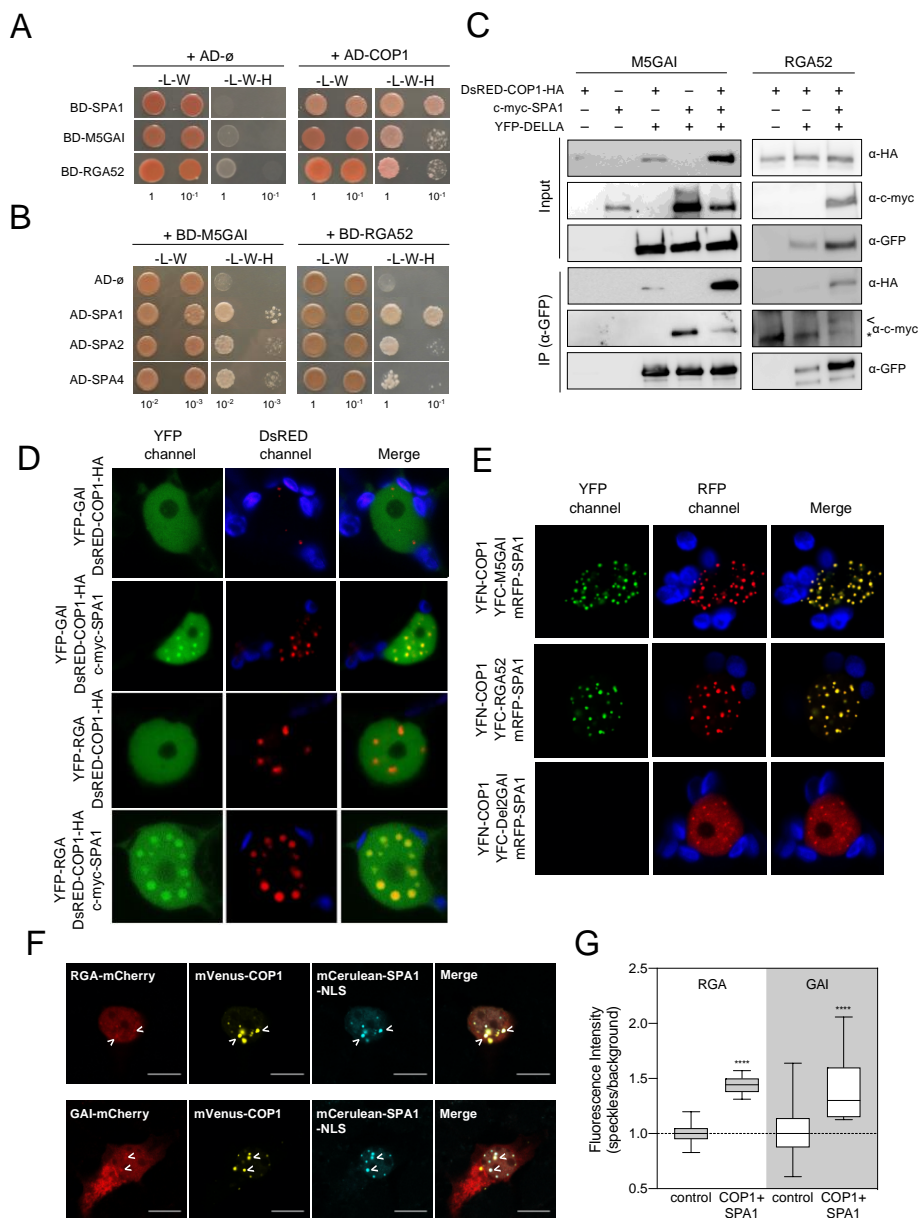


**Fig. 3. COP1 physically interacts with DELLA proteins.** (A-B) Y2H assays showing the interaction between N-terminal deleted versions of GAI and RGA with COP1 (A) and SPAs (B). L, leucine; W, tryptophan; H, histidine. Numbers indicate the dilutions used in the drop assay. (C) Co-immunoprecipitation assays showing interactions in planta. YFP-M5GAI and YFP-RGA52 were transiently expressed in leaves of *N. benthamiana* together with DsRED-COP1-HA, c-myc-SPA1 or both. Proteins were immunoprecipitated with anti-GFP antibody-coated paramagnetic beads. Leaves expressing DsRED-COP1-HA or c-myc-SPA1 alone were used as negative controls. The arrowhead and asterisk mark the co-immunoprecipitated c-myc-SPA1 and a non-specific band, respectively. (D) YFP-GAI and YFP-RGA co-localize with DsRED-COP1-HA in nuclear bodies in the presence of c-myc-SPA1. Fusion proteins were transiently expressed in

leaves of *N. benthamiana* and observed by confocal microscopy. One representative nucleus is shown. (E) BiFC assay showing that COP1 and SPA1 form a complex with M5GAI or RGA52 in nuclear bodies. The indicated proteins were expressed in leaves of *N. benthamiana* and observed by confocal microscopy. One representative nucleus is shown. (F) Representative HEK-293T cells co-transfected with mVenus-COP1, NLS-mCerulean-SPA1 and either GAI-mCherry or RGA-mCherry. Scale bar represents 10  $\mu\text{m}$ . The arrowheads point to two representative speckles co-occupied by DELLAs, SPA1 and COP1. (G) Fluorescence intensities of GAI-mCherry and RGA-mCherry in control cells and in cells co-expressing mVenus-COP1 and mCerulean-SPA1-NLS from 10-13 transfected cells. Asterisks indicate that the difference is statistically significant with the control condition (Student's *t* test, \*\*\*\*  $P < 0.0001$ ).

SPA1 complex was above 1 (Fig. 3F and G, Fig. S5), suggesting that the COP1-SPA1 complex drags RGA and GAI to the speckles by physical interaction. Taken together, these observations demonstrate that the COP1-SPA1 complex interacts with DELLA proteins.

### **COP1 ubiquitinates GAI and RGA *in vitro*.**

*In vivo* levels of ubiquitinated GFP-RGA were enhanced by over-expression of COP1 (Fig. S6). To test whether this is the result of the direct interaction between COP1 and DELLAs, we performed an *in vitro* ubiquitination assay using recombinant MBP-COP1 and 6xHis-M5GAI or 6xHis-RGA52. A slow-migrating band corresponding to the size of Ub-6xHis-M5GAI or Ub-6xHis-RGA52 was observed only when MBP-COP1 and the E2 enzyme were included in the assays (Fig. 4A and B). The delayed band did not appear, however, when  $\text{Zn}^{2+}$  ions, which are required for the proper arrangement of the RING domain of E3 ubiquitin ligases like COP1 (Von Arnim and Deng, 1993), were excluded from the reaction mixtures (Fig. 4A and B). To confirm that the slow migration of 6xHis-M5GAI and 6xHis-RGA52 is due to ubiquitination, we repeated the assay for 6xHis-M5GAI in the presence of HA-tagged ubiquitin. We detected low-migrating bands in the immunoblot with anti-GAI antibody when free ubiquitin was included in the assay, which were further upshifted when we used the HA-tagged version of ubiquitin instead (Fig. 4C). This result indicates that M5GAI and RGA52 are targets of the E3 ubiquitin ligase activity of COP1 *in vitro*.

### **COP1 controls hypocotyl elongation in a DELLA-dependent manner.**

The growth phenotypes caused by GA deficiency or *cop1* mutations in the dark (Deng et al., 1991; Von Arnim and Deng, 1993; Hoecker and Quail, 2001; Alabadí et al., 2004; Gallego-Bartolomé et al., 2012), in response to light cues from neighbors (Djakovic-Petrovic et al., 2007; Pacín et al., 2013) or to warm temperature (Stavang et al., 2009; Delker et al., 2014; Park et al., 2017b) are very similar. To determine the physiological relevance of the regulation of DELLA levels by COP1, we studied how mutations at *COP1* and *DELLA* genes

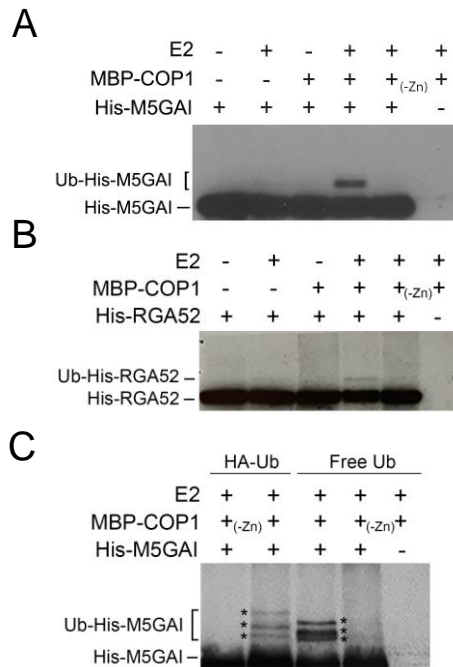


**Fig. 4. COP1 ubiquitinates GAI and RGA.** (A, B) 6xHis-M5GAI (A) and 6xHis-RGA52 (B) ubiquitination assay using recombinant MBP-COP1, rice E2 and unmodified ubiquitin. (C) 6xHis-M5GAI ubiquitination assay using unmodified and HA-tagged ubiquitin. Modified and unmodified 6xHis-M5GAI and 6xHis-RGA52 were detected with anti-GAI and anti-6xHis antibodies, respectively.

and GA-treatments impact on the hypocotyl growth rate of dark-grown seedlings transferred to light at 20 °C (de-etiolation) as well as light-grown seedlings transferred to shaded or warm environments. Noteworthy, the patterns differed between the first case, where DELLA levels build up, and the other two cases, where DELLA levels decrease (Fig. 1E). In fact, during de-etiolation, growth in the presence of 5  $\mu$ M GA<sub>4</sub> promoted the rate of hypocotyl elongation in seedlings transferred to the light but not in seedlings that remained in the dark, suggesting that endogenous GA levels are not limiting in darkness (Fig. 5). As expected, the *cop1* mutants showed reduced growth in darkness; however, they retained a significant growth response to light. This response was only marginally enhanced by adding GA<sub>4</sub> or by the *gai-td1* and *rga-29* (Cagnola et al., 2018) mutations of DELLA genes. In other words, during de-etiolation, the rapid inactivation of COP1 does not appear to be rate limiting for the RGA accumulation (Fig. 1E) or the growth inhibition (Fig. 5) responses. Addition of 5  $\mu$ M GA<sub>4</sub> promoted growth in light-grown seedlings transferred to shade or to warm temperature (Fig. 5), suggesting that GA signalling is limiting under those

conditions. The *cop1-4* and *cop1-6* mutants failed to respond to shade or warm temperatures, but the responses were restored both the application of GA<sub>4</sub> and by the presence of mutations of both *DELLA* genes. This indicates that the responses were limited by the elevated levels of DELLAs in *cop1* and reducing the DELLA pool either genetically or by the GA treatment was enough to rescue the *cop1* phenotype.

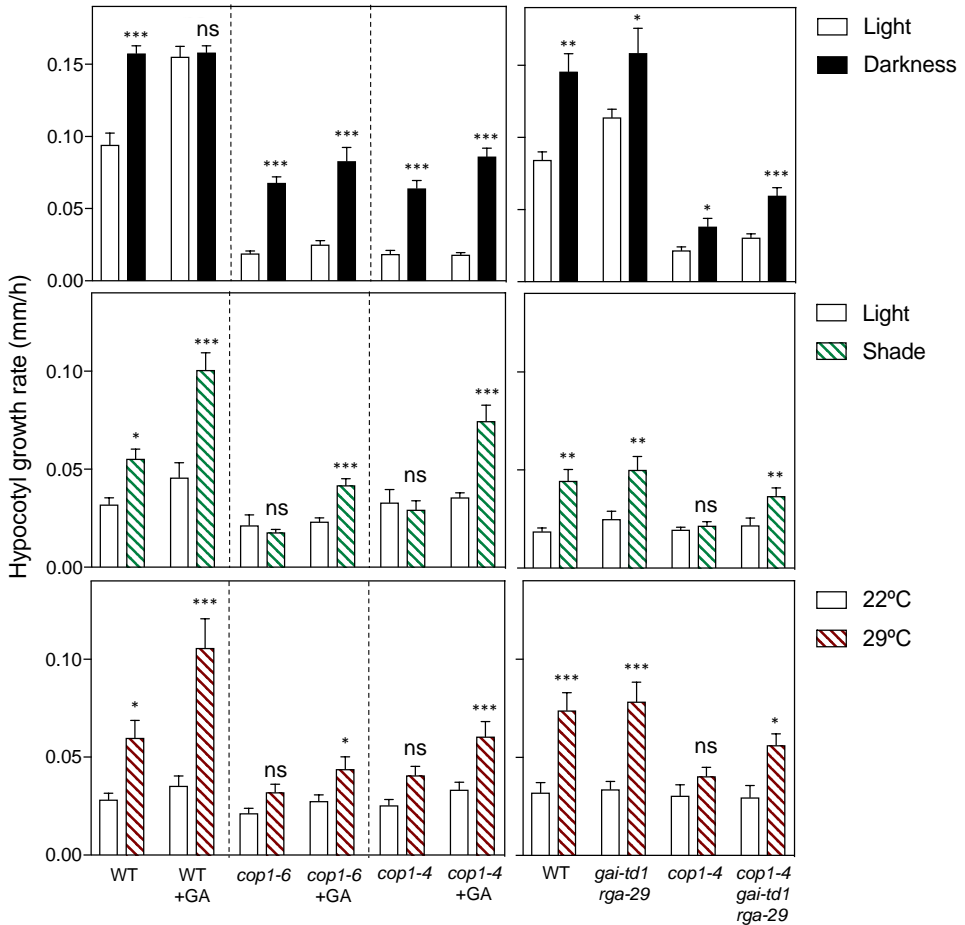


**Fig. 5. COP1 regulates the rate of hypocotyl elongation in response to shade and warm temperature in a DELLA-dependent manner.** Bars indicate the hypocotyl growth rate of seedlings of the indicated genotypes during de-etiolation or after transfer to shade or 28 °C measured over a period of 9 h. Where indicated, seedlings were germinated and grown in the presence of 5  $\mu$ M GA<sub>4</sub>. Values correspond to the mean and SE of 8 (light treatments) or 24 (temperature treatments) replicate boxes; 10 seedlings were averaged per box replicate. Asterisks indicate that the difference is statistically significant with the control condition (Student's *t* test, \*  $P < 0.05$ , \*\*  $P < 0.01$ , \*\*\*  $P < 0.005$ ; ns, non-significant).

### 3. Discussion

The results presented here establish a functional link between DELLA proteins and COP1, two of the major hubs in the control of plant architecture. The growth of the hypocotyl of *Arabidopsis* shifted from light at moderate temperatures to either warm or shade conditions requires COP1 only if DELLA proteins are present (Fig. 5). These environmental cues reduce phyB activity (Casal, 2013; Legris et al., 2016; Jung et al., 2016) and enhance COP1 nuclear abundance (Fig. 1D), while reducing the levels of RGA in a COP1-dependent manner (Fig. 1E). COP1 does not simply reduce DELLA protein abundance by increasing GA levels. First, COP1 migrates to the nucleus and mediates RGA degradation in response to warm temperature well before increasing GA levels (Fig. 1F-H, Fig. S2C). Similarly, simulated shade takes more than 4 h to modify GA levels (Bou-Torrent et al., 2014) whilst already causing large COP1-mediated effects on RGA at 2 h (Fig. 1E). Second, warm temperature or shade reduce the abundance of RGA in the presence of saturating levels of a GA synthesis inhibitor (Fig. 1A). Third, warm temperature or shade reduce the abundance of the mutant protein *rga-Δ17*, which cannot be recognized by GID1 (Willige et al., 2007) and is fully insensitive to GA (Fig. 1B and C, Fig. S2). The latter effects require COP1, providing evidence for a branch of COP1 action on DELLA that does not involve activating the canonical GA/GID1 pathway.

COP1 effects on RGA and *rga-Δ17* depend on the 26S proteasome (Fig. 2). Taking into account the well-established role of COP1 in E3-ligase complexes that ubiquitinate and target to proteasomal degradation proteins involved in environmental signalling (Lau and Deng, 2012), the simplest interpretation of the above observations is that COP1 directly regulates DELLA protein stability. Different results lend support to this hypothesis. First, RGA and GAI interact with COP1 and its complex partner SPA1 in yeast (Fig. 3A and B) and in planta (Fig. 3C). Second, COP1, SPA1 and GAI or RGA form a tertiary complex in mammalian and plant cells, and this complex is present in nuclear bodies (Fig. 3D-G, Fig. S4A-C and Fig. S5). Third, COP1 ubiquitinates RGA and GAI *in vitro* (Fig. 4) and the levels of ubiquitinated RGA *in vivo* are enhanced by COP1 (Fig. S6).

Tight regulation of abundance is a common feature of proteins that act as signalling hubs in mammals (Love and Grossman, 2012) and in yeast (Batada et al., 2006). Post-translational modifications (Conti et al., 2014; Zentella et al., 2016, 2017) and interaction with other transcriptional regulators (Yang et al., 2012; Crocco et al., 2015) modulate DELLA activity. However, the mechanism reported here is unique. In contrast to previously reported modes

of regulation of DELLA abundance, which converge to control its stability via GA/GID1, the rapid COP1-mediated regulation occurs by a mechanism that acts in parallel to the canonical GA/GID1 pathway.

COP1 might represent an ancient regulatory mechanism of control of DELLA levels, preceding the acquisition of the GA/GID1 system because the GA/GID1 system appears in lycophytes (Yasumura et al., 2007), whilst orthologs of COP1 and DELLA proteins are already present in the genome of the liverwort *Marchantia polymorpha* (Bowman et al., 2017). However, in Arabidopsis, these two pathways appear to operate in concert. Blocking GA synthesis with PAC reveals that the canonical pathway makes a negligible direct contribution to the rapid changes in RGA abundance in response to warmth or shade (Fig. 1A and H), simply because by the time GA levels increase, the COP1 pathway has already acted (Fig. 1F and G, Fig. S2C). However, the GA-pathway has a large effect in a developmental time scale, as demonstrated by the massive accumulation of RGA in the GA-deficient mutant *ga1* (Silverstone et al., 2001; Stavang et al., 2009) or the GA-insensitive version *rga-Δ17* (Fig. 1B) (Dill et al., 2001). Although *rga-Δ17* retains the COP1-mediated response (Fig. 1C, Fig. S2B), this effect is no longer rapid (Fig. S2D and E), consistently with the lack of rapid changes in RGA levels in response to warmth in the *ga1* mutant (Stavang et al., 2009). This indicates that the GA-pathway sets the sensitivity to the COP1 pathway. Co-existence of the COP1- and GA-dependent regulation would provide the advantage of a faster and tunable adjustment to the suddenly fluctuating cues of the natural environment.

## 4. Material and methods

### Plant material.

Mutants and transgenic lines used in this study that have been described previously: *cop 1-4* (Deng and Quail, 1992), *cop 1-6* (McNellis et al., 1994), *gai-td1* (Plackett et al., 2014), *rga-29* (Park et al., 2017a), *cop 1-4 gai-td1 rga-29* (Cagnola et al., 2018), *pRGA:GFP-RGA* (Silverstone et al., 2001), *pRGA:GFP-RGA cop 1-4* (Cagnola et al., 2018), *35S:YFP-COP1 cop 1-4* (Oravec et al., 2006), *pRGA:GFP-(rga-Δ17)* (Dill et al., 2001) and *35S:TAP-COP1* (Rubio et al., 2005). The *pRGA:GFP-(rga-Δ17) cop 1-4* line and the *35S:TAP-COP1 pRGA:GFP-RGA* double transgenic was prepared by genetic crosses.

## Confocal microscopy in Arabidopsis.

Seeds were sown in 0.8% agar/water and stratified at 4 °C and darkness for 3-5 days. For the de-etiolation experiments, germination was induced with a 2 h-light treatment. For confocal imaging during de-etiolation, seedlings were grown in darkness for three days and were treated on the fourth day with white light (100  $\mu\text{mol m}^{-2} \text{s}^{-1}$ , red/far-red=1). For shade treatment, 1 day after seed germination, seedlings were grown for 2 days under a 10 h light:14 h dark photoperiod (white light 100  $\mu\text{mol m}^{-2} \text{s}^{-1}$ , red:far-red= 1). One hour after the beginning of the third day seedlings were shaded with two green filters (LEE #089) following our established protocol in previous shade experiments (Pacín et al., 2013). For the temperature treatment, seedlings were grown for three days at 20 °C in continuous white fluorescent light (25  $\mu\text{mol m}^{-2} \text{s}^{-1}$ ). The fourth day plants were transferred to a chamber at 28 °C with the same lighting conditions, following our established protocol in previous temperature experiments (Stavang et al., 2009). When indicated, either paclobutrazol (a GA biosynthesis inhibitor; final concentration 0.1, 1, 10 or 100  $\mu\text{M}$ ) or MG132 (final concentration 100  $\mu\text{M}$ ) were respectively added 8 h or 3 h before starting the application of the 28 °C or shade treatments, and confocal fluorescence images of *pRGA:GFP-RGA* were taken 4 h after the application of these treatments. In kinetics experiments, confocal fluorescence images of *35S:YFP-COP1 cop 1-4* and of *pRGA:GFP-RGA* in the wild-type and *cop 1-4* backgrounds were taken at the indicated exposures to the treatments. In experiments including the *pRGA:GFP-(rga-Δ17)* line, all confocal fluorescence images were taken after 3 days of treatment because saturating levels of the GFP-(*rga-Δ17*) fluorescence signal precluded the detection of fast changes. In some of the experiments including the *pRGA:GFP-(rga-Δ17)* line, GA<sub>4</sub> (final concentration 3  $\mu\text{M}$ ) was applied to seedlings grown at 20 °C in continuous white fluorescent light (25  $\mu\text{mol m}^{-2} \text{s}^{-1}$ ). Confocal fluorescence was obtained with an LSM 5 Pascal Zeiss microscope with a water-immersion objective lens (C–Apochromat 40X/1.2; Zeiss). GFP/YFP were excited with an Argon laser (488nm) and fluorescence was detected at 505-530 nm. Fluorescence intensity was measured using ImageJ. Images were taken from the epidermis and first sub-epidermal cell layers in the upper third part of the hypocotyl. Each fluorescence intensity value in a given sample was normalized by the average fluorescence in that particular sample. In the figures where shade and 28 °C conditions are compared to a control, data were further normalized to the corresponding control condition. Chloroplasts autofluorescence was detected between 675 and 760 nm.



**Western analysis of GFP-RGA and GFP-(*rga-Δ17*).**

To detect the GFP fusions in hypocotyls, seedlings of wild-type Ler, *pRGA:GFP-RGA*, and *pRGA:GFP-(rga-Δ17)* were grown for seven days in continuous white fluorescent light ( $25 \mu\text{mol m}^{-2} \text{s}^{-1}$ ) at 20 °C or 28 °C. Hypocotyls were excised and flash frozen in liquid nitrogen. Total proteins were extracted from frozen tissue powder prepared from 20-30 hypocotyls in 1 volume of 2x Laemmli buffer, boiled at 95 °C for 5 min and clarified by centrifugation at 4 °C. Proteins were quantified using the RC DC Protein Assay (Bio-Rad). Thirty  $\mu\text{g}$  of proteins were separated in an 8% SDS-PAGE, transferred to a PVDF membrane (Life Technologies) and probed with an anti-GFP antibody (JL-8, 1:5000; Clontech). The membrane was stripped out and probed with anti-DET3 that was used to check loading. Chemiluminescence was detected with SuperSignal<sup>TM</sup> West Femto (Thermo-Fisher Scientific) and imaged with the LAS-3000 imager (Fujifilm).

**Real-time qPCR.**

Arabidopsis seedlings of *pRGA:GFP-RGA* and *pRGA:GFP-(rga-Δ17)* lines were grown for seven days in continuous white fluorescent light ( $25 \mu\text{mol m}^{-2} \text{s}^{-1}$ ) at 20 °C or 28 °C. Hypocotyls were excised and flash frozen in liquid nitrogen. RNA was extracted with the RNeasy Plant Mini Kit (Qiagen). cDNA was prepared from 1  $\mu\text{g}$  of total RNA with PrimeScript<sup>1st</sup> Strand cDNA Synthesis Kit (Takara Bio Inc). PCR was performed in a 7500 Fast Real-Time PCR System (Applied Biosystems) with SYBR premix ExTaq (Tli RNaseH Plus) Rox Plus (Takara Bio Inc). *RGA* was amplified using described primers (Gallego-Bartolomé et al., 2010). Expression levels were normalized to *EF1 $\alpha$*  (Frigerio et al., 2006).

**Gibberellin quantification.**

Seedlings were grown and harvested as described for confocal microscopy experiments with temperature treatments. The ground tissue (about 150 mg of frozen seedlings) was suspended in 80% methanol-1% acetic acid containing internal standards and mixed by shaking for one hour at 4 °C. The extract was kept a -20 °C overnight and then centrifuged and the supernatant dried in a vacuum evaporator. The dry residue was dissolved in 1% acetic acid and passed consecutively through a reverse phase column Oasis HLB (30 mg, Waters) and a cationic exchange Oasis MCX eluted with MeOH, as described elsewhere (Seo et al., 2011). The final residues were dried and dissolved in 5% acetonitrile-1% acetic acid and the hormones were separated by UHPLC with a reverse Accucore C18 column

(2.6  $\mu\text{m}$ , 100 mm length; Thermo Fisher Scientific) with a 2 to 55% acetonitrile gradient containing 0.05% acetic acid, at 400  $\mu\text{L}/\text{min}$  over 21 min. The hormones were analysed with a Q-Exactive mass spectrometer (Orbitrap detector; ThermoFisher Scientific) by targeted Selected Ion Monitoring (tSIM; capillary temperature 300°C, S-lens RF level 70, resolution 70.000) and electrospray ionization (spray voltage 3.0 kV, heater temperature 150°C, sheath gas flow rate 40  $\mu\text{L}/\text{min}$ , auxiliary gas flow rate 10  $\mu\text{L}/\text{min}$ ) in negative mode. The concentration of GA<sub>4</sub> in the extracts was determined using embedded calibration curves and the Xcalibur 4.0 and TraceFinder 4.1 SP1 programs. The internal standards for quantification were the deuterium-labeled hormones (OIChemim Ltd).

### **Degradation assays in *Nicotiana benthamiana*.**

The *GFP* CDS was cloned into pDONR207 (Thermo-Fisher Scientific) by a BP reaction (Thermo-Fisher Scientific). To prepare an entry vector with *rga-Δ17*, the CDS was amplified by PCR from a cDNA pool obtained from *pRGA:GFP-(rga-Δ17)* seedlings (Dill et al., 2001) and cloned into pDONR207. The pENTR201-RGA was obtained from the Regia collection (Paz-Ares et al., 2002). The *COP1* CDS was transferred to pEarleyGate202 (Earley et al., 2006) to create a Flag-COP1 fusion; *GFP*, *RGA*, and *rga-Δ17* CDSs were transferred to pEarleyGate201 to introduce an HA in the N-terminus of each protein; in all cases transfer to the destination vector was done by LR reaction. A pCambia-based binary vector expressing DsRED-COP1-HA under the control of the 35S promoter was also prepared by GoldenBraid (Vazquez-Vilar et al., 2017). Leaves of one-month-old *N. benthamiana* plants grown under 16 h light:8 h dark photoperiod at 25 °C were infiltrated with the different mixtures of *Agrobacterium tumefaciens* GV3101 cells carrying the vectors and the p19 silencing suppressor. Leaves were harvested at dawn of the fourth day and frozen in liquid nitrogen. For temperature experiments, *N. benthamiana* plants were grown as above and transferred to 22 °C and continuous white light (LL; 100  $\mu\text{mol m}^{-2} \text{s}^{-1}$ ) for three days after infiltration or to 30 °C and LL for the last 24 h. For MG132 treatments leaves were infiltrated with a solution of 25  $\mu\text{M}$  of the inhibitor 8 h before sampling. To determine protein levels, samples were homogenized with 3 volumes of 2x Laemmli buffer and boiled at 95 °C for 5 min. Samples were then clarified by centrifugation at room temperature and analysed by Western blot as described above. Fusion proteins were detected by HRP-conjugated Flag M2 antibody (1:2000; Sigma) and anti-HA-HRP antibody (3F10, 1:2000; Roche). Chemiluminescence was detected with the SuperSignal™ West Pico substrate

(Thermo-Fisher Scientific) and imaged with a UVP ChemiDoc imaging system (UVP, LLC). The VisionWorksLS (UVP, LLC) software was used to quantify protein levels.

### **Yeast two-hybrid assays.**

The Y2H Gateway™-adapted vectors pGBKT7 and pGADT7 were used. The *M5GAI*, *RGA52* and *Del2GAI* CDS cloned in pGBKT7 have been described (Gallego-Bartolomé et al., 2012). A pENTR-COP1 vector was prepared by cloning the *COP1* coding sequence (CDS) in the pCR8/GW/TOPO vector (Thermo-Fisher Scientific). Entry vectors for *SPA1*, *SPA2* and *SPA4* were prepared by cloning their CDS in pENTR-3C (Thermo-Fisher Scientific). *COP1*, *SPA1*, *SPA2*, and *SPA4* CDSs were transferred to the pGADT7 vector by an LR reaction (Thermo-Fisher Scientific). The yeast strains Y2HGold and Y187 (Takara Bio Inc) were transformed with the constructs in pGBKT7 and pGADT7 vectors, respectively. Interaction assays were performed in diploid cells obtained by mating and grown in selection media.

### **Co-immunoprecipitation.**

*35S:YFP-M5GAI* and *35S:YFP-RGA52* were prepared by transferring the *M5GAI* and *RGA52* CDSs from pCR8/GW/TOPO-M5GAI and pCR8/GW/TOPO-RGA52 (Gallego-Bartolomé et al., 2012) to the pEarleyGate104 vector (Earley et al., 2006). The CDS of *SPA1* was transferred by LR reaction to the pEarleyGate203 (Earley et al., 2006) to prepare the fusion c-myc-SPA1. The *35S:DsRED-COP1-HA* construct was used to express recombinant COP1. Leaves of one-month-old *N. benthamiana* plants grown under 16 h light:8 h dark photoperiod at 25 °C were infiltrated with the different mixtures of *A. tumefaciens* C58 cells carrying the vectors and the p19 silencing suppressor. Leaves were infiltrated with a solution containing 50 µM MG132 (Calbiochem) and 10 mM MgCl<sub>2</sub> 12 h before harvesting. Leaves were harvested at dawn of the fourth day and frozen in liquid nitrogen. Approximately 1 mL of ground, frozen tissue was homogenized in 0.5 mL of extraction buffer (25 mM Tris-HCl pH 7.5, 10% glycerol, 1 mM EDTA pH 8.0, 150 mM NaCl, and 1x protease inhibitor cocktail [cOmplete, EDTA-free; Roche]). Extracts were kept on ice for 15 min and cell debris was removed by centrifugation at maximum speed in a benchtop centrifuge at 4 °C twice. Total proteins were quantified by Bradford assay. One hundred and sixty µg of total proteins were denatured in Laemmli buffer and set aside to be used as input. Eight hundred µg of total protein in 1 mL of extraction buffer were incubated with 50 µL of anti-GFP-coated paramagnetic beads (Miltenyi) at 4 °C for 2 h in a rotating wheel. Extracts were loaded into µColumns (Miltenyi) at room temperature. Columns were washed four times

with 200  $\mu\text{L}$  of cold extraction buffer and proteins were eluted under denaturing conditions in 70  $\mu\text{L}$  of elution buffer following manufacturer instructions. Sixty-three  $\mu\text{L}$  of the immunoprecipitated samples (90%) were loaded in a 12% SDS-PAGE along with 60  $\mu\text{g}$  of input. Proteins were transferred to a PVDF membrane and sequentially immunodetected with an anti-HA-HRP antibody (3F10, 1:5000; Roche) and, after strip-out, with an anti-c-myc antibody (9E10, 1:1000; Roche). The remaining 10% of the immunoprecipitated samples along with 60  $\mu\text{g}$  of input were processed in the same way but immunodetected with an anti-GFP antibody (JL-8, 1:5000; Clontech). Chemiluminescence was detected with SuperSignal™ West Femto (Thermo-Fisher Scientific) and imaged with the LAS-3000 imager (Fujifilm).

### **Co-localization assays in *N. benthamiana*.**

pCambia-based binary vectors expressing RGA52-YFP alone or with DsRED-COP1-HA under the control of the 35S promoter were prepared by GoldenBraid (Vazquez-Vilar et al., 2017). 35S:YFP-GAI was described previously (Gallego-Bartolomé et al., 2011). The RGA CDS was transferred by LR reaction to pEarleyGate104 to prepare a YFP-RGA fusion. Leaves of one-month-old *N. benthamiana* plants grown under 16 h light:8 h dark photoperiod at 25 °C were infiltrated with the different mixtures of *A. tumefaciens* C58 cells carrying the vectors and the p19 silencing suppressor. Leaves were infiltrated with a solution containing 50  $\mu\text{M}$  MG132 and 10 mM  $\text{MgCl}_2$  12-16 h before imaging by confocal microscopy (Zeiss 780 Axio Observer) with a water-immersion objective lens (C-Apochromat 40X/1.2; Zeiss) the fourth day after infiltration. YFP was excited with an Argon laser (488 nm) and detected at 520-560 nm. DsRED was excited the DPSS 561-10 laser (561 nm) and detected at 580-650 nm. Samples were kept in darkness on the day of imaging. Fluorescence from YFP was detected between 520-560 nm, and fluorescence from DsRED between 580 and 650 nm. Chloroplasts autofluorescence was detected between 675 and 760 nm.

### **Bimolecular fluorescence complementation.**

The pCR8/GW/TOPO-Del2GAI has been described (Gallego-Bartolomé et al., 2012). The M5GAI, RGA52, RGA, and Del2GAI CDSs were transferred to the pMDC43-YFC (Belda-Palazón et al., 2012) vector, while the COP1 CDS was transferred to pMDC43-YFN (Belda-Palazón et al., 2012). The CDS of SPA1 was transferred by LR reaction to the pUBQ10-mRFP (Grefen et al., 2010) to prepare the fusion mRFP-SPA1. Leaves were infiltrated, treated and imaged as described for co-localization assays. *A. tumefaciens* cells carrying the

p19 silencing suppressor were not included in the mixtures. YFP fluorescence was detected as described above. mRFP fluorescence was detected as described for DsRED.

### **Co-localization assays in mammalian cells.**

The list of oligonucleotides and details for vector construction are in Supplemental Tables 1 and 2, respectively. Human embryonic kidney cells (HEK-293T, ATCC CRL-11268), were maintained in Dulbecco's modified Eagle's medium (PAN, cat. no. P04-03550) supplemented with 10% fetal calf serum (FCS, PAN, cat. no. P30-3602) and 1% penicillin/streptomycin (PAN, cat. no. P06-07100). For confocal imaging, cells were seeded onto glass coverslips placed in cell culture wells. For transfection, 40,000 cells per well of a 24-well plate, were transfected using polyethylenimine (PEI, linear, MW: 25 kDa, Polyscience) as described elsewhere (Müller et al., 2013). The medium was exchanged 5 h post transfection. In co-transfections, all plasmids were transfected in equal amounts (weight-based). For confocal imaging, cells on glass coverslips were fixed with 4% PFA for 10 min on ice followed by 10 min at room temperature. Subsequently, cells were washed once with ice-cold PBS. Coverslips were embedded in Mowiol 4-88 (Roth) containing 15 mg mL<sup>-1</sup> 1,4-diazabicyclo[2.2.2]octane (DABCO, Roth) and mounted onto glass microscope slides as described (Beyer et al., 2015). Cells were imaged with a confocal microscope (Nikon Instruments Eclipse Ti with a C2plus confocal laser scanner, 60x oil objective, NA = 1.40). mCherry, mVenus and mCerulean were visualized using excitation lasers of 561, 488, 405 nm and emission filters of 570–620, 535–550, 425–475 nm, respectively.

### **Analysis of confocal images of mammalian cells.**

Image acquisition, analysis and processing were performed with Fiji. The workflow for data analysis is as follows. The mVenus-COP1 channel image was duplicated and adjusted with a low threshold to only mark speckles as regions of interest. Then, the measurement was set to redirect to the DELLA-mCherry channel image. Particles of a size between 100–15,000 square pixels and of any shape were analysed for their mean fluorescence intensity given in absolute gray values. Additionally, 5 random areas outside of the speckles in the nucleus of each cell were analysed for their mean fluorescence intensity in the DELLA channel and the mean background fluorescence intensity was calculated. The ratio (DELLA speckle – DELLA background)/DELLA background was calculated for each speckle with the respective background. The mean ratio per cell was calculated. Outlier determination was performed using the quartile method, i.e. values smaller than  $Q1 - 1.5(Q3 - Q1)$  or larger than

Q3+1.5(Q3-Q1) were excluded in each condition (with or without mCerulean-SPA1-NLS). The co-localization assays in mammalian cells and the corresponding analysis of confocal images were performed by Nicole Heuckenf and Tim Blomeier in the lab of Matías D. Zurbriggen (University of Düsseldorf, Germany).

### **Pull-down assays with p62-beads.**

Wild-type Col-0, *pRGA:GFP-RGA* and *pRGA:GFP-RGA 35S:TAP-COP1* seedlings were grown for five days at 20 °C in continuous white light (25  $\mu\text{mol m}^{-2} \text{s}^{-1}$ ) and then temperature was shifted to 28 °C for 8 h under the same lighting condition. Seedlings were treated with 50  $\mu\text{M}$  MG132 during the high-temperature treatment. Proteins were extracted in buffer BI [50 mM Tris-HCl, pH 7.5, 20 mM NaCl, 0.1% Nonidet P-40, and 5 mM ATP, 1 mM PMSF, 50  $\mu\text{M}$  MG132, 10 nM Ub-aldehyde, 10 mM N-ethylmaleimide, and plant protease inhibitor cocktail (Sigma-Aldrich)] before incubation with pre-washed p62 agarose (Enzo Life Sciences) or the agarose alone at 4 °C for 4 h. Beads were washed twice in BI buffer and once with BI buffer supplemented with 200 mM NaCl. Proteins were eluted in Laemmli buffer at 100 °C. The eluted proteins were separated by SDS-PAGE and analysed by immunoblotting using anti-UBQ (1:1000; Enzo Life Sciences) or anti-GFP antibodies (JL-8, 1:5000; Clontech).

### **In vitro ubiquitination assay.**

Assays were performed as previously reported (Yu et al., 2008) with minor modifications. Ubiquitination reaction mixtures contained 50 ng yeast E1 (Boston Biochem), 50 ng rice 6xHis-Rad6 E2 (Yamamoto et al., 2004), 10  $\mu\text{g}$  HA-labelled or 10  $\mu\text{g}$  unlabelled ubiquitin (Boston Biochem), and 2  $\mu\text{g}$  MBP-COP1 (previously incubated with 20  $\mu\text{M}$   $\text{ZnCl}_2$ ) in 30  $\mu\text{L}$  of reaction buffer (50 mM Tris pH 7.5, 5 mM  $\text{MgCl}_2$ , 2 mM ATP and 0.5 mM DTT). As a substrate, 50 ng of 6xHis-M5GAI or 6xHis-RGA52 fusions were used per reaction. After 2 h incubation at 30 °C, reaction mixtures were stopped by adding 30  $\mu\text{L}$  of Laemmli buffer, and a half of the mixtures (30  $\mu\text{L}$ ) were boiled for 5 min and separated by 7.5% SDS-PAGE. 6xHis-M5GAI and 6xHis-RGA52 were detected using anti-GAI (Piskurewicz et al., 2008) (1:10000) and anti-6xHis (Sigma) antibodies, respectively.

### **Growth assays.**

Seeds were sown in 0.8% agar/water with or without 5  $\mu\text{M}$   $\text{GA}_4$  and stratified at 4 °C and darkness for 3-5 days. For the de-etiolation experiments, germination was induced with a 2

h-light treatment. On the day of treatment plants were imaged with a digital camera before the beginning and after the end of the 9 h-treatment and hypocotyl elongation during this period was measured with image processing software (Pacín et al., 2013). Treatments were as described for confocal imaging. Seedlings kept in darkness, unshaded or at 20 °C were used as controls of the respective treatments.

## Acknowledgements

We thank Drs Isabel Lopez-Diaz and Esther Carrera for the gibberellin quantification carried out at the Plant Hormone Quantification Service (IBMCP, Valencia, Spain) and Luís López-Molina (University of Geneva, Geneva, Switzerland) and Karin Schumacher (University of Heidelberg, Heidelberg, Germany) for the anti-GAI and anti-DET3 antibodies, respectively. We also thank Salomé Prat and all members of the SIGNAT consortium for helpful discussions about this work. This work was supported by the Spanish Ministry of Economy, Industry and Competitiveness and AEI/FEDER/EU (grants BIO2016-79133-P to DA; BIO2013-46539-R and BIO2016-80551-R to VR), the European Union SIGNAT-Research and Innovation Staff Exchange (grant H2020-MSCA-RISE-2014-644435 to MAB, DA and JJC), the Argentinian Agencia Nacional de Promoción Científica y Tecnológica (grant PICT-2016-1459 to JJC), Universidad de Buenos Aires (grant 20020170100505BA to JJC), the National Institute of General Medical Sciences of the National Institutes of Health (award numbers RO1GM067837 and RO1GM056006 to SAK), by the German Research Foundation (DFG) under Germany's Excellence Strategy/Initiative (CEPLAS – EXC-2048/1 – Project ID 390686111 to MDZ), by the International Max Planck Research School (IMPRS) of the Max Planck Society, the University of Düsseldorf and Cologne to TB, and NRW-BioSC-FocusLabs CombiCom to NH and MDZ, and MEYS of the Czech Republic (project LQ1601 CEITEC 2020 to BB and MC). NB-T, EI and MG-L were supported by MINECO FPI Program fellowships.

## 5. Supplemental information

Oligonucleotides used for cloning in mammalian expression plasmids as well as the plasmids used for expression in mammalian cells are shown in Supplemental Tables 1 and 2, respectively. Both tables are available on the following website (Password: NBTVALENCIA2020): <http://plasticity.ibmcp.csic.es/downloads.html>

Supplemental figures (Figs. S1 to S6) are shown below:

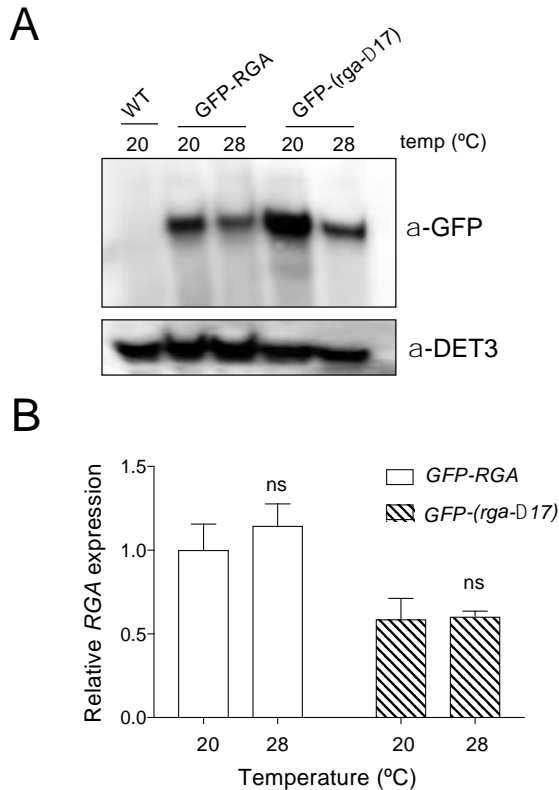


**Fig. S1. The GA-resistant *rga-Δ17* is regulated post-translationally by warm temperature.** (A) Western analysis of GFP-RGA and GFP-(*rga-Δ17*) in hypocotyls of seedlings grown in continuous light at 20 °C or 28 °C. Membrane was sequentially probed with anti-GFP and anti-DEET3 antibodies. (B) RGA expression in hypocotyls was analysed by RT-qPCR. Data correspond to mean and standard deviation from three technical replicates. The analysis was performed twice with similar results. ns indicates that the difference is non-significant with the control condition (Student's *t* test).



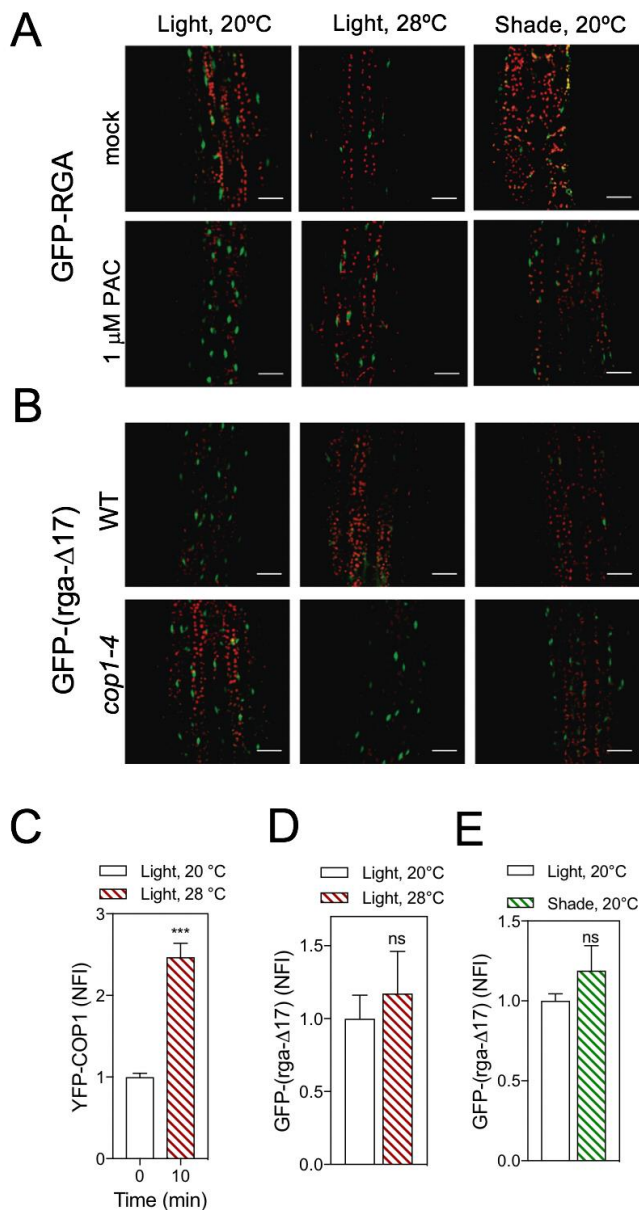


**Fig. S2. COP1 regulates RGA levels.** (A) Representative confocal images of GFP-RGA in hypocotyls used for fluorescence quantifications shown in main Figure 1A. (B) Representative confocal images of GFP-(rga-Δ17) in hypocotyls used for fluorescence quantifications shown in main Figure 1C. (C) YFP-COP1 accumulates rapidly in nuclei after transfer to 28 °C. (D and E) GFP-(rga-Δ17) levels do not change after transfer to 28 °C (D) or shade (E) for 4 h. Bars in A and B represent 35 μm. Confocal data (C-E) show the normalized fluorescence intensity (NFI) in nuclei (NFI=1 in the control seedlings). Confocal microscopy data (C-E) are means and SE of 9-12 seedlings (a minimum of 10 and up to 30 nuclei were averaged per seedling replicate). Asterisks indicate that the difference is statistically significant with the control condition (Student's *t* test, \*\*\*  $P < 0.001$ ; ns, non-significant).

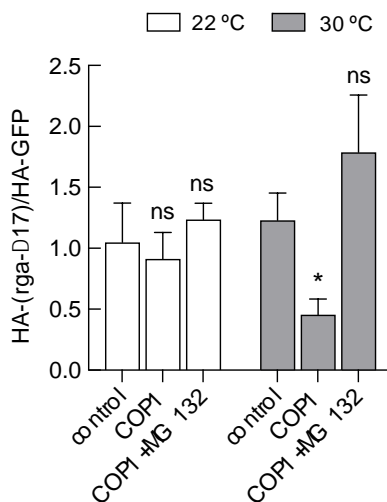
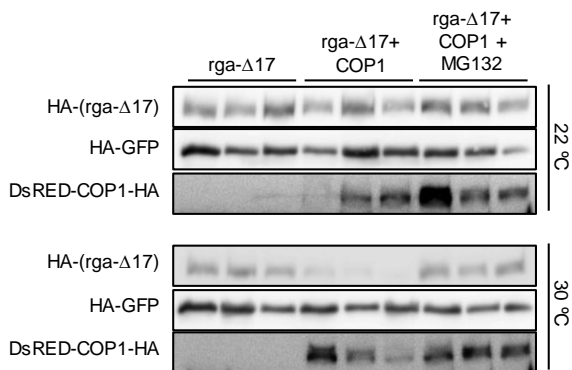


**Fig. S3. Destabilization of the GA-resistant *rga-Δ17* by warm temperature in *N. benthamiana* leaves is dependent on COP1.** HA-(*rga-Δ17*) was transiently expressed alone or with DsRED-COP1-HA in leaves of *N. benthamiana* plants that were transferred to continuous light at 22 °C for three days or 30 °C for the last 24 h. For MG132 treatments leaves were infiltrated with a solution of 25 μM of the inhibitor 8 h before sampling. HA-GFP was used as control to demonstrate the specificity of COP1 action. Blots show data from three individual infiltrated leaves per mixture. Plot shows HA-(*rga-Δ17*) normalized against HA-GFP. Data are means and SE of 3 leaves from one experiment, repeated twice with similar results. The asterisk indicates that the difference is statistically significant with the control condition (Student's *t* test, \*  $P < 0.05$ ; ns, non-significant).

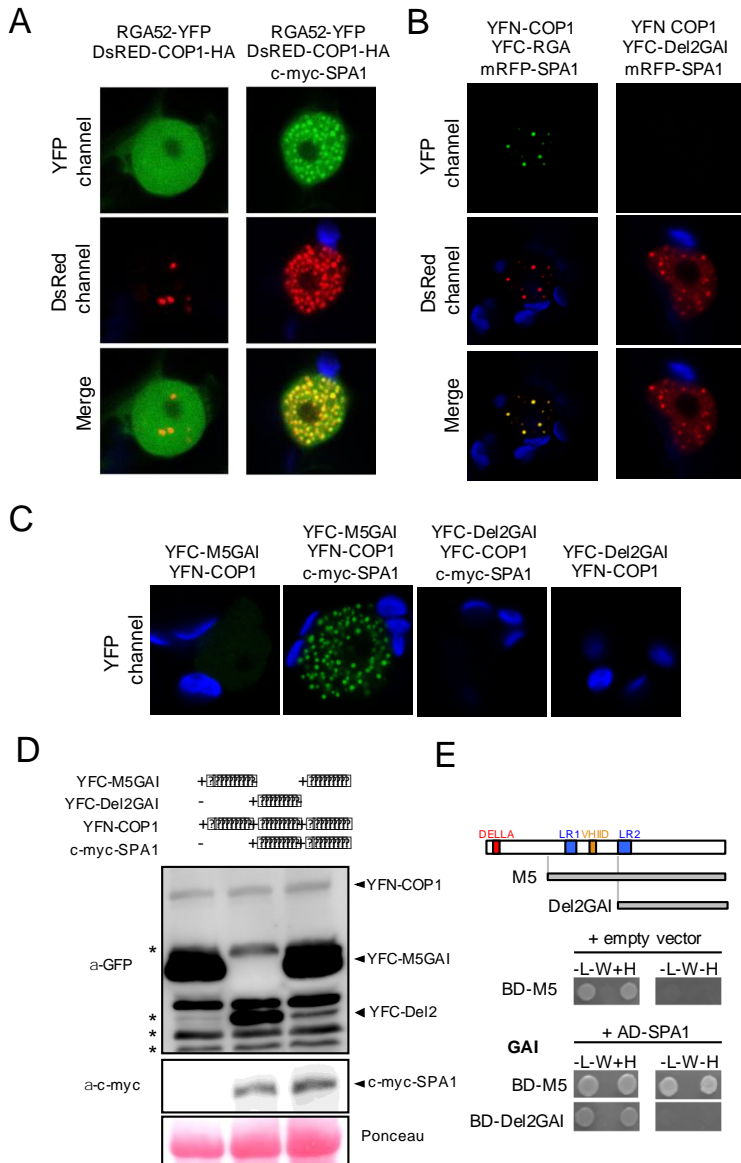


**Fig. S4. SPA1 helps COP1 recruiting DELLA proteins to nuclear bodies.** (A) RGA52-YFP co-localizes with DsRED-COP1-HA in nuclear bodies in the presence of c-myc-SPA1. Fusion proteins were transiently expressed in leaves of *N. benthamiana* and observed by confocal microscopy. One representative nucleus is shown. (B-C) BiFC assay showing that RGA (B) and M5-GAI (C) form a complex with COP1 and SPA1 in nuclear bodies, along with negative controls. The indicated proteins were expressed in leaves of *N. benthamiana* and observed by confocal microscopy. One representative nucleus is shown. (D) Immunoblot analysis of fusion proteins from leaves used for BiFC. The fusion proteins have the expected size: YFN-COP1 (97 KDa), YFC-M5GAI (55 KDa), YFC-Del2GAI (40 KDa) and c-myc-SPA1 (117 KDa). Asterisks indicate non-specific bands, one of them overlapping with YFC-Del2GAI. (E) Y2H assay showing that the GAI deletion Del2GAI does not interact with SPA1.

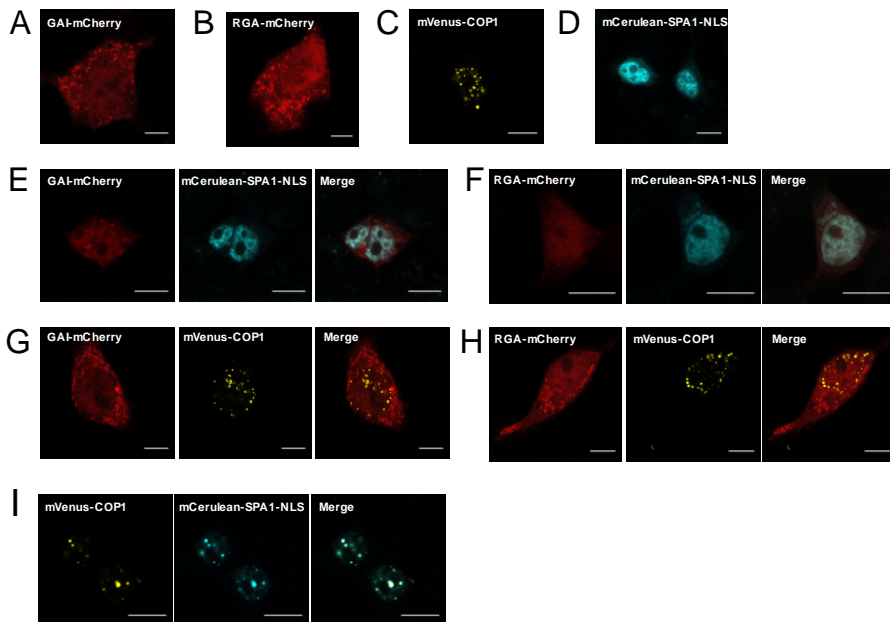


**Fig. S5. Confocal microscopy analysis of the localization of GAI, RGA, COP1 and SPA1 in animal cells.** (A-D) The fusion proteins GAI-mCherry (A), RGA-mCherry (B), mVenus-COP1 (C) and mCerulean-SPA1-NLS (D) were transfected into Human Embryonic Kidney 293T (HEK-293T) cells. GAI and RGA are distributed throughout the whole cell. mVenus-COP1 localizes to nuclear speckle-like structures. mCerulean-SPA1-NLS localizes to the nucleus. (E-I) HEK-293T cells were co-transfected with GAI-mCherry and mCerulean-SPA1-NLS (E), RGA-mCherry and mCerulean-SPA1-NLS (F), GAI-mCherry and mVenus-COP1 (G), RGA-mCherry and mVenus-COP1 (H), or mVenus-COP1 and mCerulean-SPA1-NLS (I). Representative cells are shown. Scale bar represents 10  $\mu\text{m}$ . Note that even when expressed separately, COP1 or SPA1 had weak interactions with DELLAs. For instance, GAI showed more fluorescence inside the COP1 nuclear speckles than outside them (speckles / background fluorescence in G:  $1.16 \pm 0.02$ ,  $P < 0.05$ ) and inside the nucleus where SPA1 was present than in the cytosol (bright areas in E correspond to the nucleus and in A to the whole cell).

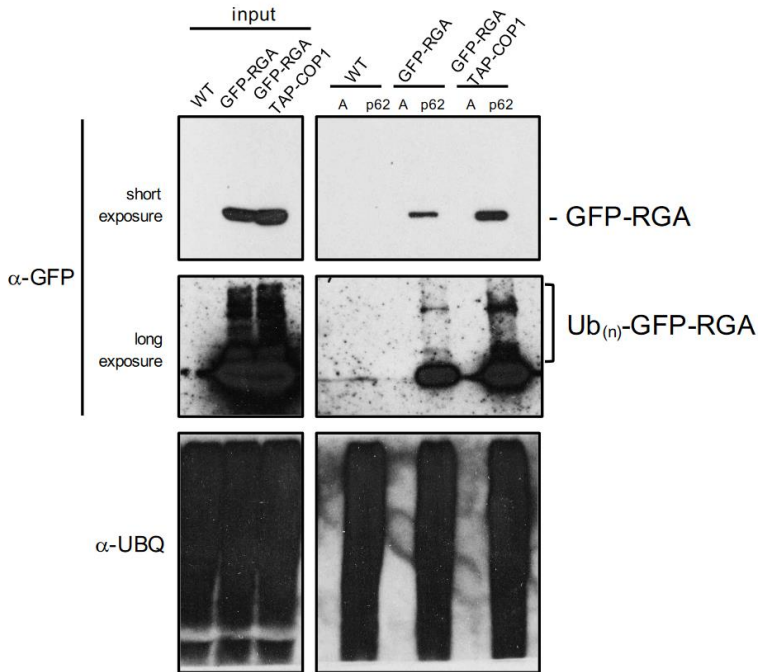


**Fig. S6. RGA ubiquitination *in vivo* is enhanced by COP1.** *pRGA:GFP-RGA* and *pRGA:GFP-RGA 35S:TAP-COP1* seedlings along with the WT were grown for 5 days at 20 °C and then transferred at 28 °C and treated with 50 μM MG132 for 8 h. Proteins were pulled down with p62 beads or agarose beads (A) as negative control. GFP-RGA and its polyubiquitinated forms were detected with an anti-GFP antibody. Total ubiquitinated proteins were detected with an anti-UBQ antibody.

## 6. References

- Achard, P., Liao, L., Jiang, C., Desnos, T., Bartlett, J., Fu, X., and Harberd, N.P.** (2007). DELLAs contribute to plant photomorphogenesis. *Plant Physiol.* **143**: 1163–1172.
- Alabadí, D. and Blázquez, M.A.** (2009). Molecular interactions between light and hormone signaling to control plant growth. *Plant Mol. Biol.* **69**: 409–417.
- Alabadí, D., Gallego-Bartolomé, J., Orlando, L., García-Cárcel, L., Rubio, V., Martínez, C., Frigerio, M., Iglesias-Pedraz, J.M., Espinosa, A., Deng, X.W., and Blázquez, M.A.** (2008). Gibberellins modulate light signaling pathways to prevent Arabidopsis seedling de-etiolation in darkness. *Plant J.* **53**: 324–335.
- Alabadí, D., Gil, J., Blázquez, M.A., and García-Martínez, J.L.** (2004). Gibberellins repress photomorphogenesis in darkness. *Plant Physiol.* **134**: 1050–1057.
- Arana, M.V., Marín-De La Rosa, N., Maloof, J.N., Blázquez, M.A., and Alabadí, D.** (2011). Circadian oscillation of gibberellin signaling in Arabidopsis. *Proc. Natl. Acad. Sci. U. S. A.* **108**: 9292–9297.
- Batada, N.N., Hurst, L.D., and Tyers, M.** (2006). Evolutionary and physiological importance of hub proteins. *PLoS Comput. Biol.* **2**: e88.
- Belda-Palazón, B., Ruiz, L., Martí, E., Tárraga, S., Tiburcio, A.F., Culiáñez, F., Farràs, R., Carrasco, P., and Ferrando, A.** (2012). Aminopropyltransferases Involved in Polyamine Biosynthesis Localize Preferentially in the Nucleus of Plant Cells. *PLoS One.* **7**: e46907.
- Beyer, H.M., Juillot, S., Herbst, K., Samodelov, S.L., Müller, K., Schamel, W.W., Römer, W., Schäfer, E., Nagy, F., Strähle, U., Weber, W., and Zurbriggen, M.D.** (2015). Red Light-Regulated Reversible Nuclear Localization of Proteins in Mammalian Cells and Zebrafish. *ACS Synth. Biol.* **4**: 951–958.
- Bou-Torrent, J., Galstyan, A., Gallemí, M., Cifuentes-Esquivel, N., Molina-Contreras, M.J., Salla-Martret, M., Jikumaru, Y., Yamaguchi, S., Kamiya, Y., and Martínez-García, J.F.** (2014). Plant proximity perception dynamically modulates hormone levels and sensitivity in Arabidopsis. *J. Exp. Bot.* **65**: 2937–2947.
- Bowman, J.L. et al.** (2017). Insights into Land Plant Evolution Garnered from the *Marchantia polymorpha* Genome. *Cell.* **171**: 287–304.
- Cagnola, J.I. et al.** (2018). Long-day photoperiod enhances jasmonic acid-related plant defense. *Plant Physiol.* **178**: 163–173.
- Casal, J.J.** (2013). Photoreceptor Signaling Networks in Plant Responses to Shade. *Annu. Rev. Plant Biol.* **64**: 403–427.
- Casal, J.J., Fankhauser, C., Coupland, G., and Blázquez, M.A.** (2004). Signalling for developmental plasticity. *Trends Plant Sci.* **9**: 309–314.
- Catalá, R., Medina, J., and Salinas, J.** (2011). Integration of low temperature and light signaling during cold acclimation response in Arabidopsis. *Proc. Natl. Acad. Sci. U. S. A.* **108**: 16475–16480.
- Claeys, H., De Bodt, S., and Inzé, D.** (2014). Gibberellins and DELLAs: Central nodes in growth regulatory networks. *Trends Plant Sci.* **19**: 231–239.
- Conti, L., Nelis, S., Zhang, C., Woodcock, A., Swarup, R., Galbiati, M., Tonelli, C., Napier, R., Hedden, P., Bennett, M., and Sadanandom, A.** (2014). Small Ubiquitin-like Modifier Protein SUMO Enables Plants to Control Growth Independently of the Phytohormone

- Gibberellin. *Dev. Cell.* **28**: 102–110.
- Crocco, C.D., Locascio, A., Escudero, C.M., Alabadí, D., Blázquez, M.A., and Botto, J.F.** (2015). The transcriptional regulator BBX24 impairs DELLA activity to promote shade avoidance in *Arabidopsis thaliana*. *Nat. Commun.* **6**: 6202.
- De Lucas, M., Davière, J.M., Rodríguez-Falcón, M., Pontin, M., Iglesias-Pedraz, J.M., Lorrain, S., Fankhauser, C., Blázquez, M.A., Titarenko, E., and Prat, S.** (2008). A molecular framework for light and gibberellin control of cell elongation. *Nature*. **451**: 480–484.
- Delker, C. et al.** (2014). The DET1-COP1-HY5 Pathway Constitutes a Multipurpose Signaling Module Regulating Plant Photomorphogenesis and Thermomorphogenesis. *Cell Rep.* **9**: 1983–1989.
- Deng, X.W. and Quail, P.H.** (1992). Genetic and phenotypic characterization of *cop1* mutants of *Arabidopsis thaliana*. *Plant J.* **2**: 83–95.
- Deng, X.W., Caspar, T., and Quail, P.H.** (1991). *cop1*: A regulatory locus involved in light-controlled development and gene expression in *Arabidopsis*. *Genes Dev.* **5**: 1172–1182.
- Dill, A., Jung, H.S., and Sun, T.P.** (2001). The DELLA motif is essential for gibberellin-induced degradation of RGA. *Proc. Natl. Acad. Sci. U. S. A.* **98**: 14162–14167.
- Djakovic-Petrovic, T., Wit, M. De, Voesenek, L.A.C.J., and Pierik, R.** (2007). DELLA protein function in growth responses to canopy signals. *Plant J.* **51**: 117–126.
- Earley, K.W., Haag, J.R., Pontes, O., Opper, K., Juehne, T., Song, K., and Pikaard, C.S.** (2006). Gateway-compatible vectors for plant functional genomics and proteomics. *Plant J.* **45**: 616–629.
- Frigerio, M., Alabadí, D., Pérez-Gómez, J., García-Cárcel, L., Phillips, A.L., Hedden, P., and Blázquez, M.A.** (2006). Transcriptional regulation of gibberellin metabolism genes by auxin signaling in *Arabidopsis*. *Plant Physiol.* **142**: 553–563.
- Gallego-Bartolomé, J., Minguet, E.G., Grau-Enguix, F., Abbas, M., Locascio, A., Thomas, S.G., Alabadí, D., and Blázquez, M.A.** (2012). Molecular mechanism for the interaction between gibberellin and brassinosteroid signaling pathways in *Arabidopsis*. *Proc. Natl. Acad. Sci. U. S. A.* **109**: 13446–13451.
- Gallego-Bartolomé, J., Arana, M. V., Vandenbussche, F., Žádníková, P., Minguet, E.G., Guardiola, V., Van Der Straeten, D., Benkova, E., Alabadí, D., and Blázquez, M.A.** (2011). Hierarchy of hormone action controlling apical hook development in *Arabidopsis*. *Plant J.* **67**: 622–634.
- Gallego-Bartolomé, J., Minguet, E.G., Marín, J.A., Prat, S., Blázquez, M.A., and Alabadí, D.** (2010). Transcriptional diversification and functional conservation between DELLA proteins in *Arabidopsis*. *Mol. Biol. Evol.* **27**: 1247–1256.
- Gil, J. and García-Martínez, J.L.** (2000). Light regulation of gibberellin A1 content and expression of genes coding for GA 20-oxidase and GA 3 $\beta$ -hydroxylase in etiolated pea seedlings. *Physiol. Plant.* **108**: 223–229.
- Grefen, C., Donald, N., Hashimoto, K., Kudla, J., Schumacher, K., and Blatt, M.R.** (2010). A ubiquitin-10 promoter-based vector set for fluorescent protein tagging facilitates temporal stability and native protein distribution in transient and stable expression studies. *Plant J.* **64**: 355–365.
- Hoecker, U.** (2017). The activities of the E3 ubiquitin ligase COP1/SPA, a key repressor in light signaling. *Curr. Opin. Plant Biol.* **37**: 63–69.

- Hoecker, U. and Quail, P.H.** (2001). The Phytochrome A-specific Signaling Intermediate SPA1 Interacts Directly with COP1, a Constitutive Repressor of Light Signaling in Arabidopsis. *J. Biol. Chem.* **276**: 38173–38178.
- Jung, J.H. et al.** (2016). Phytochromes function as thermosensors in Arabidopsis. *Science*. **354**: 886–889.
- Lantzouni, O., Alkofer, A., Falter-Braun, P., Schwechheimer, C.** (2020). GROWTH-REGULATING FACTORS Interact with DELLAs and Regulate Growth in Cold Stress. *Plant Cell*. **32**: 1018–1034.
- Lau, O.S. and Deng, X.W.** (2012). The photomorphogenic repressors COP1 and DET1: 20 years later. *Trends Plant Sci.* **17**: 584–593.
- Legris, M., Klose, C., Burgie, E.S., Rojas, C.C., Neme, M., Hiltbrunner, A., Wigge, P.A., Schäfer, E., Vierstra, R.D., and Casal, J.J.** (2016). Phytochrome B integrates light and temperature signals in Arabidopsis. *Science*. **354**: 897–900.
- Lian, H.L., He, S.B., Zhang, Y.C., Zhu, D.M., Zhang, J.Y., Jia, K.P., Sun, S.X., Li, L., and Yang, H.Q.** (2011). Blue-light-dependent interaction of cryptochrome 1 with SPA1 defines a dynamic signaling mechanism. *Genes Dev.* **25**: 1023–1028.
- Liu, B., Zuo, Z., Liu, H., Liu, X., and Lin, C.** (2011). Arabidopsis cryptochrome 1 interacts with SPA1 to suppress COP1 activity in response to blue light. *Genes Dev.* **25**: 1029–1034.
- Love, I.M. and Grossman, S.R.** (2012). It Takes 15 to Tango: Making Sense of the Many Ubiquitin Ligases of p53. *Genes and Cancer*. **3**: 249–263.
- Lu, X.D., Zhou, C.M., Xu, P.B., Luo, Q., Lian, H.L., and Yang, H.Q.** (2015). Red-light-dependent interaction of phyB with SPA1 promotes COP1-SPA1 dissociation and photomorphogenic development in Arabidopsis. *Mol. Plant*. **8**: 467–478.
- McNellis, T.W., von Arnim, A.G., Araki, T., Komeda, Y., Misera, S., and Deng X. W.** (1994). Genetic and molecular analysis of an allelic series of *cop1* mutants suggests functional roles for the multiple protein domains. *Plant Cell*. **6**: 487–500.
- Müller, K., Engesser, R., Schulz, S., Steinberg, T., Tomakidi, P., Weber, C.C., Ulm, R., Timmer, J., Zurbriggen, M.D., and Weber, W.** (2013). Multi-chromatic control of mammalian gene expression and signaling. *Nucleic Acids Res.* **41**: e124.
- Oravecz, A., Baumann, A., Máté, Z., Brzezinska, A., Molinier, J., Oakeley, E.J., Ádám, É., Schäfer, E., Nagy, F., and Ulm, R.** (2006). CONSTITUTIVELY PHOTOMORPHOGENIC1 is required for the UV-B response in Arabidopsis. *Plant Cell*. **18**: 1975–1990.
- Pacín, M., Legris, M., and Casal, J.J.** (2014). Rapid decline in nuclear COP1 abundance anticipates the stabilisation of its target HY5 in the light. *Plant Physiol.* **164**: 1134–1138.
- Pacín, M., Legris, M., and Casal, J.J.** (2013). COP1 re-accumulates in the nucleus under shade. *Plant J.* **75**: 631–641.
- Park, J., Oh, D.H., Dassanayake, M., Nguyen, K.T., Ogas, J., Choi, G., and Sun, T.P.** (2017a). Gibberellin signaling requires chromatin remodeler PICKLE to promote vegetative growth and phase transitions. *Plant Physiol.* **173**: 1463–1474.
- Park, Y.J., Lee, H.J., Ha, J.H., Kim, J.Y., and Park, C.M.** (2017b). COP1 conveys warm temperature information to hypocotyl thermomorphogenesis. *New Phytol.* **215**: 269–280.
- Paz-Ares, J. et al.** (2002). REGIA an EU project on functional genomics of transcription factors from *Arabidopsis thaliana*. *Comp. Funct. Genomics*. **3**: 102–108.



- Piskurewicz, U., Jikumaru, Y., Kinoshita, N., Nambara, E., Kamiya, Y., and Lopez-Molina, L.** (2008). The gibberellic acid signaling repressor RGL2 inhibits Arabidopsis seed germination by stimulating abscisic acid synthesis and ABI5 activity. *Plant Cell*. **20**: 2729–2745.
- Plackett, A.R.G., Ferguson, A.C., Powers, S.J., Wanchoo-Kohli, A., Phillips, A.L., Wilson, Z.A., Hedden, P., and Thomas, S.G.** (2014). DELLA activity is required for successful pollen development in the Columbia ecotype of Arabidopsis. *New Phytol.* **201**: 825–836.
- Quint, M., Delker, C., Franklin, K.A., Wigge, P.A., Halliday, K.J., and Van Zanten, M.** (2016). Molecular and genetic control of plant thermomorphogenesis. *Nat. Plants*. **2**: 15190.
- Rubio, V., Shen, Y., Saijo, Y., Liu, Y., Gusmaroli, G., Dinesh-Kumar, S.P., and Deng, X.W.** (2005). An alternative tandem affinity purification strategy applied to Arabidopsis protein complex isolation. *Plant J.* **41**: 767–778.
- Seo, H.S., Yang, J.Y., Ishikawa, M., Bolle, C., Ballesteros, M.L., and Chua, N.H.** (2003). LAF1 ubiquitination by COP1 controls photomorphogenesis and is stimulated by SPA1. *Nature*. **423**: 995–999.
- Seo, M., Jikumaru, Y., and Kamiya, Y.** (2011). Profiling of hormones and related metabolites in seed dormancy and germination studies. *Methods Mol. Biol.* **773**: 99–111.
- Sheerin, D.J., Menon, C., Oven-Krockhaus, S. Zur, Enderle, B., Zhu, L., Johnen, P., Schleifenbaum, F., Stierhof, Y.D., Huq, E., and Hiltbrunner, A.** (2015). Light-activated phytochrome A and B interact with members of the SPA family to promote photomorphogenesis in Arabidopsis by reorganizing the COP1/SPA complex. *Plant Cell*. **27**: 189–201.
- Silverstone, A.L., Jung, H.S., Dill, A., Kawaide, H., Kamiya, Y., and Sun, T.P.** (2001). Repressing a repressor: Gibberellin-induced rapid reduction of the RGA protein in Arabidopsis. *Plant Cell*. **13**: 1555–1566.
- Stavang, J.A., Gallego-Bartolomé, J., Gómez, M.D., Yoshida, S., Asami, T., Olsen, J.E., García-Martínez, J.L., Alabadí, D., and Blázquez, M.A.** (2009). Hormonal regulation of temperature-induced growth in Arabidopsis. *Plant J.* **60**: 589–601.
- Sun, T.P.** (2011). The molecular mechanism and evolution of the GA-GID1-DELLA signaling module in plants. *Curr. Biol.* **21**: R338–R345.
- Van De Velde, K., Ruelens, P., Geuten, K., Rohde, A., and Van Der Straeten, D.** (2017). Exploiting DELLA Signaling in Cereals. *Trends Plant Sci.* **10**: 880–893.
- Vazquez-Vilar, M., Quijano-Rubio, A., Fernandez-Del-Carmen, A., Sarrion-Perdigones, A., Ochoa-Fernandez, R., Ziarso, P., Blanca, J., Granell, A., and Orzaez, D.** (2017). GB3.0: a platform for plant bio-design that connects functional DNA elements with associated biological data. *Nucleic Acids Res.* **45**: 2196–2209.
- Von Arnim, A.G. and Deng, X.W.** (1993). Ring finger motif of *Arabidopsis thaliana* COP1 defines a new class of zinc-binding domain. *J. Biol. Chem.* **268**: 19626–19631.
- Weller, J.L., Hecht, V., Schoor, J.K.V., Davidson, S.E., and Ross, J.J.** (2009). Light regulation of gibberellin biosynthesis in pea is mediated through the COP1/HY5 pathway. *Plant Cell*. **21**: 800–813.
- Willige, B.C., Ghosh, S., Nill, C., Zourelidou, M., Dohmann, E.M.N., Maier, A., and Schwechheimer, C.** (2007). The DELLA domain of GA INSENSITIVE mediates the interaction with the GA INSENSITIVE DWARF1A gibberellin receptor of Arabidopsis. *Plant Cell*. **19**: 1209–1220.
- Yamamoto, T., Mori, Y., Ishibashi, T., Uchiyama, Y., Sakaguchi, N., Furukawa, T.,**

- Hashimoto, J., Kimura, S., and Sakaguchi, K.** (2004). Characterization of Rad6 from a higher plant, rice (*Oryza sativa* L.) and its interaction with Sgt1, a subunit of the SCF ubiquitin ligase complex. *Biochem. Biophys. Res. Commun.* **314**: 434–439.
- Yang, D.L. et al.** (2012). Plant hormone jasmonate prioritizes defense over growth by interfering with gibberellin signaling cascade. *Proc. Natl. Acad. Sci. U. S. A.* **109**: E1192–1200.
- Yasumura, Y., Crumpton-Taylor, M., Fuentes, S., and Harberd, N.P.** (2007). Step-by-Step Acquisition of the Gibberellin-DELLA Growth-Regulatory Mechanism during Land-Plant Evolution. *Curr. Biol.* **17**: 1225–1230.
- Yu, J.W. et al.** (2008). COP1 and ELF3 Control Circadian Function and Photoperiodic Flowering by Regulating GI Stability. *Mol. Cell.* **32**: 617–630.
- Zentella, R., Sui, N., Barnhill, B., Hsieh, W.P., Hu, J., Shabanowitz, J., Boyce, M., Olszewski, N.E., Zhou, P., Hunt, D.F., and Sun, T.P.** (2017). The Arabidopsis O-fucosyltransferase SPINDLY activates nuclear growth repressor DELLA. *Nat. Chem. Biol.* **13**: 479–485.
- Zentella, R. et al.** (2016). O-GlcNAcylation of master growth repressor DELLA by SECRET AGENT modulates multiple signaling pathways in Arabidopsis. *Genes Dev.* **30**: 164–176.
- Zhao, X., Yu, X., Foo, E., Symons, G.M., Lopez, J., Bendehakalu, K.T., Xiang, J., Weller, J.L., Liu, X., Reid, J.B., and Lin, C.** (2007). A study of gibberellin homeostasis and cryptochrome-mediated blue light inhibition of hypocotyl elongation. *Plant Physiol.* **145**: 106–118.

## Chapter 2

### **DELTA proteins are required for the recruitment of Paf1c to its target genes**

Blanco-Touriñán N, Bourbousse C, Latrasse D, Ait-Mohamed O, Forment J, Deton-Cabanillas AF, De Lucas M, Benhamed M, Barneche F, Blázquez MA, Alabadí D.

**(unpublished)**

DELLA proteins are plant-specific transcriptional regulators that act as negative elements in the gibberellin (GA) signalling pathway in vascular plants. An ever-increasing number of studies support a central role for DELLAs in connecting environmental signals with the transcriptional networks that control growth and development. The current model for DELLAs action considers a transcription regulatory function through physical interaction with multiple transcription factors (TFs). DELLAs may trigger TF sequestration away from their target promoters or act on site with TFs as transcriptional co-activators. Interestingly, DELLAs also occupy chromatin along gene bodies, suggesting that there may be additional mechanisms by which these proteins modulate transcription. Here, we report that GAI and RGA DELLA proteins interact in a yeast two-hybrid system and *in vivo* with the Polymerase-Associated Factor 1 complex (Paf1c) core subunit ELF7. Paf1c is required for the monoubiquitination of histone H2B (H2Bub) to facilitate RNA Polymerase II (RNAPII) transcription elongation. Transcriptomic analyses identified that ELF7 and GAs regulate the expression of a common set of genes, suggesting that DELLAs and ELF7 act in the same pathway. CHIP-seq profiling further showed that H2Bub and ELF7 largely target the same transcribed genes and are both affected by GA-treatment. Hence, defects in H2Bub chromatin enrichment upon GA treatment appear to be caused, at least in part, by decreased occupancy of ELF7 at its targets. Consistently, we found that both RNAPII occupancy and distribution were similarly altered upon GA-treatment and *ELF7* loss-of-function. Taken together, our findings unveil a new mechanism by which DELLAs directly act with transcription elongation factors to regulate gene expression.

## 1. Introduction

DELLA proteins are master negative elements in the gibberellin (GA) signalling pathway. They allow the integration of external information on the plant environment with the transcriptional networks that control growth and development. DELLAs have been proposed to modulate gene expression through different molecular mechanisms, including (i) the inhibition of the activity of transcription factors (TFs) and other transcriptional regulators through sequestration from chromatin; and, (ii) the activation of TF activity in the context of their target genes (Davière and Achard, 2016; Vera-Sirera et al., 2016). Nevertheless, observations that DELLAs occupy gene bodies (Marín-de la Rosa et al., 2015; Serrano-Mislata et al., 2017) also suggest a model in which DELLAs regulate gene expression through other mechanisms, for instance affecting directly RNA polymerase II (RNAPII) transcription.

RNAPII transcription follows an conserved three-step cycle (initiation, elongation and termination) that is tightly regulated to fine-tune gene expression (Hsin and Manley, 2012; Conaway and Conaway, 2015). This regulation involves numerous accompanying factors (proteins or protein complexes), most of them being evolutionarily conserved in all eukaryotes (Lijsebettens and Grasser, 2014). In fact, a recent study has identified several of these factors associated to RNAPII in Arabidopsis cell suspensions (Antosz et al., 2017), one of which is the Polymerase-Associated Factor 1 complex (Paf1c) (Van Oss et al., 2017).

The current model of how Paf1c acts on RNAPII is based on studies in yeast and mammals (Van Oss et al., 2017). Paf1c was first shown to regulate transcription through the establishment of co-transcriptional histone modifications (e.g. Histone 3 lysine 4 methylation [H3K4me], H3K36me and H2Bub), which influence chromatin dynamics to facilitate RNAPII progression (Van Oss et al., 2017). In particular, Paf1c stimulates the monoubiquitination of H2B (H2Bub) through different mechanisms in yeast and mammals. In yeast, it promotes de activity of the enzymes involved in H2Bub, the Rad6 E2 ubiquitin-conjugating enzyme and Bre1 E3 ubiquitin ligase (Wood et al., 2003), whereas in mammals, it is required for the recruitment of RNF20/40 (the mammalian orthologs of Bre1) to the chromatin (Wu et al., 2014).

Several subunits of the plant Paf1c have been identified genetically owing to the early flowering phenotype of Arabidopsis mutants (Zhang and Van Nocker, 2002; Zhang et al., 2003; Oh et al., 2004; He et al., 2004; Yu and Michaels, 2010). The plant complex contains

six subunits, as described in animals, PLANT HOMOLOGOUS TO PARAFIBROMIN (PHP)/CDC73, VERNALIZATION INDEPENDENCE (VIP) 2 (also known as EARLY FLOWERING 7, ELF7; Paf1), VIP3 (Ski8), VIP4 (Ctr1), VIP5 (Rtf1) and VIP6 (also known as ELF8; Leo) (Jaehning, 2010). In line with the role of Paf1c in animals and yeast, recent studies suggest the involvement of Paf1c in H2B monoubiquitination and in transcriptional elongation in plants: (i) mutations in *ELF7*, *VIP4*, *VIP5* and *ELF8* subunits cause a global decrease in H2Bub analysed by immunoblot (Cao et al., 2015); (ii) the levels of H2Bub at the *FLC/MAF* loci are reduced in *elf7-3* mutant (Cao et al., 2015); (iii) Paf1c subunits interact in plant cells with different RNAPII subunits and with other transcription elongation factors such as TFIIIS, SPT5, SPT6 and FACT (Antosz et al., 2017); and (iv) the Paf1c subunit ELF7 is associated with the Ser2P-RNAPII elongating form (Antosz et al., 2017).

To investigate if the presence of DELLAs in gene bodies reflects a role in the regulation of transcription elongation, we carried out a targeted yeast two-hybrid (Y2H) screening and identified the Paf1c subunit ELF7 as an interactor of GAI and RGA. Molecular characterization of these interactions *in vivo* indicates the participation of DELLAs in the regulation of chromatin remodelling during transcription elongation.

## 2. Results

### DELLAs interact with the Paf1c subunit ELF7

In a targeted Y2H screen that included proteins involved in several stages of transcriptional regulation (Fig. S1), we found that the GRAS domain of the DELLA proteins GAI (M5-GAI) and RGA (RG52) interacted with the Paf1c subunit ELF7 (Fig. 1A and B, Fig. S1). Further analysis confirmed that ELF7 interacted with the other Arabidopsis DELLAs (RGL1, RGL2 and RGL3) (Fig. S2). The interaction was restricted to the ELF7 subunit as no interactions were detected with the other four Paf1c subunits tested (Fig. 1A and B, Fig. S2). The interaction of ELF7 with GAI and RGA was confirmed in plant cells by Bimolecular Fluorescence Complementation (BiFC) (Fig. 1C) and co-immunoprecipitation (co-IP) (Fig. 1D), respectively. In the BiFC experiment, the fluorescence from the reconstituted yellow fluorescent protein (YFP) was observed in nuclei of epidermal cells of *Nicotiana benthamiana* co-infiltrated with YFC-GAI and YFN-ELF7 (Fig. 1C). The fluorescent signal showed a homogeneous nuclear distribution, in contrast to the speckles observed for the interaction of ELF7 with other proteins (Cao et al., 2015), suggesting that the interactions may occur in different locations depending on the partner. Flag-ELF7 was also specifically co-

immunoprecipitated with anti-GFP antibodies from extracts of *RGAp:GFP-RGA ELF7p:Flag-ELF7* double transgenic plants, confirming the interaction between RGA and ELF7 in Arabidopsis (Fig. 1D). In summary, these findings identify a physical association of DELLAs with the transcription elongation complex Paf1c through its subunit ELF7.

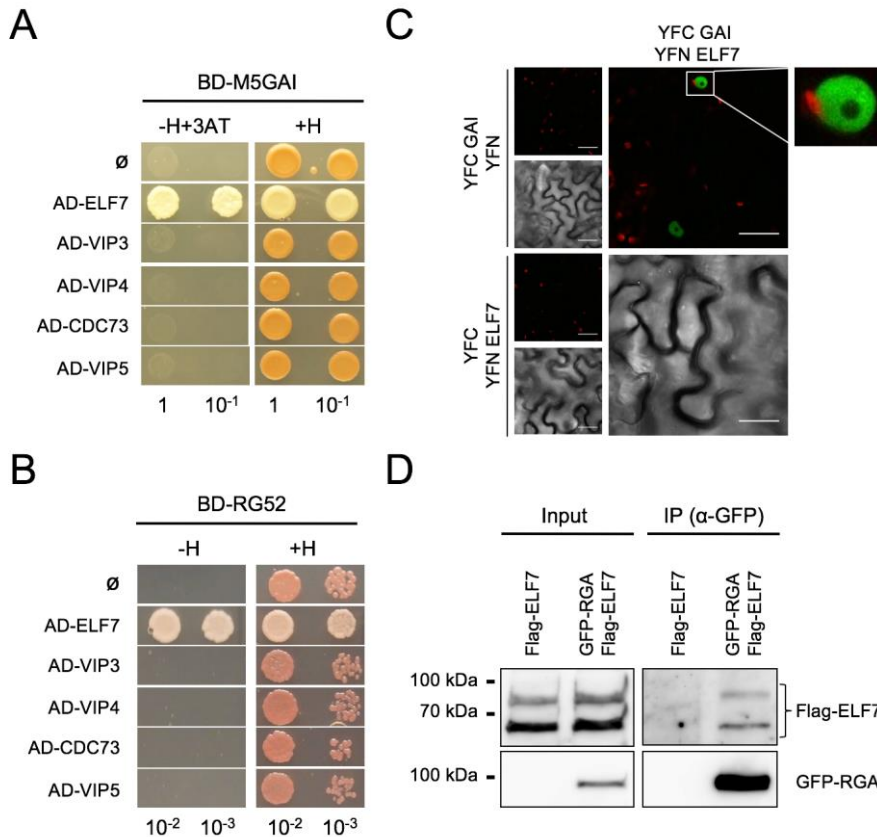


**Fig. 1. DELLAs interact with ELF7 in plant cells.** (A-B) Y2H assays of five subunits of the Paf1c (ELF7, VIP3, VIP4, CDC73 and VIP5) with M5GAI (A) and RG52 (B). ∅ represents negative control where no sequence was cloned into the activation domain (AD). The serial dilutions (1:10) shown are indicated. +H, control medium depleted of leucine and tryptophan. -H, selective medium also lacking histidine and containing in (A) 5 mM 3-aminotriazol (3-AT). (C) BiFC analysis in *N. benthamiana* leaves of ELF7 and GAI fusions to N- and C-terminal fragments of YFP, respectively. YFP fluorescence and bright-field images are shown. Scale bars: 40 μm. A zoom depicting BiFC signal is shown. (D) Co-IP assay showing the interaction between RGA and ELF7 in Arabidopsis seedlings. Soluble proteins from *Flag-ELF7* and the double transgenic *GFP-RGA Flag-ELF7* seedlings grown in the presence of paclobutrazol were used for the IP with anti-GFP paramagnetic beads and were detected by immunoblotting with either anti-Flag or anti-GFP antibodies. The position of molecular weight markers is shown on the left. The sizes of the bands correspond to the expected sizes of the fusion proteins although Flag-ELF7 was also detected around 90 KDa (expected size = 68.4KDa).

## DELLAs are part of a gene regulatory network with Paf1c

To investigate a possible functional relationship between DELLAs and Paf1c, we first examined the transcriptomic changes caused by reducing DELLA or Paf1c activity. For that purpose, we compared the transcriptomes of 7-day-old seedlings of wild-type (WT), WT grown in medium containing 100  $\mu$ M GA<sub>3</sub> (hereafter WT+GA; this treatment causes the depletion of DELLA proteins) and *elf7-3*. This showed that 631 genes were differentially expressed in WT+GA seedlings (245 up-regulated and 386 down-regulated) and 1381 in the *elf7-3* mutant compared to WT plants (725 up-regulated and 656 down-regulated) ( $p$  adj <0.01, fold change (FC)  $\geq$ 1.5) (Fig. 2A-C, Supp. Table 1). As expected, the transcriptional response to GA included the down-regulation of prototypical marker genes, such as GA 3-OXIDASE1 and GA 20-OXIDASE2 transcripts (Fig. S5A, Supp. Table 1), while *elf7-3* samples presented a significant reduction of *ELF7* mRNA levels (Log<sub>2</sub> FC of -2.2, Supp. Table 1). Importantly, 202 genes displayed similar misregulation in WT+GA and *elf7-3* seedlings, representing a statistically significant overlap (Fig. 2C and D, Supp. Table 1). This is compatible with a model in which DELLAs and Paf1c act on a common pathway, with DELLAs having a positive effect on Paf1c activity. Gene Ontology (GO) analysis of DEGs showed an enrichment in functional categories related to external stimulus, such as response to chitin or fungus, response to absence of light or cellular response to phosphate starvation (Fig. 3A and B, Supp. Table 2). The list of co-regulated genes includes several that encode enzymes involved in glucosinolate metabolism (*SUR1/ALF1*, *UGT74B1*, *SOT18*, *IMS2/MAM3*, *CYP81F2*, *IPM11* –most of them up-regulated) (Gigolashvili et al., 2009; Bell, 2019) as well as some involved in the phosphate starvation responses (*SPX1*, *SPX3*, *SPX4*, *SQD1* and 2, *PHF1* –most of them up-regulated) (Essigmann et al., 1998; Yu et al., 2002; González et al., 2005; Liu et al., 2018b) (Fig. 3B, Supp. Tables 1 and 2). The identification of misregulated phosphate response genes is in agreement with previous studies showing that both GA and Paf1c are involved in the control of phosphate homeostasis (Jiang et al., 2007; Zhang et al., 2019; Ellison et al., 2019). However, to the best of our knowledge, neither GA nor Paf1c have been previously related to glucosinolates. Overall, these results suggest that DELLAs may regulate gene expression through Paf1c, with a specific relevance in certain cellular processes.



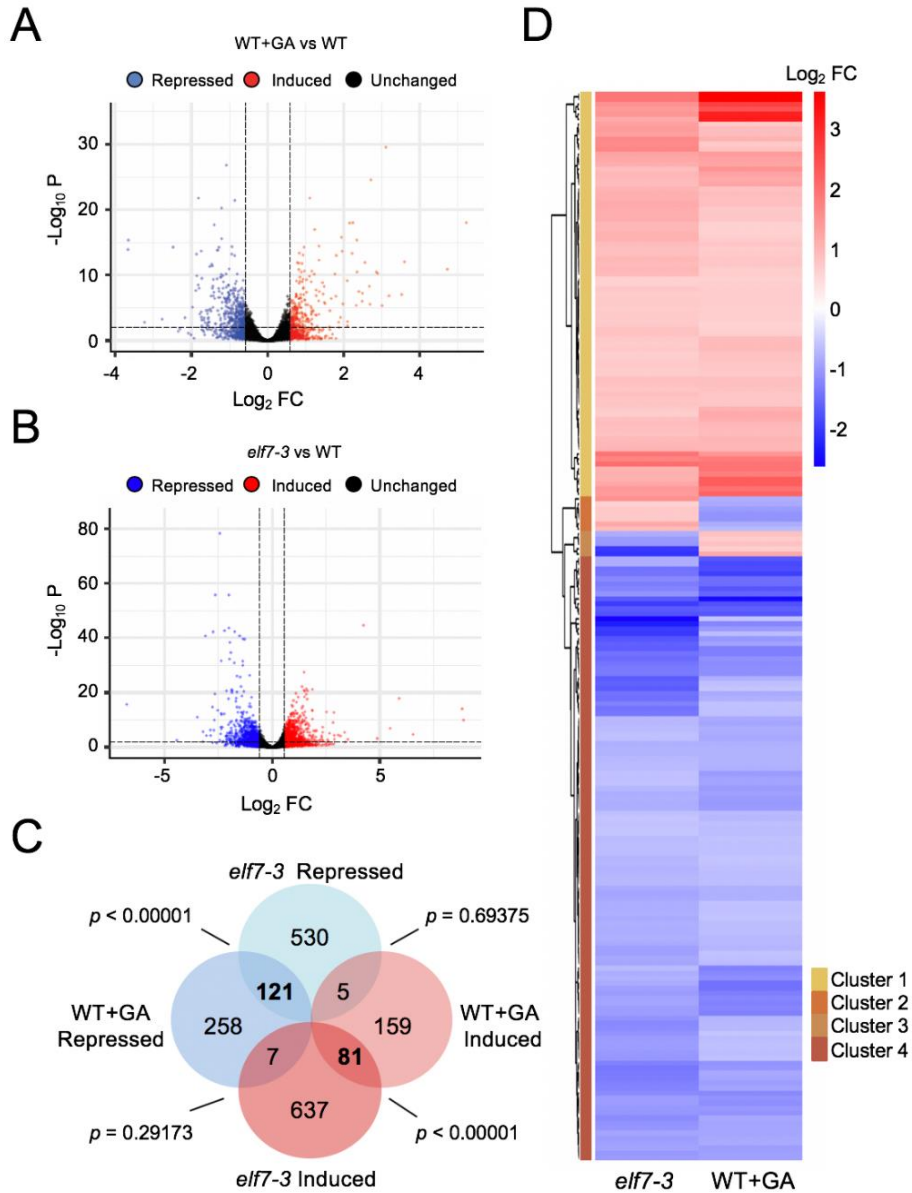
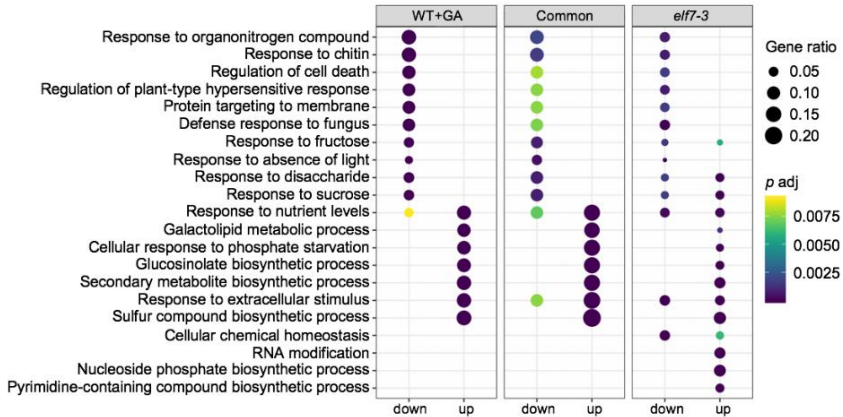


**Fig. 2. Transcriptomic analysis of WT+GA and *elf7-3* seedlings.** (A-B) Volcano plots showing the genes expressed in WT+GA (N=18557, A) and *elf7-3* seedlings (N=18590, B). Expressed genes are referred to those with  $\geq 1$  RPKM in the three replicates of each condition/genotype. The red and blue dots indicate induced and repressed genes, respectively. DEGs were considered when  $FC \geq 1.5$  and  $p \text{ adj} < 0.01$ . (C) Venn diagram showing total and overlapping DEGs in WT+GA and *elf7-3* seedlings. The  $p$ -values  $< 0.05$  show significant differences according to the chi square test. (D) Heatmap representing the log<sub>2</sub>FC of the common DEGs in both WT+GA and *elf7-3* seedlings (N=214).

A



B

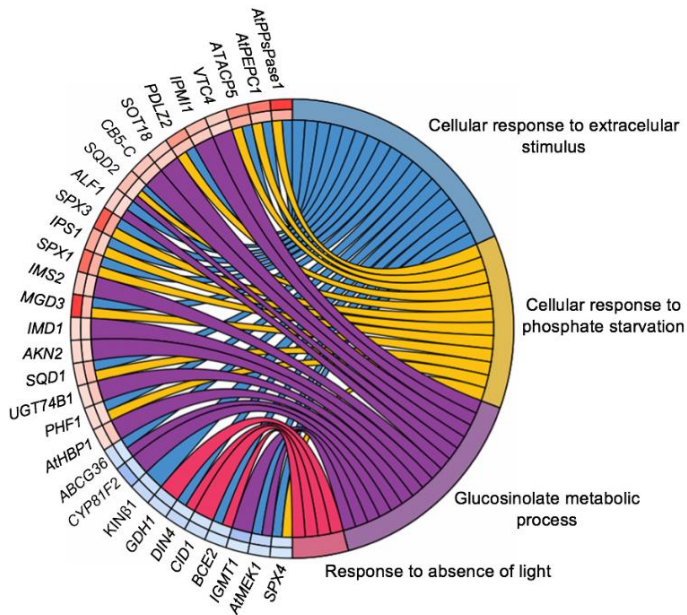


**Fig. 3. Gene Ontology enrichment among genes that are differentially expressed in WT+GA and *elf7-3* seedlings.** (A) Plot showing “Biological process” categories over-represented in WT+GA, *elf7-3* and “common”. The latter referred to those common DEGs that showed a similar behaviour in both WT+GA and *elf7-3* (N=202). GO categories were filtered as described in material and methods section and those that were largely redundant were also removed. All the GO are included in Supp. Table 2. The number of genes contained, and the significance of each term were indicated according to the size and the brightness of the circles, respectively. (B) GOChord plot showing a few common DEGs in WT+GA and *elf7-3* mutant seedlings in five GO categories. On the left, a heatmap showing the induced and repressed genes in red and blue, respectively. The column on the left includes WT+GA data while the one on the right the data from *elf7-3* transcriptome.

**Both DELLAs and ELF7 influence H2Bub general abundance and distribution**

Paf1c is required for efficient deposition of the H2Bub mark in different organisms, including plants (Wood et al., 2003; Cao et al., 2015; Hou et al., 2019). Therefore, to explore the potential influence of DELLAs on Paf1c activity, we investigated the global distribution of H2Bub in GA-treated and *elf7-3* seedlings by Chromatin Immunoprecipitation-Rx (ChIP-Rx). This modified version of ChIP-seq allows for accurate quantitative comparisons of samples with genome-wide differences in a chromatin mark abundance (Orlando et al., 2014). As previously described (Nassrallah et al., 2018), all samples were “spiked-in” with *Drosophila* chromatin prior to IP. The amount of exogenous DNA was subsequently determined in all inputs and IP samples and taken into account as a reference to avoid the effects of technical variations. We further determined H2Bub peaks after normalization to histone H2B occupancy profiled in the same samples by ChIP-Rx (see Methods). In agreement with previous profiling studies in *Arabidopsis* (Roudier et al., 2011; Bourbousse et al., 2012; Nassrallah et al., 2018), H2Bub was exclusively enriched in the transcribed regions (Fig. 4A and B, Fig. S3). Importantly, the deposition of the H2Bub mark was strongly affected in *elf7-3* and WT+GA seedlings. H2Bub peak detection showed that *elf7-3* and WT+GA seedlings had significantly less H2Bub-marked genes with a reduction of ca. 30% (3402 fewer genes) and 16% (1758 fewer genes) as compared to untreated WT plants, respectively (Fig. 4C, Supp. Table 3). Still, two thirds of H2Bub peaks were maintained upon GA treatment or in *elf7-3* plants but with much lower levels (Fig. 4A and B, Fig. S3). Identification of differentially ubiquitinated genes (DUGs) confirmed a general tendency for reduced H2Bub enrichment over most genes in *elf7-3* plants, which was also apparent in WT+GA with a lower amplitude (orange/pink dots in Fig. 4D and E, Supp. Table 4).

In mammals, chromatin recruitment of Paf1c and RFN20/40 is inter-dependent, which provides an explanation for the reduction of H2Bub mark in *paf1* knock-down cells, i.e. lower binding of RFN20/40 to their targets (Wu et al., 2014). We next tested whether this mechanism operates in plants. Subcellular fractionation analysis showed that the loss of function of *ELF7* did not lead to decreased chromatin enrichment of HUB1/HUB2 (Fig. S4A), the *Arabidopsis* orthologs of RFN20/40 and Bre1 (Liu et al, Plant Cell 2007; Fleury et al., Plant Cell 2007; Feng and Shen, 2014). Amounts of HUB1/2 in the chromatin fraction, detected by custom-made anti-HUB1/2 (see Methods), were also not altered in WT+GA seedlings (Fig. S4B). These results suggest that Paf1c and DELLAs might be required for HUB1/2 E3 ligase activity but not for their recruitment to chromatin, similar to what

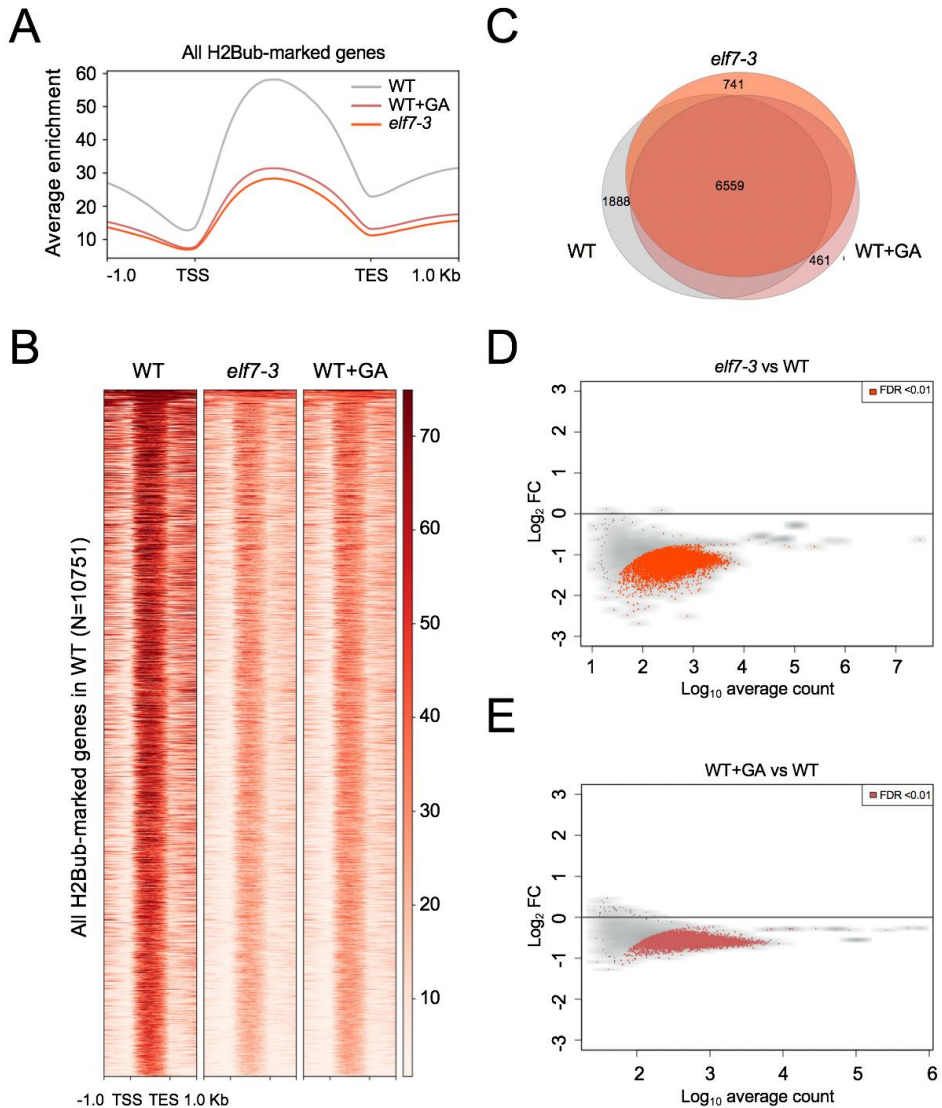


**Fig. 4. DELLAs and ELF7 are required for H2Bub enrichment over protein-coding genes.** (A) Metagene plot of H2Bub distribution over the genes marked in WT seedlings (N=10751). (B) Heatmap showing H2Bub enrichment in WT, WT+GA and *elf7-3* over the genes marked in WT seedlings. Genes are ranked from top to down according to the H2Bub enrichment in the WT. TSS refers to “transcription start sites” and TES to “transcription end sites”. Genes are equally scaled and 1 kb up- and downstream regions are additionally considered. Note that low H2Bub levels were observed in *elf7-3* and WT+GA. (C) Venn diagram showing the number of H2Bub-marked genes in WT, WT+GA and *elf7-3* seedlings and the overlap between the different conditions. (D-E) Differentially ubiquitinated genes (DUGs) are shown as orange or pink dots in *elf7-3* and WT+GA seedlings, respectively. They were determined by Rx-normalised DESeq2 analysis ( $\text{FDR} < 0.01$ ) as described in material and methods section.

happens in the well-characterized Paf1c-dependent Bre1 pathway in yeast (Wood et al., 2003). Hence, in agreement with our hypothesis of DELLAs and Paf1c acting in the same pathway, our data demonstrate that DELLAs and the Paf1c subunit ELF7 are required for H2Bub enrichment over most genes through a mechanism that does not seem to involve the regulation of HUB1/2 chromatin recruitment.

### **DELLAs are required for the recruitment of Paf1c to the chromatin**

The physical interaction of DELLAs with ELF7 provided an appealing hypothesis to explain the observed defects in the H2Bub mark. Still, to rule out that defects observed in WT+GA seedlings were not due to secondary effects from gene expression misregulation, we examined the levels of transcripts encoding Paf1 complex subunits or histone H2B ubiquitination (HUB1/2, UBC1/2 -the Arabidopsis orthologs of Rad6-) or deubiquitination (UBP22, SGF11, ENY2) machineries. Our transcriptomic analysis showed that the transcript levels of all these genes were not affected by the GA treatment (Fig. S5A, Supp. Tables 1 and 5). Analysis of *gai-1* seedlings encoding a GA-resistant version of GAI (Koorneef et al., 1985) grown under the same conditions as for the ChIP-seq gave similar results (Fig. S5B, Supp. Table 5). These results suggested that DELLAs might rather act more directly on H2Bub deposition with Paf1c.

We next investigated the possibility that the DELLA-ELF7 interaction affects Paf1c or HUB1/2 activity at the post-transcriptional level, for instance, affecting protein levels of Paf1c subunits. To test this possibility, we analysed the protein levels response to a GA-treatment by taking advantage of available Arabidopsis transgenic lines expressing tagged subunits, e.g. Flag-ELF7, VIP3-GFP and PHP-Flag (Park et al., 2010; Dorcey et al., 2012; Cao et al., 2015), and also anti-VIP5 (Lu et al., 2017) and anti-HUB1/2 antibodies. As shown in Fig. S6, neither endogenous HUB1/2 and VIP5 proteins nor the tagged proteins Flag-ELF7, VIP3-GFP and PHP-Flag were affected by GA treatments.

Given that both DELLAs and the Arabidopsis Paf1c subunits ELF7, CDC73 and VIP5 have been found to occupy the coding region of a few genes (Yu and Michaels, 2010; Cao et al., 2015; Marín-de la Rosa et al., 2015; Lu et al., 2017; Serrano-Mislata et al., 2017), we wondered if DELLAs affect the recruitment of Paf1c to the chromatin. To address this question, we first determined whether ELF7 association to gene bodies is a general trend in

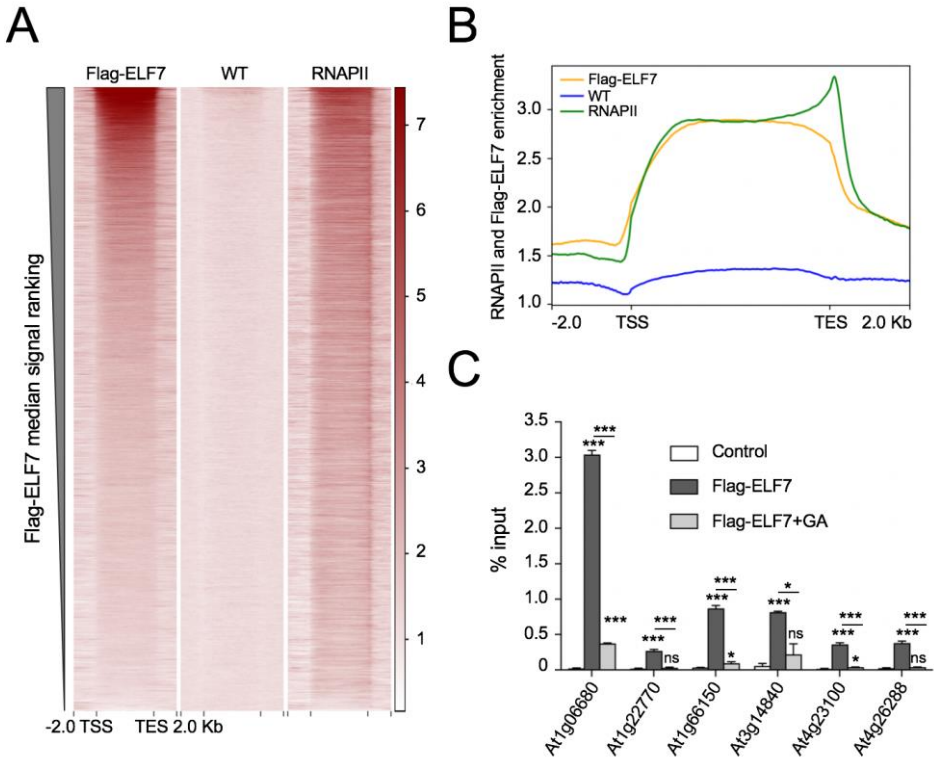


**Fig. 5. DELLAs regulate Paf1c recruitment to the chromatin.** (A) Heatmap showing that Flag-ELF7 associates over a large gene repertoire ( $N=11,708$ ) and its occupancy correlates with RNAPII. Genes are ranked from top to down according to Flag-ELF7 signal. (B) Median enrichment of Flag-ELF7 over the 11,708 genes targeted by Flag-ELF7. The distribution of RNAPII is also shown. TSS refers to “transcription start sites” and TES to “transcription end sites”. Genes are equally scaled and 2 kb up- and downstream regions are additionally considered. (C) ChIP-qPCR analysis of Flag-ELF7 at the gene bodies or 5' end (only for GI) of six randomly selected genes in the presence vs the absence of GA in the growth media. Fold enrichment is given as percentage of IP/Input. Error bars represent standard deviation from 3 technical replicates. The experiment was repeated three times and similar results were obtained. Unpaired t-test was performed to evaluate the statistical significance of differences between each line/condition: \*  $p < 0.01$ ; \*\*  $p < 0.001$ ; \*\*\*  $p < 0.0001$ ; ns, non-significant.

Arabidopsis as in yeast and mammals (Mayer et al., 2010; Yang et al., 2016) by ChIP-seq analysis of the Flag-ELF7 transgenic line. To improve the ChIP efficiency, we used an EGS/formaldehyde dual crosslinking to obtain robust signals with discrete peaks in the transgenic line while no significant background was found in WT plants used as mock (Fig. 5A, Fig.S7). Flag-ELF7 profiles display several notable features. First, 11,708 ELF7 peaks were identified (usually one peak per protein-coding gene) (Fig. 5A, Supp. Table 6). This number is considerably higher than the 1,381 DEGs identified by RNA-seq analysis (Fig. 2B and C,

Supp. Tables 1), a situation that parallels what occurs in human cell lines (Yu et al., 2015). Still, ELF7 appears to target 56% of misregulated genes in *elf7-3* seedlings (Fig S8A, Supp. Table 6) and 75% of the genes commonly misregulated in *elf7-3* and WT+GA seedlings (Fig S8B, Supp. Table 6). Second, the genomic profile of ELF7 along the genes is similar to that of the yeast ortholog Paf1 (Mayer et al., 2010), exhibiting the most significant enrichment over gene bodies and tapering off toward the transcription start sites (TSS) and transcription end sites (TES) (Fig. 5A and B). Its genomic distribution also matches the distribution of RNAPII obtained using seedlings grown under similar conditions (Fig. 5B) and is positively correlated with transcript level, i.e. higher Flag-ELF7 enrichment over most expressed genes (Fig. S9A). This is in agreement with a conserved role of Paf1c being required for efficient transcription elongation in plants. Third, comparison with our H2Bub profiles revealed that almost two-thirds of the H2Bub-marked genes are occupied by Flag-ELF7 at the seedling stage (Fig. S9B, Supp. Table 6). Nevertheless, ELF7 chromatin association is also found over hundreds of genes without H2Bub marking (Fig. S9B and C, Supp. Table 6), and we identified hundreds of genes with a Flag-ELF7 peak but no H2Bub (see examples in Fig. S7 and 9C). The latter observations suggest that, as in mammalian cells (Yang et al., 2016), ELF7 may not be strictly linked to H2B monoubiquitination. They could also possibly rely on H2Bub dynamic erasure during transcription or, conversely, on differential steady levels of ELF7 and H2Bub.

Taken together, our genome wide analyses indicate that ELF7 specifically targets transcriptional domains of genes. To test whether this association was responsive to GA, we next determined Flag-ELF7 enrichment upon GA treatment. Remarkably, the six randomly selected target genes examined by ChIP-qPCR (described in Fig. S7 and Supp. Table 6) displayed lower Flag-ELF7 peaks in the presence of GA (Fig. 5C). These results strongly suggest that DELLAs are required for proper recruitment of ELF7 to target loci.

### **RNAPII occupancy and distribution is dependent on DELLAs and ELF7**

Paf1c is required to define the global distribution of RNAPII in metazoans (Yu et al., 2015; Chen et al., 2015). Hence, we investigated if Paf1c performs a similar role in plants and the possible influence of DELLAs. For that purpose, we determined the global occupancy of total RNAPII by ChIP-seq in same genotypes as the H2Bub analysis. The RNAPII showed a biphasic distribution over the ELF7-occupied genes in the WT, with peaks around the TSS and TES (Fig. 6A and B). Both the occupancy and distribution were, nonetheless, affected in



*elf7-3* seedlings (Fig. 6A and B). The overall occupancy was reduced in the mutant, being more evident around the TSS, where the RNAPII peak was strongly reduced (see Fig. 6C for an example). Importantly, the same trend was observed in WT+GA seedlings, albeit of reduced magnitude. These results suggest (i) that Paf1c is required for RNAPII to reach proper levels and distribution, at least over ELF7-target genes, in agreement with ELF7 interacting with elongating RNAPII and other transcription elongation factors in Arabidopsis (Antosz et al., 2017); and (ii) that this role is likely dependent on DELLA activity.

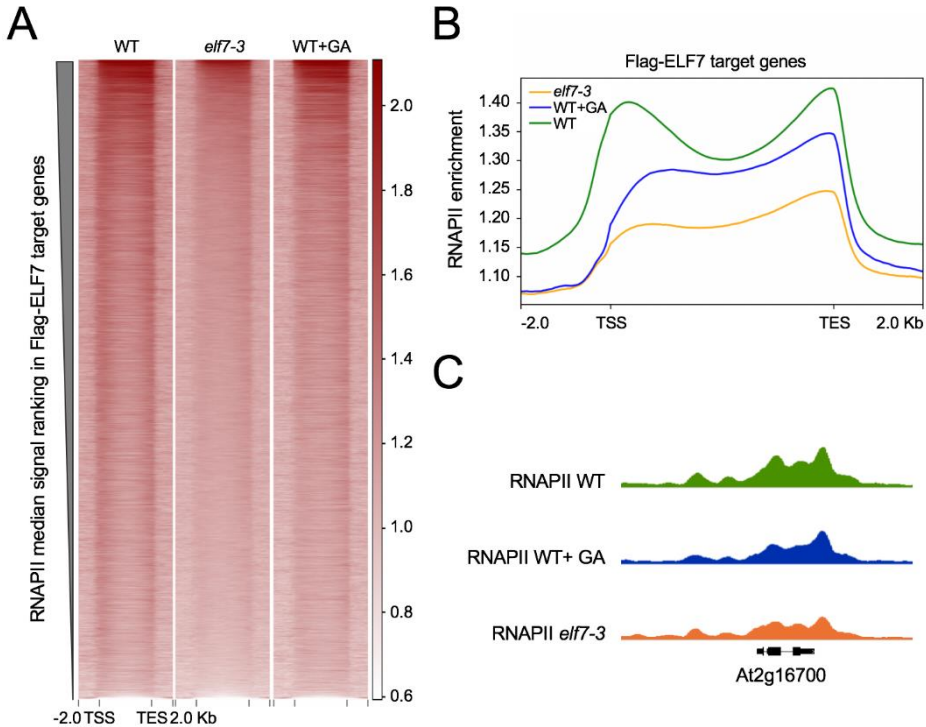


**Fig. 6. RNAPII distribution is altered in WT+GA and *elf7-3* seedlings.** (A) Heatmap showing RNAPII median signal in Flag-ELF7 target genes (N=11,708). Genes are ranked from top to down according to RNAPII signal. (B) Median enrichment of RNAPII over the 11,708 genes targeted by Flag-ELF7 in WT, WT+GA and *elf7-3* seedlings. TSS refers to “transcription start sites” and TES to “transcription end sites”. Genes are equally scaled and 2 kb up- and downstream regions are additionally considered. (C) Genome browser track example of RNAPII ChIP-seq in WT, WT+GA and *elf7-3* seedlings. All tracks are equally scaled. At2g16700 encodes the actin depolymerizing factor 5 (ADF5) and it is a Flag-ELF7 target gene. ADF5 gene is not misregulated in WT+GA or *elf7-3* mutant seedlings. Note that graphs shown (A-C) results from the data of a single biological replicate.



### 3. Discussion

The current evidence supporting a role for the Paf1c as a transcription elongation factor in plants relies in its interaction *in vivo* with transcription elongation factors and with elongating RNAPII (Antosz et al., 2017), and in the reduction in the transcription elongation mark H2Bub in mutants with impaired Paf1c, analysed by immunoblots (Cao et al., 2015). In this work, we show that the scope of Paf1c action is genome-wide, being required for the global distribution of H2Bub and the RNAPII in plants, acting therefore as a transcription elongation factor. Importantly, we show Paf1c activity is dependent on the presence of DELLA proteins, uncovering a mechanistic connection between DELLAs and Paf1c that broadens the portfolio of mechanisms by which DELLA proteins regulate gene expression.

A relevant question is whether the activity of the plant Paf1c is required for RNAPII activity, as occurs in yeast and animals. Paf1c is necessary for the deposition in gene bodies of H3 marks associated to active gene transcription in Arabidopsis (Oh et al., 2008). We show here that it is also required for the genome-wide distribution of H2Bub, another well-known mark that stimulates transcription elongation in different organisms and whose defects cause gene expression alterations (Weake and Workman, 2008; Feng and Shen, 2014; Van Lijsebettens and Grasser, 2014). Our results point out that Paf1c recruitment to chromatin and the associated histone H2B monoubiquitination leads to RNAPII chromatin enrichment along transcriptional units. The reduction in chromatin associated RNAPII would result in lower transcription. Indeed, our observations indicate that either absence of DELLA proteins or impaired Paf1c function cause a qualitatively similar, global reduction in the amount of RNAPII along the ELF7 target genes, especially along the 5' domains of gene bodies (Fig. 6). Interestingly, the particular reduction of RNAPII around TSSs is reminiscent of the situation observed in the human cells where knocking-down the Paf1 subunit reduces RNAPII pausing just downstream of the TSS and acts as a regulatory checkpoint for transcription (Chen et al., 2015). Although recent studies indicate that pausing also occurs in Arabidopsis (Zhu et al., 2018; Kindgren et al., 2020), no regulators of this process have been identified so far. Collectively, these observations led us to propose that Paf1c and DELLAs are required for proper RNAPII distribution in genes and that both might exert a role in RNAPII pausing regulation.

In future studies, stronger evidence is needed to demonstrate our model. In particular, our RNAPII ChIP-seq experiments indifferently detects all chromatin-bound RNAPII isoforms, including elongating and stalled ones, which reduces the resolution of our approach. To

determine whether RNAPII engagement and elongation is actually targeted by DELLAs and Paf1c, an analysis by plant native elongating transcript sequencing would be required (pNET-seq, Zhu et al., 2018; Kindgren et al., 2020).

Our data indicate that the role of DELLAs in the regulation of gene expression goes well beyond the modulation of the activity of TFs through a modulation of RNAPII elongation itself. Given the emerging role of DELLAs as modulators of a broad range of genetic circuits and the intrinsic benefit of coordinating successive steps during transcription, it is not surprising that DELLAs also influence the activity of the basal transcriptional machinery. Nonetheless, what is more striking to us is that their effect on the activity of the transcription elongation factor Paf1c appears on such a global scale, most likely resulting from an upstream process (Fig. 4, 5, and 6). Several lines of evidence suggest that DELLAs are necessary for Paf1c recruitment to target genes. First, the behavior of H2Bub and RNAPII in the absence of DELLAs or in the *elf7-3* mutant is qualitatively similar, still being stronger in the case of *ELF7* loss-of-function (Fig. 4 and 6). Second, the amount of recruited Flag-ELF7 to the loci tested is strongly reduced in the absence of DELLAs (Fig. 5C). Third, protein levels of Paf1c subunits do not change in response to GAs (Fig. S6). The simplest model to explain the above observations is that DELLAs modulate the recruitment of Paf1c (or at least of ELF7) to the chromatin (Figure 7). The physical interaction between DELLAs and ELF7, led us to speculate about two non-mutually excluding possibilities to explain this modulation. First, DELLAs might facilitate the assembly of Paf1c, assuming this step is necessary for its chromatin recruitment. Second, DELLAs might promote post-translational modifications of ELF7 necessary for its activity. Accordingly, ELF7 is phosphorylated in at least seven residues in Arabidopsis (<https://www.psb.ugent.be/webtools/ptm-viewer/protein.php?id=AT1G79730.1>). Although the direct interaction DELLA-ELF7 seems a plausible explanation for the effect of DELLAs, we cannot rule out the possibility of them being required for the expression or the activity of proteins involved in the recruitment of Paf1c to chromatin. In order to discriminate between these possibilities, the generation of the double transgenic line *gai-1-GR Flag-ELF7* will be very useful, since we could assay the inducible activity of the GA-insensitive *gai-1-GR* fusion in the absence of protein synthesis by simultaneous treatment with the inductor dexamethasone and the translation inhibitor cycloheximide, and thus check whether the *gai-1-GR* can restore the Flag-ELF7 association to its target genes in the presence of GAs.

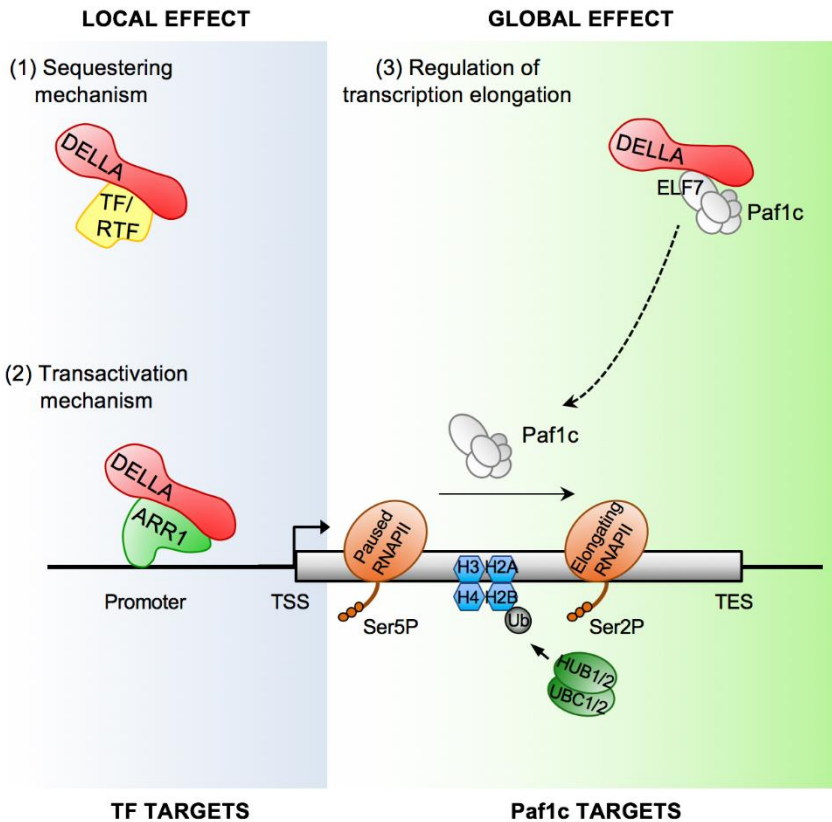


**Fig. 7. Proposed model depicting the role of DELLAs regulating transcription elongation.** In addition to their role modulating the activity of TFs or regulators of TFs (RTF) [see mechanisms (1) and (2)], DELLAs are required for the recruitment of Paf1c to the chromatin, which is necessary to reach adequate levels of H2Bub (mediated by HUB1/2-UBC1/2) and RNAPII.

The presence of DELLAs in gene bodies was the initial observation that prompted us to investigate novel mechanisms of DELLA action. Our results showing that effects of reduced DELLA activity on the H2Bub mark and in the distribution of the RNAPII are genome-wide, paralleling those caused by impaired Paf1c, would argue, however, against such effects being local at each ELF7-targeted locus, as DELLAs seem to occupy a much smaller number of gene bodies (Serrano-Mislata et al., 2017) than Flag-ELF7 (Fig. 5A, Supp. Table 6). DELLAs, therefore, would be recruited to gene bodies by other proteins/protein complexes different to Paf1c.

The activity of the RNAPII has to be tuned with the environment. The current view indicates that the Mediator complex relays environmental information to the RNAPII by integrating signalling from TFs (Samanta and Thakur, 2015). We propose that the DELLA-Paf1c pathway also feeds the RNAPII with information from the surrounding environment, thanks to the high sensibility of GA and DELLA levels to changes in the environmental conditions (Sun, *Curr Biol*, 2011; Chapter 1). But, what could be its physiological relevance? It is tempting to speculate that GAs have a negative impact on transcription (due to lower levels of chromatin associated RNAPII), causing a general reduction in the transcription regime led to save energy and re-allocate resources. GA levels are tightly regulated in the plant and bursts in GA production, leading to a reduction in DELLA levels, are usually associated to particular windows of its life cycle (e.g. germination, skotomorphogenesis, flowering, etc), developmental transitions when most energy resources need to be dedicated to rapid growth. This also includes the reversible response to changes in the light quality (shade) or ambient temperature (warmth) that provoke rapid elongation of different organs. In these cases, if the environmental change persists, GAs finally contribute to accelerate flowering to rapidly complete the life cycle of the plant. This situation would be reminiscent of COP1 function, as high COP1 activity is normally associated to physiological responses where GA levels are also high (see Chapter 1). In all these contexts, proper re-allocation of energy resources by reducing the transcription of all Paf1c-dependent genes by GAs might be key for adaptation to the environmental change or for the progression of the developmental response. This mechanism could act simultaneously with other DELLA-dependent gene regulation mechanisms (Fig. 7). The quantification of transcription rates in response to different environments and the determination of the influence of Paf1c and DELLAs would help us to ascertain if our hypothesis holds.

## 4. Material and methods

### Plant material.

All the Arabidopsis lines used in this work have been previously described: *elf7-3* (He et al., 2004), *hub 1-3 hub2-2* (Liu et al., 2007), *pRGA:GFP-RGA* (Silverstone et al., 2001), *PHHp:PHP-Flag php-1* (Park et al., 2010) and *ELF7p:Flag-ELF7 elf7-3* (Cao et al., 2015) are in the Col-0 background; *gai-1* (Koorneef et al., 1985) in the Ler background; and, *VIP3-GFP* was obtained in the Sav-0 ecotype (Dorcey et al., 2012). The *pRGA:GFP-RGA ELF7p:Flag-ELF7* double transgenic line was generated by genetic crosses.

## Growth conditions and treatments

All seeds were surface sterilized and sown on half-strength MS (Duchefa) plates containing 1% (w/v) sucrose, 8 g/L agar (pH 5.7). Seedlings were grown at 22°C under continuous light (50-60  $\mu\text{mol m}^{-2} \text{s}^{-1}$ ) (our standard conditions). WT+GA samples were obtained by directly sowing seeds in MS plates supplemented with 100  $\mu\text{M}$  GA<sub>3</sub> (Sigma). For the Co-IP experiment, 3-day-old seedlings grown on sterile filter papers placed on MS plates were transferred to MS supplemented with 10  $\mu\text{M}$  paclobutrazol (PAC) or the corresponding control (acetone) for 4 days.

## Yeast two-hybrid assays

pENTR223 vectors carrying the coding sequence (CDS) of UBC1, SAP18, MED31, ELF7, VIP3, VIP4, CDC73, Phf5a, CDKD;2, CDKC;2, CYCT1;4, LSM1b, LSM2, LSM3a, LSM5, LSM6, LSM7, LSM8, SmB, SmD1a and SmEb were obtained from SALK Institute and transferred to the pGADT7 vector (Clontech) by an LR reaction (Thermo-Fisher Scientific). pDONR221 LSM4 was obtained by a BP reaction (Thermo-Fisher Scientific) after amplifying LSM4 by two consecutive PCRs, using first the oligos

Fw\_CAGGCTTCATGCTTCCTCTATCGCTGCTT  
and Rv\_GCTGGGTCTCAACCACGGCCGCGACC

and then the oligos

Fw\_GGGGACAAGTTTGTACAAAAAAGCAGGCTTC  
and Rv\_GGGGACCACTTTGTACAAGAAAGCTGGGTC).

The pGADT7 LSM4 was obtained as described above. The pGADT7 VIP5 vector was generated using gene synthesis (GenScript, USA). pGBKT7 M5-GAI and RG52 plasmids were previously described (Marín-de la Rosa et al., 2015). The M5-truncated versions for RGL1, RGL2 and RGL3 in pGBKT7 were kindly provided by Prof Salomé Prat (CNB, Spain). The yeast strains Y2HGold and Y187 (Takara Bio Inc) were transformed with the constructs in pGBKT7 and pGADT7 vectors, respectively, following the Clontech small-scale LiAc yeast transformation procedure. Yeast diploid cells carrying both plasmids were obtained by mating, and interaction tests were assayed on selective media (SD/-Trp/-Leu/-His) containing 3-aminotriazol (3-AT) (Sigma).

### **Bimolecular fluorescence complementation assay**

The pMDC43-YFC GAI vector was previously used (Crocco et al., 2015). ELF7 CDS was transferred into pMDC43-YFN vector (Belda-Palazón et al., 2012) by Gateway using the LR clonase (Thermo-Fisher Scientific). Each construct was introduced into *Agrobacterium tumefaciens* C58 cells which were used to infiltrate 4-week-old *Nicotiana benthamiana* leaves. BiFC samples were mixed in a 1:1 ratio to a total optical density (OD<sub>600nm</sub>) of 0.2. After 3 days, microscopy images were collected using a Zeiss LSM780 confocal microscope. YFP fluorescence was detected at 520-560 nm after excitation with an Argon laser (488 nm).

### **Co-immunoprecipitation assays**

The ground frozen tissue (occupying a volume of 1 mL) was homogenized in 500 µL of extraction buffer (25 mM Tris-HCl pH 7.5, 10% glycerol, 1 mM EDTA pH 8.0, 150 mM NaCl, 10 mM DTT, and 1x protease inhibitor cocktail [cComplete, EDTA-free; Roche]) and incubated on ice for 15 min. Extracts were centrifuged twice for 15 min at full speed at 4°C and proteins were then quantified by the Bradford assay. 100 µg of total proteins were denatured in Laemmli buffer and set aside to be used as input. One mg of total proteins was incubated for 2 h at 4°C in a rotating wheel with 50 µL of anti-GFP-coated paramagnetic beads and loaded onto µColumns (Miltényi) at room temperature. Columns were washed twice with 700 µL of cold extraction buffer and proteins were eluted under denaturing conditions in 70 µL of elution buffer following manufacturer's instructions. The inputs and immunoprecipitates were analysed by Western blot (see immunoblot analysis section).

### **Gene expression analysis**

Two different RNA-seq with three independent biological replicates for each condition/genotype were performed. In both cases, seedlings were grown under our standard conditions (see growth conditions and treatments section). For the first RNA-seq, 7-day-old WT Col-0, WT+GA and *elf7-3* seedlings were collected. A second RNA-seq series was performed using 7-day-old WT Ler and *gai-1* seedlings. Total RNA was extracted with a RNeasy Plant Mini Kit (Qiagen) according to the manufacturer's instructions. The RNA concentration and integrity [RNA integrity number (RIN)] were measured in an RNA nanochip (Bioanalyzer, Agilent Technologies 2100) by the IBMCP Genomics Service. The preparation of the libraries and the sequencing were carried out by the Genomics Service of the University of Valencia. Reads were mapped to the Arabidopsis reference genome

using TopHat (Trapnell et al., 2012) with default parameters. Transcripts counts were calculated with HTSeq-count software (Anders et al., 2015) and differentially expressed genes (DEG) were identified with DESeq2 (FC  $\geq 1.5$ ,  $p$  adj. value  $< 0.01$ ) (Supp. Table 1). The normalized expression values for each gene were calculated as reads per kilobase million (RPKM) (Supp. Table 5). The volcano plots and the heatmap representation were generated with the EnhancedVolcano (Blighe, 2019) and Pheatmap (Kolde, 2015) R packages, respectively. GO annotations (including biological processes(BP), molecular functions(MF) and cellular components(CC); see Supp. Table 2) were assigned with the clusterProfiler R package (Yu et al., 2012) using as  $p$ -value and  $q$ -value cut-offs 0.01 and 0.05, respectively. BP categories that were over-represented among the DEG were summarized in Fig. 3A through the method implemented by Wang et al (2007) in the GOSemSim R package (Yu et al., 2010) using the adjusted  $p$ -value and applying a similarity cut-off of 0.7. The GOChord plot was done with GOplot (Walter et al., 2015) in order to show some common DEG in WT+GA and *elf7-3* mutant seedlings in certain GO categories. For the meta-analysis with the Flag-ELF7 genomic distribution (see chromatin immunoprecipitation analysis section), genes were split into 5 groups based on the RPKM in WT Col-0 seedlings (RPKM=0-1, RPKM=1-10, RPKM=10-100, RPKM=100-1000, RPKM above 1000).

## ChIP experiments

H2B and H2Bub ChIP-Rx were conducted in parallel using the same two biological replicates of 7-day-old WT, WT+GA and *elf7-3* seedlings grown under our standard conditions. For each biological replicate, two immunoprecipitations (IP) were performed using an anti-H2Bub antibody (MM-0029-P, Medimabs) and one using an anti-H2B (ab1790, abcam). 100  $\mu$ g of Arabidopsis chromatin mixed with 3  $\mu$ g of *Drosophila* chromatin was used for each IP as previously described (Nassrallah et al., 2018). DNA eluted from the two technical replicates of H2Bub IP was pooled before library preparation. Library preparation and sequencing were carried out by the CRG Genomics Core Facility (Barcelona, Spain). In a second series, Flag-ELF7 ChIP-seq was performed using 7-day-old WT Col-0 and Flag-ELF7 *elf7-3* samples and an anti-Flag M2 antibody (F1804, Sigma) and a double *in vitro* crosslinking as recently described (Bourbousse et al., 2018; Fiorucci et al., 2019) using 1.5 mM ethylene glycol bis (succinimidyl succinate) for 20 min and then with 1% formaldehyde for 10 min at room temperature. Library preparation and sequencing were carried out by the CRG Genomics Core Facility (Barcelona, Spain). A third series was performed using the anti-RNAPII antibody (active motif, Clone: 4H8) using similar growth conditions and protocol

than for H2Bub profiling without *Drosophila* cells spike-in. Library preparation and sequencing were carried out by the Epigenomics platform at IPS2 (Paris, France). Finally, ChIP-qPCR experiments were performed using the primers described by (Bourbousse et al., 2012) and included in Supp. Table 7. ChIP DNA was analysed on 7500 Fast Real-Time PCR System (Applied Biosystems) with SYBR Premix Ex Taq II (Tli RNaseH Plus) ROX plus (Takara Bio) according to the supplier's instructions. Three biological replicates, each including three technical qPCR replicates, were performed. Enrichments were determined as IP/Input ratios.

### ChIP-seq bioinformatics

H2B and H2Bub ChIP-Rx data were analysed using the corresponding *Arabidopsis* and *Drosophila* reads in each Input and IP samples individually according to Nassrallah et al. (2018). To account for an additional normalization of H2Bub levels with respect to histone H2B occupancy, H2Bub enrichment was determined using H2B ChIP IP/Input ratio as Input instead of cognate H2Bub Input from the same sample (as described in Zhang et al., 2008). For tracks visualization, IGV version 2.7.22.7.2 (Thorvaldsdóttir et al., 2013) browser tracks were obtained by scaling MACS2 values in the bedgraph pilup files with the Rx normalization factors described above. Upon confirmation of consistency between biological replicates by Hierarchical dendrogram clustering based on Spearman correlation, by Heatmap representation based on Euclidean distance between samples based on read counts per gene, and by Principal component analysis (PCA) projection, values obtained for replicates were averaged and converted to bigwig files. To determine H2Bub-marked genes (included in Supp. Table 3), H2Bub enriched domains reproducibly detected using MACS2 in the two biological replicates with an FDR<0.01 were intersected using Bedtools Utility Intersect version v2.27.1 (Quinlan and Hall, 2010). Only peaks exhibiting intersection regions beyond 10 % of input peak lengths were kept. The resulting peaks from all samples were merged and annotated with TAIR10 gene coordinates extended to -250 pb from gene TSS to TES. Only genes that had intersection regions greater than 150 bp (~one nucleosome) with the resulting peaks were kept. To determine the differentially marked genes by H2Bub (Supp. Table 4), the number of reads mapping into the peak coordinates of each replicate sample was calculated using Bedtools Utility Multicov and the peaks from all samples were grouped by gene-ID to obtain unique peak coordinates per marked gene using Bedtools Utility Groupby (Quinlan and Hall, 2010). The coverage values from all samples were then scaled



using Rx factors, and used for DESeq2 version 1.19.37 (Love et al., 2014) analysis using Wald test. Plots were produced with R software version 3.5.2.

ChIP-seq analysis of Flag-ELF7 and RNAPII samples were conducted as in (Fiorucci et al., 2019). Briefly, reads were mapped to TAIR10 genome and peaks were identified using MACS2 (see Sup. Table 6). Flag-ELF7 target genes were considered when a peak overlapped at least 150 pb within the gene body and 250 pb upstream of the TSS (considered as promoter region). For the meta-analysis with RNAPII occupancy shown in Fig. 5B, the RNAPII data was obtained from (Fiorucci et al., 2019). Metagene plots and heatmaps were drawn with Deeptools protProfile and plotHeatmap, respectively.

### Subcellular fractionation

Cytoplasmic, nucleoplasmic and chromatin-associated fractions were obtained as described (Liu et al., 2018a) with minor modifications. Briefly, about 1.5 grams of 7-day-old seedlings were ground in liquid nitrogen and homogenized in 3-4 mL of Honda buffer (0.44 M Sucrose, 20 mM HEPES KOH pH 7.4, 2.5% Percoll, 5% Dextran T40, 10 mM MgCl<sub>2</sub>, 0.5% Triton X-100, 5mM DTT, 1 mM PMSF, and 1x protease inhibitor cocktail [cOmplete, EDTA-free; Roche]). The homogenate was filtered through two double layers of Miracloth and the flow-through was centrifuged at 2,400g for 10 min at 4°C. The supernatant (1 mL) was spun at 10,000 g for 10 min at 4°C and collected as cytoplasmic fraction. The pellet was resuspended in 1 mL Honda buffer and centrifuged at 1,800 g for 5 min at 4°C to concentrate crude nuclei. This pellet was then washed for 4-6 times with Honda buffer and rinsed with PBS buffer (137 mM NaCl, 2.7 mM KCl, 10 mM Na<sub>2</sub>HPO<sub>4</sub>, 2 mM KH<sub>2</sub>PO<sub>4</sub>) containing 1 mM EDTA. The pellet was resuspended in 150 µL of cold glycerol buffer (20 mM Tris-HCl pH 7.9, 50% glycerol, 75 mM NaCl, 0.5 mM EDTA, 0.85 mM DTT, 0.125 mM PMSF, and 1x protease inhibitor cocktail [cOmplete, EDTA-free; Roche]) and gently vortexed twice after adding 150 µL of cold nuclei lysis buffer (10 mM HEPES KOH pH 7.4, 7.5 mM MgCl<sub>2</sub>, 0.2 mM EDTA, 0.3 M NaCl, 1 M urea, 1% NP-40, 1 mM DTT, 0.5 mM PMSF, 10 mM β-mercaptoethanol, and 1x protease inhibitor cocktail [cOmplete, EDTA-free; Roche]). The mixture was incubated for 2 min on ice and centrifuged at 14,000 rpm for 2 min at 4°C. The supernatant was collected as nucleoplasmic fraction. The chromatin-associated pellet was rinsed with PBS buffer containing 1 mM EDTA and then resuspended in 150 µL cold glycerol buffer and 150 µL cold nuclei lysis buffer. Protein concentrations were determined by using the Pierce 660 nm protein assay (Ref. 22662) according to the manufacturer's

instructions. The different fractions were analysed by Western blot (see immunoblot analysis section).

### Immunoblot analysis

Total protein extracts, immunoprecipitates and subcellular fractionation samples were separated by SDS-PAGE, transferred to PVDF membranes and immunolabeled with specific antibodies against anti-Flag (1:1000, Sigma, Ref #F1804), anti-GFP (1:5000, JL-8 Takara Bio Clontech), anti-HUB1/2 (1:2000, this study), anti-DET3 (1:10000, provided by Karin Schumacher), anti-Rtf1 (1:1000, ab84564, abcam), anti-H3 (1:5000, ab1791, abcam) or anti-tubulin (1:1000, Invitrogen, Ref #62204). Chemiluminescence was detected with the Supersignal west FEMTO maximum sensitivity substrate (Thermo-Fisher Scientific) and protein bands were detected and quantified using the LAS-3000 Imaging system (Fujifilm) and NIH ImageJ software, respectively. Custom-made rabbit anti-HUB1/2 antibody was obtained by SDIX (USA) using the immunogen sequence MQDTLLIDKYIMDKDIQQGSAYASFLSKKSSRIEDQLRFCTDQFQKLAEDKYQKSVSLENLQKKRADIGNGLEQARSRLSEESHKVEQSRLDYGALELEL.

### Acknowledgements

We thank Christian S. Hardtke (University of Lausanne, Switzerland) for sharing *VIP3-GFP* line, Steven van Nocker (Michigan State University, USA) for *PHPp:PHP-Flag php-1* seeds and Ligeng Ma (Capital Normal University, China) for *elf7-3* and *ELF7p:Flag-ELF7 elf7-3* seeds. We also thank Salomé Prat (CNB, Spain) for providing pGBKT7 RGL1, RGL2 and RGL3 plasmids and Karin Schumacher (University of Heidelberg, Germany) for anti-DET3 antibody. N.B-T was supported by a fellowship from MINECO [BES-2014-068868] and an EMBO Short-Term fellowship (STF n°8047) to visit the Barneche lab. Research in the Alabadí and Blázquez lab was supported by BIO2013-43184-P and BIO2016-79133-P grants from the Spanish Ministry of Economy and Innovation. Research in the Barneche lab was supported by CNRS EPIPLANT Action (France), the COST Action CA16212 INDEPTH (E.U.), the Agence Nationale de la Recherche grants MEMOLIFE (ANR-10-LABX- 54) and ChromaLight (ANR-18-CE13-0004-01).

## 5. Supplemental information

Supplemental tables derived from our RNA-seq and ChIP-seq (Supp. Tables 1 to 7) experiments are available on the following website (Password: NBTVALENCIA2020):

<http://plasticity.ibmcp.csic.es/downloads.html>

**Suppl. Table 1:** Gene lists summarizing differentially expressed genes (DEGs) identified by RNA-seq in WT+GA and *elf7-3* samples. This file also includes the common DEGs of WT+GA and *elf7-3*.

**Suppl. Table 2:** File including GO enrichment categories for WT+GA and *elf7-3* DEGs and for the 202 DEGs that showed a similar trend in WT+GA and *elf7-3*. “BP” is referred to biological processes, “MF” to molecular function and “CC” to cellular components.

**Suppl. Table 3:** File including the genes that are marked with H2Bub in each condition (WT, WT+GA and *elf7-3*).

**Suppl. Table 4:** Differentially ubiquitinated genes (DUGs) in WT+GA and *elf7-3* obtained by DeSeq2.

**Suppl. Table 5:** File including RPKM values for each gene in each biological replicate of WT Col-0, WT+GA, *elf7-3*, WT Ler and *gai-1*.

**Suppl. Table 6:** Gene lists summarizing ChIP-seq analysis of Flag-ELF7 occupancy in WT seedlings and the meta-analysis with H2Bub-marked genes. Flag-ELF7 targets that are also misregulated in *elf7-3* or in WT+GA and *elf7-3* in the same direction are also included.

**Supp. Table 7:** List of primers used for ChIP-qPCR analysis

Primer name	Sequence	Reference
At1g06680(Psb1)Fw	5'-GATCACAGCAACCGTGAATG-3'	Bourbousse et al. (2012)
At1g06680(Psb1)Rv	5'-TGAAGAAAGCAAGCAGAGCA-3'	Bourbousse et al. (2012)
At1g22770(GI)Fw	5'-CATCCGTTTGCCTCTTTCAT-3'	Bourbousse et al. (2012)
At1g22770(GI)Rv	5'-ATTTCTCCACATGCCAAAGC-3'	Bourbousse et al. (2012)
At1g66150(TMK1)Fw	5'-CGTAAGCGTTGGAGGGATAA-3'	Bourbousse et al. (2012)
At1g66150(TMK1)Rv	5'-TTAACCGCAATCTTCGTTCC-3'	Bourbousse et al. (2012)
At3g14840Fw	5'-CTGCAAACAAGATCGGAGAAG-3'	Bourbousse et al. (2012)
At3g14840Rv	5'-GCTTCACCGCGATTACAGTT-3'	Bourbousse et al. (2012)
At4g23100Fw	5'-GGCTGGAAGCCAATTCCTA-3'	Bourbousse et al. (2012)
At4g23100Rv	5'-GCCAATGCTCTCACCTAAA-3'	Bourbousse et al. (2012)
At4g26288Fw	5'-GTCATGCTGCAAAAGGGATT-3'	Bourbousse et al. (2012)
At4g26288Rv	5'-TCATTTAGCTTGGGGCAAC-3'	Bourbousse et al. (2012)

Supplemental figures (Figs. S1 to S9) are shown below:

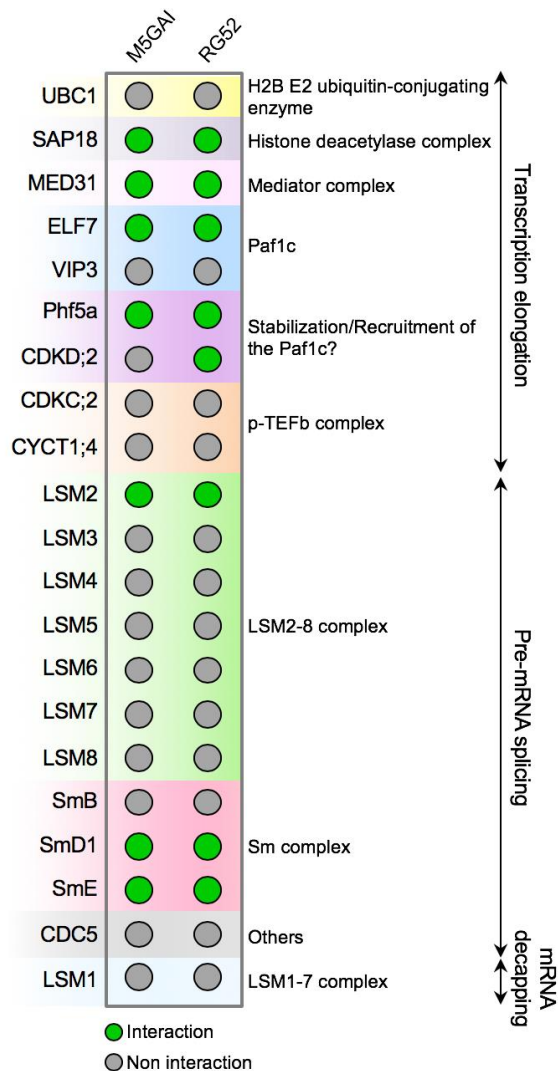


**Fig. S1. DELLA protein interactors found in our Y2H targeted screening.** Representation summarizing the results obtained in our yeast screening using M5-GAI and RG52 as bait and several proteins involved in transcription elongation, pre-mRNA splicing and mRNA decapping as prey. Note that Sm-like proteins (LSMs) LSM2 to 7 are core components of both LSM2-8 and LSM1-7 complexes that are required for pre-mRNA splicing and mRNA decapping, respectively (Perea-Resea et al., 2015; Carrasco-López et al., 2017; Catalá et al., 2019). UBC1, UBIQUITIN CARRIER PROTEIN1 (Cao et al., 2008); SAP18, SIN3 ASSOCIATED POLYPEPTIDE18 (Song and Galbraith, 2006); MED31; MEDIATOR31 (Zhang et al., 2018); ELF7, EARLY FLOWERING 7 (He et al., 2004); VIP3, VERNALIZATION INDEPENDENCE 3 (Park et al., 2010); Phf5a, PHD finger protein 5A (Strikoudis et al., 2016); CDKD;2, Cyclin-dependent kinase D2 (Lu et al., 2017); CDKC;2 CYCLIN DEPENDENT KINASE GROUP C2 (Wang et al., 2014); CYCT1;4, CYCLIN T1;4 (Wang et al., 2014); CDC5; CELL DIVISION CYCLE 5 (Zhang et al., 2013).

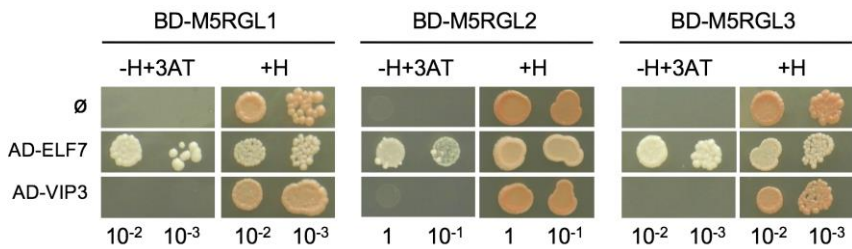


**Fig. S2. RGL1, RGL2 and RGL3 interact with ELF7 but not with VIP3 in yeast.** Y2H assays of the M5 truncated versions of RGL1, RGL2 and RGL3 with the Paf1c subunits ELF7 and VIP3. Ø represents negative control where no sequence was cloned into the activation domain (AD). The serial dilutions (1:10) shown are indicated. +H, control medium depleted of leucine and tryptophan. -H, selective medium also lacking histidine and containing 10 mM 3-aminotriazol (3-AT).

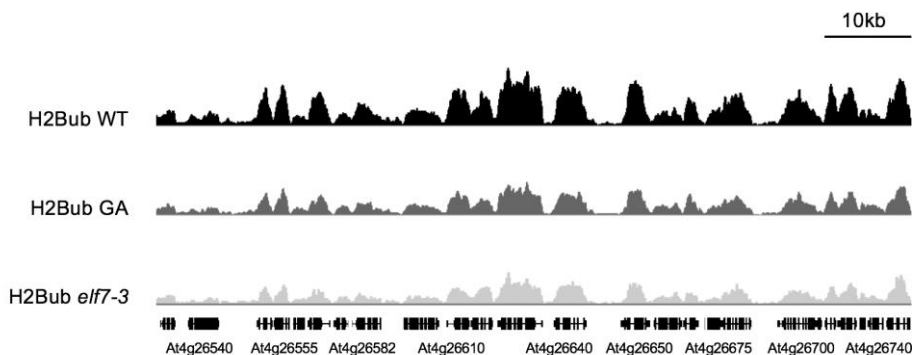


**Fig. S3. H2Bub peaks are lower in the absence of DELLAs or ELF7.** Genome browser snapshots showing H2Bub profiles in WT, WT+GA and *elf7-3* seedlings. All tracks are equally scaled. Each track represents the average data of two independent biological replicates for H2Bub ChIP-Rx.

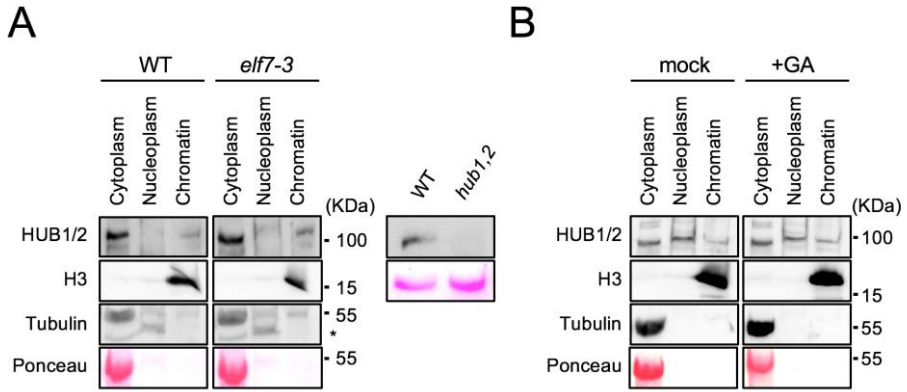


**Fig. S4. Neither loss of function of *ELF7* nor GA treatment result in decrease of HUB1/2 chromatin binding.** (A-B) Detection by Western blot of endogenous HUB1/2 in cytoplasmic, nucleoplasmic and chromatin-associated fractions in wild-type and *elf7-3* mutant seedlings (A) as well as in wild-type seedlings grown in MS+100 $\mu$ M GA<sub>3</sub> (B). Tubulin and Rubisco and Histone H3 were used as cytoplasmic and chromatin-associated fraction markers, respectively. Note that four times less extracts were loaded for the nucleoplasm fraction. The position of molecular weight markers is shown on the right. The asterisk indicates a nonspecific band. The analysis was performed twice with similar results.



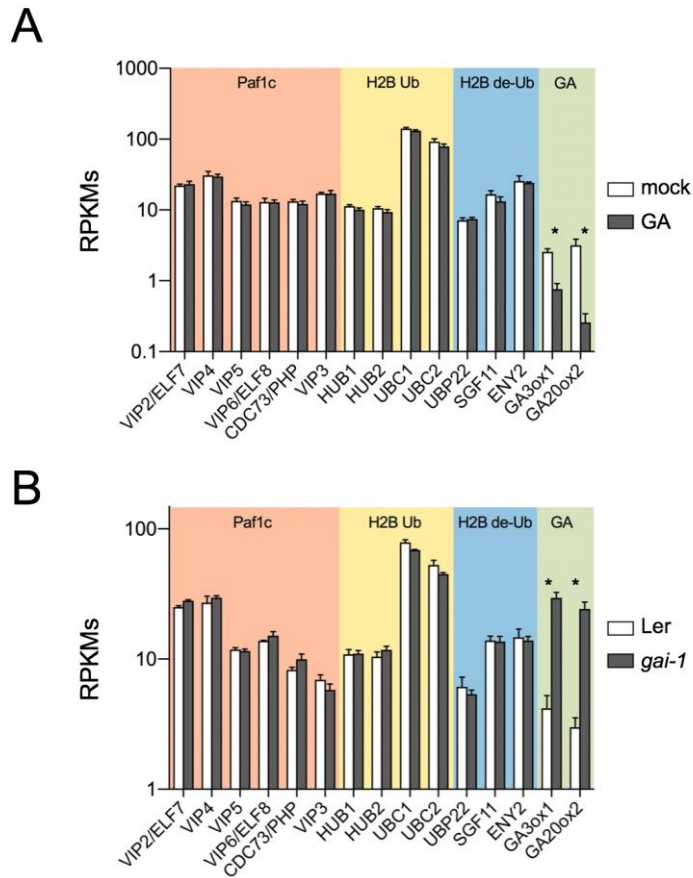


**Fig. S5. H2Bub-related genes expression in Col-0 seedlings grown with GA or mock and in Ler and *gai-1* mutant seedlings.** Note that defects in H2Bub caused by altering DELLA levels are not due to changes in the expression of genes encoding subunits of Paf1c or H2B ubiquitination (Ub)/deubiquitination (de-Ub) modules. *GA3ox1* and *GA20ox2* are shown as examples of differentially expressed genes in GA-treated and *gai-1* mutant seedlings. Both plots show the transcript levels in RPKM extracted from our RNA-seq experiments. Asterisks represent significant differences ( $p < 0.01$ ).

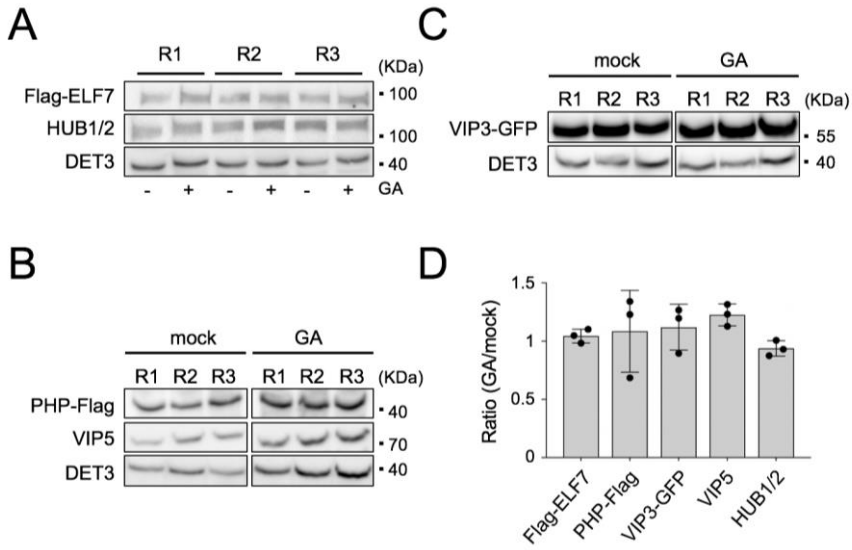


**Fig. S6. Paf1c and HUB1/2 protein levels are not altered by a GA treatment.** (A-D) The levels of Flag-ELF7, HUB1/2 (A), PHP-Flag, VIP5 (B) and GFP-VIP3 (C) were determined in mock- and GA-treated seedlings by Western blot. DET3 was used as loading control. The position of molecular weight markers is shown on the right. The size of the bands corresponds to the expected sizes of the endogenous or the fusion proteins: HUB1 (99.7 KDa), DET3 (42.6 KDa), PHP-Flag (48.5 KDa), VIP5 (71.3 KDa) and VIP3-GFP (61.2 KDa). Flag-ELF7 band was detected around 90-100 KDa (expected size = 68.4KDa). (D) Plot showing the ratio of Paf1c or HUB1,2/DET3 in GA-treated seedlings with respect to mock conditions. Data are average from three biological replicates (shown in plots from A to C). No significant differences were obtained between the two conditions (GA- or mock-treatment) of each genotype ( $p < 0.01$ ).

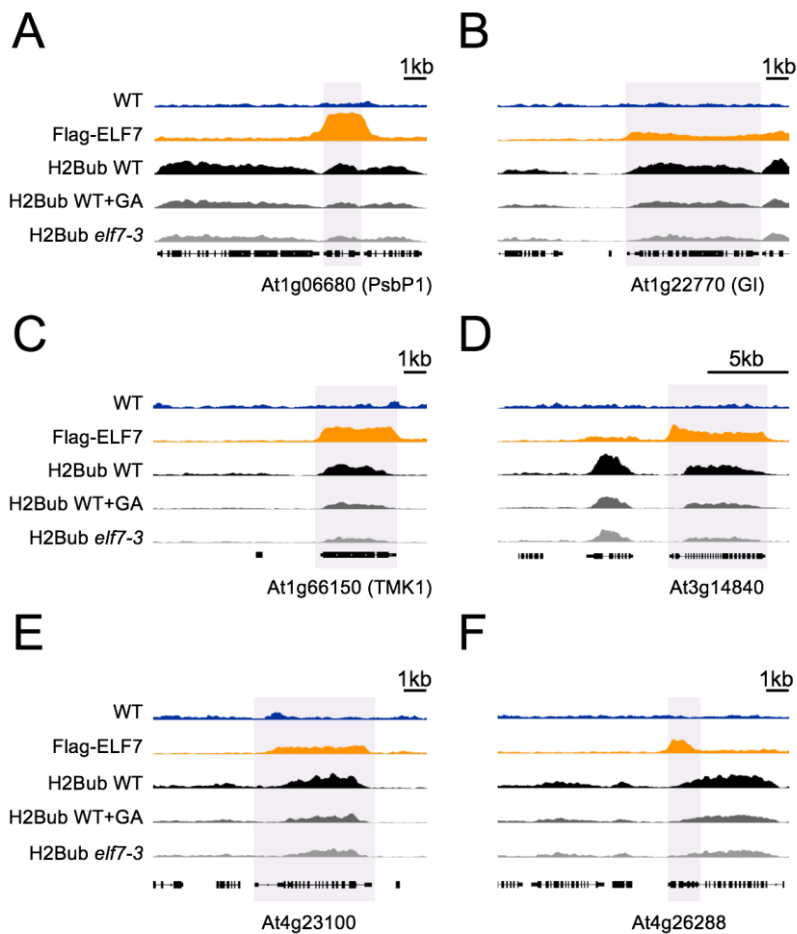
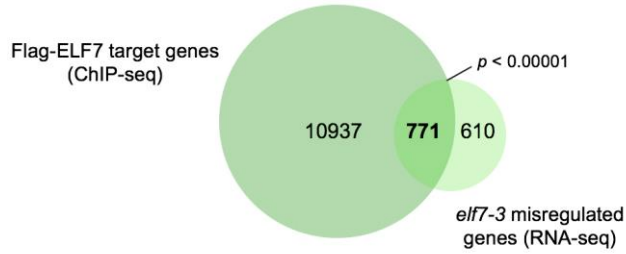


**Fig. S7. The Paf1c subunit ELF7 is recruited to gene bodies.** (A-F) Genome browser track examples of Flag-ELF7 ChIP-seq and of H2Bub ChIP-Rx in WT, WT+GA and *elf7-3*. Each track represents the average data of two independent biological replicates for H2Bub ChIP-Rx and a single replicate for Flag-ELF7 ChIP-seq. The binding of Flag-ELF7 to the highlighted genes was confirmed by ChIP-qPCR as shown in Fig. 5.

2

A



B

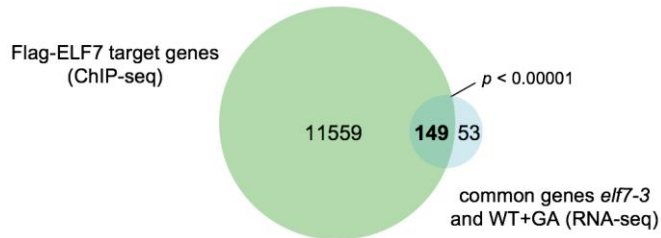
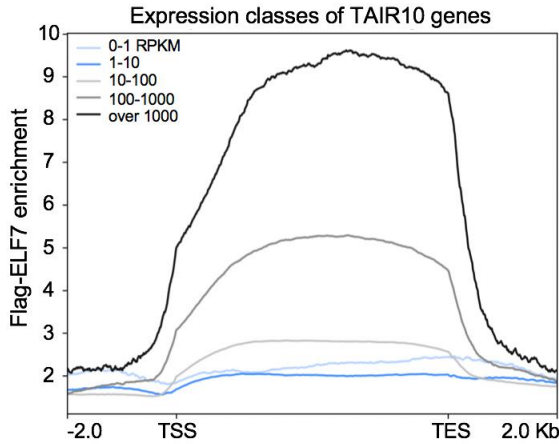
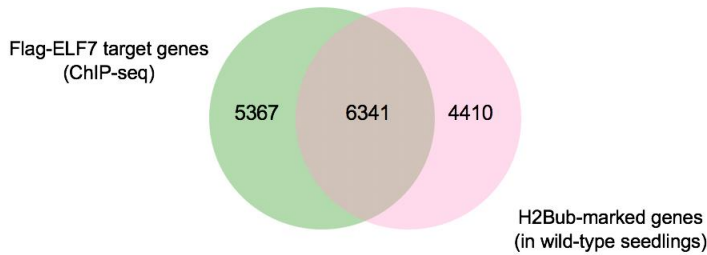


**Fig. S8. Meta-analysis of Flag-ELF7 ChIP-seq data and the transcriptomes of *elf7-3* and WT+GA seedlings.** (A-B) Venn diagram showing the overlap of Flag-ELF7 target genes identified by ChIP-seq and the DEGs identified by RNA-seq in the *elf7-3* mutant (A) or the 202 genes misregulated in the same direction in *elf7-3* and WT+GA seedlings (B).  $p < 0.05$  show significant differences according to the chi square test.

A



B



C

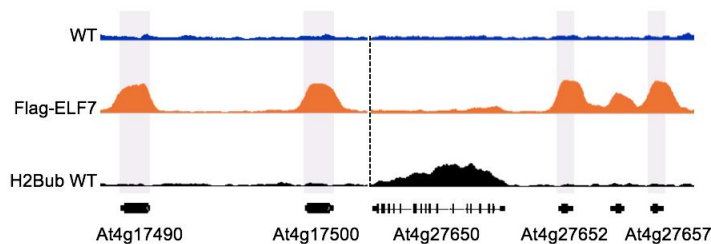


**Fig. S9. Flag-ELF7 occupancy associates with highly expressed genes but is not strictly linked to H2Bub-marked genes.** (A) Mean enrichment of Flag-ELF7 on TAIR10 genes grouped into 5 classes ranked by expression level in wild-type Col-0 seedlings. The five chosen classes include the following number of Flag-ELF7 targets: Group 1 (0-1 RPKM)=825 genes, Group 2 (1-10 RPKM)=2,365 genes, Group 3 (10-100 RPKM)=6,440 genes, Group 4 (100-1000 RPKM)=1,062 genes and Group 5 (over 1000 RPKM)=68 genes. (B) Venn diagram showing the overlap of Flag-ELF7 target genes identified by ChIP-seq and the H2Bub-marked genes. (C) Genome browser track examples of Flag-ELF7 binding in genes without H2Bub mark (also included in Supp. Table 6). Each track represents the average data of two independent biological replicates for H2Bub ChIP-Rx and a single replicate for Flag-ELF7 ChIP-seq.

## 6. References

- Anders, S., Pyl, P.T., and Huber, W.** (2015). HTSeq-A Python framework to work with high-throughput sequencing data. *Bioinformatics*. **31**: 166–169.
- Antosz, W. et al.** (2017). The composition of the Arabidopsis RNA polymerase II transcript elongation complex reveals the interplay between elongation and mRNA processing factors. *Plant Cell*. **29**: 854–870.
- Belda-Palazón, B., Ruiz, L., Martí, E., Tárraga, S., Tiburcio, A.F., Culiáñez, F., Farràs, R., Carrasco, P., and Ferrando, A.** (2012). Aminopropyltransferases Involved in Polyamine Biosynthesis Localize Preferentially in the Nucleus of Plant Cells. *PLoS One*. **7**: e46907.
- Bell, L.** (2019). The Biosynthesis of Glucosinolates: Insights, Inconsistencies, and Unknowns. In *Annual Plant Reviews online*, J.A. Roberts (Ed.).
- Blighe, K.** (2019). Publication-ready volcano plots with enhanced colouring and labeling. R-Package.
- Bourbousse, C., Vegesna, N., and Law, J.A.** (2018). SOG1 activator and MYB3R repressors regulate a complex DNA damage network in Arabidopsis. *Proc. Natl. Acad. Sci. U. S. A.* **115**: E12453–E12462.
- Bourbousse, C., Ahmed, I., Roudier, F., Zabulon, G., Blondet, E., Balzergue, S., Colot, V., Bowler, C., and Barneche, F.** (2012). Histone H2B monoubiquitination facilitates the rapid modulation of gene expression during Arabidopsis photomorphogenesis. *PLoS Genet.* **8**: e1002825.
- Cao, Y., Wen, L., Wang, Z., and Ma, L.** (2015). SKIP Interacts with the Paf1 Complex to Regulate Flowering via the Activation of FLC Transcription in Arabidopsis. *Mol. Plant*. **8**: 1816–1819.
- Cao, Y., Dai, Y., Cui, S., and Ma, L.** (2008). Histone H2B monoubiquitination in the chromatin of Flowering Locus C regulates flowering time in Arabidopsis. *Plant Cell*. **20**: 2586–2602.
- Carrasco-López, C., Hernández-Verdeja, T., Perea-Resa, C., Abia, D., Catalá, R., and Salinas, J.** (2017). Environment-dependent regulation of spliceosome activity by the LSM2-8 complex in Arabidopsis. *Nucleic Acids Res.* **45**: 7416–7431.
- Catalá, R., Carrasco-López, C., Perea-Resa, C., Hernández-Verdeja, T., and Salinas, J.** (2019). Emerging roles of LSM complexes in posttranscriptional regulation of plant response to abiotic stress. *Front. Plant Sci.* **10**: 167.
- Chen, F.X., Woodfin, A.R., Gardini, A., Rickels, R.A., Marshall, S.A., Smith, E.R., Shiekhhattar, R., and Shilatifard, A.** (2015). PAF1, a Molecular Regulator of Promoter-Proximal Pausing by RNA Polymerase II. *Cell*. **162**: 1003–1015.
- Conaway, R.C. and Conaway, J.W.** (2015). Orchestrating transcription with the pol II CTD. *Nat. Rev. Mol. Cell Biol.* **16**: 128.
- Crocco, C.D., Locascio, A., Escudero, C.M., Alabadí, D., Blázquez, M.A., and Botto, J.F.** (2015). The transcriptional regulator BBX24 impairs DELLA activity to promote shade avoidance in *Arabidopsis thaliana*. *Nat. Commun.* **6**: 6202.
- Davière, J.M. and Achard, P.** (2016). A Pivotal Role of DELLAs in Regulating Multiple Hormone Signals. *Mol. Plant*. **9**: 10–20.
- Dorcey, E., Rodriguez-Villalon, A., Salinas, P., Santuari, L., Pradervand, S., Harshman, K., and Hardtke, C.S.** (2012). Context-dependent dual role of SKI8 homologs in mRNA synthesis and turnover. *PLoS Genet.* **8**: 1–9.

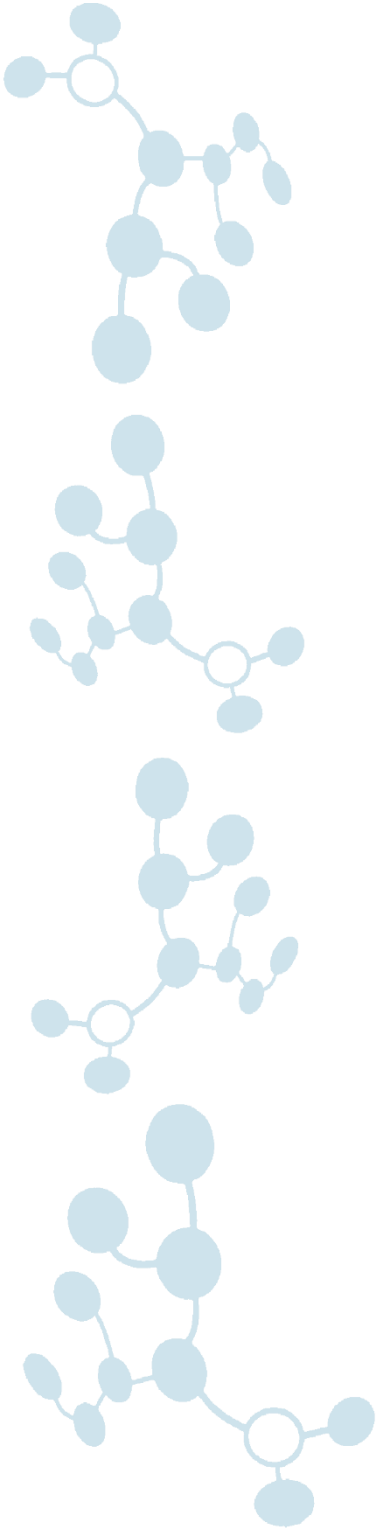
- Ellison, M.A., Lederer, A.R., Warner, M.H., Mavrich, T.N., Raupach, E.A., Heisler, L.E., Nislow, C., Lee, M.T., and Arndt, K.M.** (2019). The Paf1 complex broadly impacts the transcriptome of *Saccharomyces cerevisiae*. *Genetics*. **212**: 711–728.
- Essigmann, B., Güler, S., Narang, R.A., Linke, D., and Benning, C.** (1998). Phosphate availability affects the thylakoid lipid composition and the expression of *SQD1* a gene required for sulfolipid biosynthesis in *Arabidopsis thaliana*. *Proc. Natl. Acad. Sci. U. S. A.* **95**: 1950–1955.
- Feng, J. and Shen, W.H.** (2014). Dynamic regulation and function of histone monoubiquitination in plants. *Front. Plant Sci.* **5**: 1–9.
- Fiorucci, A.S. et al.** (2019). Arabidopsis S2Lb links AtCOMPASS-like and SDG2 activity in H3K4me3 independently from histone H2B monoubiquitination. *Genome Biol.* **20**: 1–21.
- Gigolashvili, T., Yatusевич, R., Rollwitz, I., Humphry, M., Gershenzon, J., and Flügge, U.I.** (2009). The plastidic bile acid transporter 5 is required for the biosynthesis of methionine-derived glucosinolates in *Arabidopsis thaliana*. *Plant Cell.* **21**: 1813–1829.
- González, E., Solano, R., Rubio, V., Leyva, A., and Paz-Ares, J.** (2005). PHOSPHATE TRANSPORTER TRAFFIC FACILITATOR1 is a plant-specific SEC12-related protein that enables the endoplasmic reticulum exit of a high-affinity phosphate transporter in Arabidopsis. *Plant Cell.* **17**: 3500–3512.
- He, Y., Doyle, M.R., and Amasino, R.M.** (2004). PAF1-complex-mediated histone methylation of FLOWERING LOCUS C chromatin is required for the vernalization-responsive, winter-annual habit in Arabidopsis. *Genes Dev.* **18**: 2774–2784.
- Hou, L., Wang, Y., Liu, Y., Zhang, N., Shamovsky, I., Nudler, E., Tian, B., and Dynlacht, B.D.** (2019). Paf1C regulates RNA polymerase II progression by modulating elongation rate. *Proc. Natl. Acad. Sci. U. S. A.* **116**: 14583–14592.
- Hsin, J.P. and Manley, J.L.** (2012). The RNA polymerase II CTD coordinates transcription and RNA processing. *Genes Dev.* **26**: 2119–2137.
- Jaehning, J.A.** (2010). The Paf1 complex: Platform or player in RNA polymerase II transcription? *Biochim. Biophys. Acta - Gene Regul. Mech.* **1799**: 379–388.
- Jiang, C., Gao, X., Liao, L., Harberd, N.P., and Fu, X.** (2007). Phosphate starvation root architecture and anthocyanin accumulation responses are modulated by the gibberellin-DELLA signaling pathway in Arabidopsis. *Plant Physiol.* **145**: 1460–1470.
- Kindgren, P., Ivanov, M., and Marquardt, S.** (2020). Native elongation transcript sequencing reveals temperature dependent dynamics of nascent RNAPII transcription in Arabidopsis. *Nucleic Acids Res.* **48**: 2332–2347.
- Kolde, R.** (2015). pheatmap: Pretty Heatmaps. R Packag. version 1.0.8.
- Koorneef, M., Elgersma, A., Hanhart, C.J., van Loenen-Martinet, E.P., van Rijn, L., and Zeevaart, J.A.D.** (1985). A gibberellin insensitive mutant of *Arabidopsis thaliana*. *Physiol. Plant.* **65**: 33–39.
- Liu, C., Xin, Y., Xu, L., Cai, Z., Xue, Y., Liu, Y., Xie, D., Liu, Y., and Qi, Y.** (2018a). Arabidopsis ARGONAUTE 1 Binds Chromatin to Promote Gene Transcription in Response to Hormones and Stresses. *Dev. Cell.* **44**: 348–361.e7.
- Liu, N., Shang, W., Li, C., Jia, L., Wang, X., Xing, G., and Zheng, W.M.** (2018b). Evolution of the *SPX* gene family in plants and its role in the response mechanism to phosphorus stress. *Open Biol.* **8**: 170231.
- Liu, Y., Koorneef, M., and Soppe, W.J.J.** (2007). The absence of histone H2B

- monoubiquitination in the *Arabidopsis hub1 (rdo4)* mutant reveals a role for chromatin remodeling in seed dormancy. *Plant Cell*. **19**: 433–444.
- Love, M.I., Huber, W., and Anders, S.** (2014). Moderated estimation of fold change and dispersion for RNA-seq data with DESeq2. *Genome Biol*. **15**: 1–21.
- Lu, C., Tian, Y., Wang, S., Su, Y., Mao, T., Huang, T., Chen, Q., Xu, Z., and Ding, Y.** (2017). Phosphorylation of SPT5 by CDKD;2 is required for VIP5 recruitment and normal flowering in *Arabidopsis thaliana*. *Plant Cell*. **29**: 277–291.
- Marín-de la Rosa, N. et al.** (2015). Genome Wide Binding Site Analysis Reveals Transcriptional Coactivation of Cytokinin-Responsive Genes by DELLA Proteins. *PLoS Genet*. **11**: 1–20.
- Mayer, A., Lidschreiber, M., Siebert, M., Leike, K., Söding, J., and Cramer, P.** (2010). Uniform transitions of the general RNA polymerase II transcription complex. *Nat. Struct. Mol. Biol*. **17**: 1272–1278.
- Nassrallah, A. et al.** (2018). DET1-mediated degradation of a SAGA-like deubiquitination module controls H2Bub homeostasis. *Elife*. **7**: 1–29.
- Oh, S., Park, S., and Van Nocker, S.** (2008). Genic and global functions for Paf1C in chromatin modification and gene expression in *Arabidopsis*. *PLoS Genet*. **4**: e1000077.
- Oh, S., Zhang, H., Ludwig, P., and Van Nocker, S.** (2004). A mechanism related to the yeast transcriptional regulator Paf1c is required for expression of the *Arabidopsis* FLC/MAF MADS box gene family. *Plant Cell*. **16**: 2940–53.
- Orlando, D.A., Chen, M.W., Brown, V.E., Solanki, S., Choi, Y.J., Olson, E.R., Fritz, C.C., Bradner, J.E., and Guenther, M.G.** (2014). Quantitative ChIP-Seq normalization reveals global modulation of the epigenome. *Cell Rep*. **9**: 1163–1170.
- Park, S., Oh, S., Ek-Ramos, J., and van Nocker, S.** (2010). Plant homologous to parafibromin is a component of the Paf1 complex and assists in regulating expression of genes within h3k27me3-enriched chromatin. *Plant Physiol*. **153**: 821–831.
- Perea-Resa, C., Carrasco-López, C., Catalá, R., Turečková, V., Novak, O., Zhang, W., Sieburth, L., Jiménez-Gómez, J.M., and Salinas, J.** (2015). The LSM1-7 complex differentially regulates *Arabidopsis* tolerance to abiotic stress conditions by promoting selective mRNA decapping. *Plant Cell*. **28**: 505–520.
- Quinlan, A.R. and Hall, I.M.** (2010). BEDTools: A flexible suite of utilities for comparing genomic features. *Bioinformatics*. **26**: 841–842.
- Roudier, F. et al.** (2011). Integrative epigenomic mapping defines four main chromatin states in *Arabidopsis*. *EMBO J*. **30**: 1928–1938.
- Samanta, S. and Thakur, J.K.** (2015). Importance of mediator complex in the regulation and integration of diverse signaling pathways in plants. *Front. Plant Sci*. **6**: 1–16.
- Serrano-Mislata, A., Bencivenga, S., Bush, M., Schiessl, K., Boden, S., and Sablowski, R.** (2017). DELLA genes restrict inflorescence meristem function independently of plant height. *Nat. Plants*. **3**: 749–754.
- Silverstone, A.L., Jung, H.-S., Dill, A., Kawaide, H., Kamiya, Y., and Sun, T.** (2001). Repressing a Repressor. *Plant Cell*. **13**: 1555–1566.
- Song, C.P. and Galbraith, D.W.** (2006). AtSAP18, an orthologue of human SAP18, is involved in the regulation of salt stress and mediates transcriptional repression in *Arabidopsis*. *Plant Mol. Biol*. **60**: 241–257.



- Strikoudis, A. et al.** (2016). Regulation of transcriptional elongation in pluripotency and cell differentiation by the PHD-finger protein Phf5a. *Nat. Cell Biol.* **18**: 1127–1138.
- Thorvaldsdóttir, H., Robinson, J.T., and Mesirov, J.P.** (2013). Integrative Genomics Viewer (IGV): High-performance genomics data visualization and exploration. *Brief. Bioinform.* **14**: 178–192.
- Trapnell, C., Roberts, A., Goff, L., Pertea, G., Kim, D., Kelley, D.R., Pimentel, H., Salzberg, S.L., Rinn, J.L., and Pachter, L.** (2012). Differential gene and transcript expression analysis of RNA-seq experiments with TopHat and Cufflinks. *Nat. Protoc.* **7**: 562–578.
- Van Lijsebettens, M. and Grasser, K.D.** (2014). Transcript elongation factors: Shaping transcriptomes after transcript initiation. *Trends Plant Sci.* **19**: 717–726.
- Van Oss, S.B., Cucinotta, C.E., and Arndt, K.M.** (2017). Emerging Insights into the Roles of the Paf1 Complex in Gene Regulation. *Trends Biochem. Sci.* **42**: 788–798.
- Vera-Sirera, F., Gomez, M.D., and Perez-Amador, M.A.** (2016). DELLA Proteins, a Group of GRAS Transcription Regulators that Mediate Gibberellin Signaling. In *Plant Transcription Factors: Evolutionary, Structural and Functional Aspects*. D. H. Gonzalez (Ed.).
- Walter, W., Sánchez-Cabo, F., and Ricote, M.** (2015). GOplot: An R package for visually combining expression data with functional analysis. *Bioinformatics.* **31**: 2912–2914.
- Wang, J.Z., Du, Z., Payattakool, R., Yu, P.S., and Chen, C.F.** (2007). A new method to measure the semantic similarity of GO terms. *Bioinformatics.* **23**: 1274–1281.
- Wang, Z.W., Wu, Z., Raitskin, O., Sun, Q., and Dean, C.** (2014). Antisense-mediated FLC transcriptional repression requires the P-TEFb transcription elongation factor. *Proc. Natl. Acad. Sci. U. S. A.* **111**: 7468–7473.
- Weake, V.M. and Workman, J.L.** (2008). Histone Ubiquitination: Triggering Gene Activity. *Mol. Cell.* **29**: 653–663.
- Wood, A., Schneider, J., Dover, J., Johnston, M., and Shilatifard, A.** (2003). The Paf1 complex is essential for histone monoubiquitination by the Rad6-Bre1 complex, which signals for histone methylation by COMPASS and Dot1p. *J. Biol. Chem.* **278**: 34739–34742.
- Wu, L., Li, L., Zhou, B., Qin, Z., and Dou, Y.** (2014). H2B Ubiquitylation Promotes RNA Pol II Processivity via PAF1 and pTEFb. *Mol. Cell.* **54**: 920–931.
- Yang, Y., Li, W., Hoque, M., Hou, L., Shen, S., Tian, B., and Dynlacht, B.D.** (2016). PAF Complex Plays Novel Subunit-Specific Roles in Alternative Cleavage and Polyadenylation. *PLoS Genet.* **12**: 1–28.
- Yu, B., Xu, C., and Benning, C.** (2002). Arabidopsis disrupted in SQD2 encoding sulfolipid synthase is impaired in phosphate-limited growth. *Proc. Natl. Acad. Sci. U. S. A.* **99**: 5732–5737.
- Yu, G., Wang, L.G., Han, Y., and He, Q.Y.** (2012). ClusterProfiler: An R package for comparing biological themes among gene clusters. *Omi. A J. Integr. Biol.* **6**: 284–287.
- Yu, G., Li, F., Qin, Y., Bo, X., Wu, Y., and Wang, S.** (2010). GOSemSim: An R package for measuring semantic similarity among GO terms and gene products. *Bioinformatics.* **26**: 976–978.
- Yu, M., Yang, W., Ni, T., Tang, Z., Nakadai, T., Zhu, J., and Roeder, R.G.** (2015). RNA polymerase II-associated factor 1 regulates the release and phosphorylation of paused RNA polymerase II. *Science.* **350**: 1383–1386.

- Yu, X. and Michaels, S.D.** (2010). The Arabidopsis Paf1c complex component CDC73 participates in the modification of FLOWERING LOCUS C chromatin. *Plant Physiol.* **153**: 1074–1084.
- Zhang, H., Ransom, C., Ludwig, P., and Van Nocker, S.** (2003). Genetic analysis of early flowering mutants in Arabidopsis defines a class of pleiotropic developmental regulator required for expression of the flowering-time switch FLOWERING LOCUS C. *Genetics.* **164**: 347–358.
- Zhang, H. and Van Nocker, S.** (2002). The Vernalization Independence 4 gene encodes a novel regulator of Flowering Locus C. *Plant J.* **31**: 663–673.
- Zhang, S., Xie, M., Ren, G., and Yu, B.** (2013). CDC5, a DNA binding protein, positively regulates posttranscriptional processing and/or transcription of primary microRNA transcripts. *Proc. Natl. Acad. Sci. U. S. A.* **110**: 17588–17593.
- Zhang, X., Zhou, W., Chen, Q., Fang, M., Zheng, S., Scheres, B., and Li, C.** (2018). Mediator subunit MED31 is required for radial patterning of Arabidopsis roots. *Proc. Natl. Acad. Sci. U. S. A.* **115**: E5624–E5633.
- Zhang, Y., Zhou, Y., Chen, S., Liu, J., Fan, K., Li, Z., Liu, Z., and Lin, W.** (2019). Gibberellins play dual roles in response to phosphate starvation of tomato seedlings, negatively in shoots but positively in roots. *J. Plant Physiol.* **234**: 145–153.
- Zhang, Y., Liu, T., Meyer, C.A., Eeckhoutte, J., Johnson, D.S., Bernstein, B.E., Nussbaum, C., Myers, R.M., Brown, M., Li, W., and Shirley, X.S.** (2008). Model-based analysis of CHIP-Seq (MACS). *Genome Biol.* **9**: R137.
- Zhu, J., Liu, M., Liu, X., and Dong, Z.** (2018). RNA polymerase II activity revealed by GRO-seq and pNET-seq in Arabidopsis. *Nat. Plants.* **4**: 1112–1123.



## **General discussion**



DELLA proteins have been proposed to coordinate growth in response to the environment (Claeys et al., 2014). This idea is sustained by two main features: (i) DELLAs are destabilized by GAs, whose levels are very sensitive to changes in the environmental conditions (Alabadí and Blázquez, 2009; Sun, 2011); and (ii) they have the ability to interact with and regulate multitude of transcription factors (TFs), with impact in growth and developmental outputs (Marín-de La Rosa et al., 2014). Interestingly, the physical interaction between DELLAs and chromatin remodelers (Sarnowska et al., 2013; Zhang et al., 2014; Park et al., 2017a) also hinted towards an additional mechanism by which they would regulate transcription, although its relevance has not been proven so far. The work presented in this Thesis expands our view of these two features of DELLA proteins –how they are regulated and how they transduce the information to the transcription machinery–, both of which enhance the view of DELLAs as core components of the network that mediates between the environment and cellular functions.

Our demonstration that DELLAs are physiologically relevant targets of the E3 ubiquitin ligase COP1 expands the set of mechanisms that regulate DELLA levels in response to the environment. It is well-known that DELLAs levels can be regulated by other post-translational modifications (PTM), such as SUMOylation and phosphorylation, but COP1-mediated degradation is unique in that it degrades DELLAs directly without converging in the GA/GID1 pathway, contrary to the effect of phosphorylation and SUMOylation that simply modify the capacity of DELLAs to be degraded by the GA/GID1 pathway. This does not mean that COP1 interferes with DELLA signalling only through its direct physical interaction. We and others have shown that COP1 also has an indirect effect in GA biosynthesis in a longer time frame (Weller et al., 2009; this work). This sort of complex networks is typical of plant regulatory circuits, especially around important regulatory nodes, and allow them to properly adjust growth preventing over-regulation of downstream pathways. Levels of proteins that function as “signalling hubs” are indeed tightly regulated in other organisms as well. For example, the tumour suppressor p53 is targeted for degradation by at least fifteen E3 ubiquitin ligases in mammals (Love and Grossman, 2012) and many “signalling hub” proteins are encoded by short-lived mRNAs in yeast (Batada et al., 2006).

Furthermore, our observation that DELLAs not only regulate gene expression through TFs but also through the activity of the transcription elongation factor Paf1c, also place DELLAs in a central position in the transcriptional network, influencing several consecutive steps of

the process, from the initiation of transcription to the ability of RNAPII to proceed through the gene body.

In summary, our results add two novel players to the DELLA signalling pathway that (i) increases connectivity with the environmental sensors (COP1) and (ii) broadens the scope of DELLA action on the target genes (Paf1c). However, several questions arise in the light of the various mechanisms that converge in the same regulatory circuit: What is the particular relevance of the different mechanisms? What are the evolutionary implications of the coexistence of alternative mechanisms? How can this knowledge be useful in the development of new biotechnological strategies?

## 1. Relative importance of the different mechanisms

When several mechanisms operate on a common process, it is common that each of them provides differential regulatory layers. In the case of COP1-mediated DELLAs degradation, we have shown in Chapter 1 that this mode of regulation is particularly relevant in response to shade or warmth, but not during photomorphogenesis, indicating that the contribution of this pathway depends on the biological context. Therefore, further work is required to know whether this pathway also operates under other physiological contexts, for instance, in germination, root growth, flowering or response to cold, under which both COP1 and DELLAs have been involved (at least separately) (Tyler et al., 2004; Ubeda-Tomás et al., 2008; Achard et al., 2008; Catalá et al., 2011; Galvão et al., 2012; Sassi et al., 2012; Deng et al., 2016; Yu et al., 2016). For instance, accumulation of DELLAs in the root in response to cold is mediated by a reduction in bioactive GA levels (Achard et al., 2008). Equally to the situation in the hypocotyl, disappearance of COP1 from root nuclei when temperature drops (Catalá et al., 2011) might contribute to DELLA accumulation. Thus, the fact that there are several physiological situations in which both pathways regulate DELLA stability still begs for an explanation.

COP1 defines a faster path to destabilize DELLAs compared to that defined by GA/GID1. In fact, the rapid response to warmth or shade is mostly dependent on COP1, while the GA pathway is more relevant on a developmental scale. In addition to the rapid accumulation of COP1 in nuclei in response to warmth shown here, inactivation of phyB as temperature increases (Legris et al., 2016; Jung et al., 2016) or due to a reduction in the red (R) to far-red (FR) ratio, would trigger the activation of the pool of COP1 already present in the nucleus previous to the environmental change (Park et al., 2017b), being thus

available to de-repress the growth restraint imposed by DELLAs. This initial growth de-repression might represent an adaptive advantage for seedlings facing the environmental challenge, awaiting further accumulation of COP1 in the nucleus and the up regulation of the GA pathway, which occurs later and that will consolidate the response. Interestingly, the growth restraint imposed by DELLA stabilization after salt stress is first achieved by DELLA SUMOylation (Conti et al., 2014), suggesting that post-translational mobilization of DELLAs prior to changes in bioactive GAs is not restricted to responses to light or temperature and might represent a fast, widespread way to transmit environmental changes to growth outputs.

Our results also indicate that the two seemingly independent pathways (COP1 and GA/GID1) are interconnected. This view is supported not only by the finding that COP1 promotes GA accumulation (Weller et al., 2009; this work), but also by the observation that degradation by COP1 becomes quantitatively relevant only below a certain threshold of DELLA levels, which may be established by the GA/GID1 pathway. The co-existence of these interconnected mechanisms might for instance reinforce the cellular commitment to grow when conditions are favourable by reducing DELLA levels, in other words, providing robustness.

Regarding the role of DELLA in transcription, what is the benefit of having several DELLA-operated strategies to regulate gene expression for plants? We propose that the two mechanisms proposed in this work complement each other to coordinate different steps during gene transcription, from the formation of the pre-initiation complex to the recruitment of the transcription elongation factor Paf1c. In addition to this, both confer particularities to the regulation: the interaction with TFs provides specificity that might be required to regulate gene expression in a specific process, whereas the DELLA-Paf1c module would operate on a broader scale to set the pace of transcription of Paf1c-target genes. It is worth mentioning that we assume a “global effect” of DELLAs on Paf1c activity because we observed global defects on H2Bub, although only a particular set of genes were misregulated in seedlings lacking DELLAs or ELF7. It is not surprising, since the “final” effect on gene expression likely depend on other mechanisms as well.

## 2. Evolutionary implications

It has been shown DELLAs predate the origin of GA metabolism and perception, which seems to coincide with the appearance of the ancestor of vascular plants (Miyazaki et al.,

2018; Yoshida et al., 2018; Hernández-García et al., 2019; Blázquez et al., 2020). The function of DELLAs in early-diverging land plants is still under investigation, but there are strong indications that they regulate transcription too (Briones-Moreno et al., 2017; Hernández-García et al., 2019). Then, (i) how is DELLA activity regulated in land plants? And, (ii) what is the ancestral mechanism for the regulation of transcription in those plants? Regarding the first question, several pieces of evidence allow us to propose that, at least in the case of the liverwort *Marchantia polymorpha*, the DELLA protein might be regulated by COP1. First, MpDELLA stability is dependent on the 26S proteasome, indicating that there may exist a mechanism to ubiquitinate this protein (Hernández-García et al, unpublished); and second, the orthologs of COP1 and DELLA interact each other in this species (Fig. 1). Therefore, it is tempting to speculate that COP1 might represent an ancestral mechanism for the regulation of DELLA stability, which was later refined or taken over by the GA/GID1 pathway.

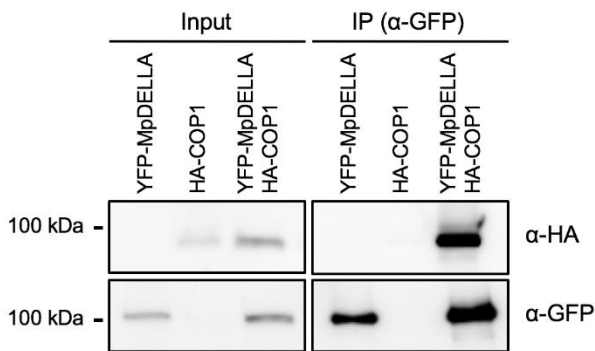


**Fig. 1. MpDELLA interacts with MpCOP1 in plant cells.** Co-IP assay showing the interaction between YFP-MpDELLA and HA-COP1 in *Nicotiana benthamiana* leaves. Soluble proteins were incubated with anti-GFP paramagnetic beads and were detected by immunoblotting with either anti-HA-HRP or anti-GFP antibodies. The position of molecular weight markers is shown on the left. The sizes of the bands correspond to the expected sizes of the fusion proteins.

Work with *M. polymorpha* could also shed light on the evolutionary relevance of the regulation by DELLAs of RNAPII activity. Unpublished work in our laboratory shows that the orthologs of several TFs, chromatin remodelers (e.g. SWI3C) and Paf1c physically interact with MpDELLA (Briones-Moreno et al, unpublished). Future work should address the question of the relative contribution of the role of the ancestral DELLA in transcriptional initiation vs transcriptional elongation.



### 3. Biotechnological implications

Since their discovery, GAs and their inhibitors (e.g. paclobutrazol) have been widely used as a biotechnological tool to improve many agronomic traits (see examples in Kaya et al., 2006; Zhang et al., 2019). However, their application also provokes undesired effects, indicating the need for different GA-related biotechnological strategies. The identification of DELLAs as core elements of GA signalling shifted the focus of biotechnological applications towards the modification of these proteins. Nevertheless, the fact that DELLAs are “signalling hubs” makes their use as biotechnological tools difficult: their activity is so intertwined with multiple processes (upstream and downstream) that any slight modification of DELLAs affects the desired process and, potentially, also have undesired side effects. Several strategies could be applied to overcome such difficulties: (i) the selection of DELLA edgetic alleles that interfere only with the interaction between DELLAs and the growth-promoting TFs, maintaining the DELLA interaction with defence-related TFs unaffected; (ii) the search for compounds that specifically inhibit the interaction between DELLAs and growth-promoting TFs; (iii) the manipulation of DELLA targets instead of DELLAs themselves; and, (iv) the alteration of *DELLA* expression or protein slightly. Although all the different new DELLA-based biotechnological tools are complementary, the focus on the manipulation of the transcriptional or post-translational mechanisms involving DELLA protein stability rather than activity might be successful for one reason: it is likely that the affinity of DELLAs for the different interactors (be it TFs or transcriptional elongation factors) must be different. Thus, altering the levels will necessarily affect the ones with lower affinity preferentially.

The results in this Thesis provide two additional mechanisms to alter DELLA signalling only slightly. First, we have shown that despite DELLAs affecting Paf1c activity in a very general manner, this causes a relatively stronger effect only in smaller subset of genes. Therefore, a strategy targeting the interaction between DELLA and Paf1c might allow us the modification of certain GA-related traits without the undesired lateral effects. Second, the construction of DELLA alleles insensitive to COP1 degradation, but still sensitive to the GA/GID1 pathway, could be very useful from a biotechnological point of view since each pathway seems to be more relevant in specific biological contexts. Probably, these COP1-insensitive DELLA alleles would reduce the waste of resources in competition among crop plants (shade response) and excessive stem elongation (in both shade and warm responses). In addition to this, the reduction of this response might increase the tolerance to biotic stress

since several works indicate that shaded plants are more susceptible to pathogens (Chico et al., 2014; Cerrudo et al., 2017). In fact, DELLA alleles with increased resistance to GA-induced degradation had been already spontaneously selected as the basis for the new grass varieties established during the Green Revolution: the enhanced resistance to fungal infections semi dwarf varieties (Peng et al., 1999).



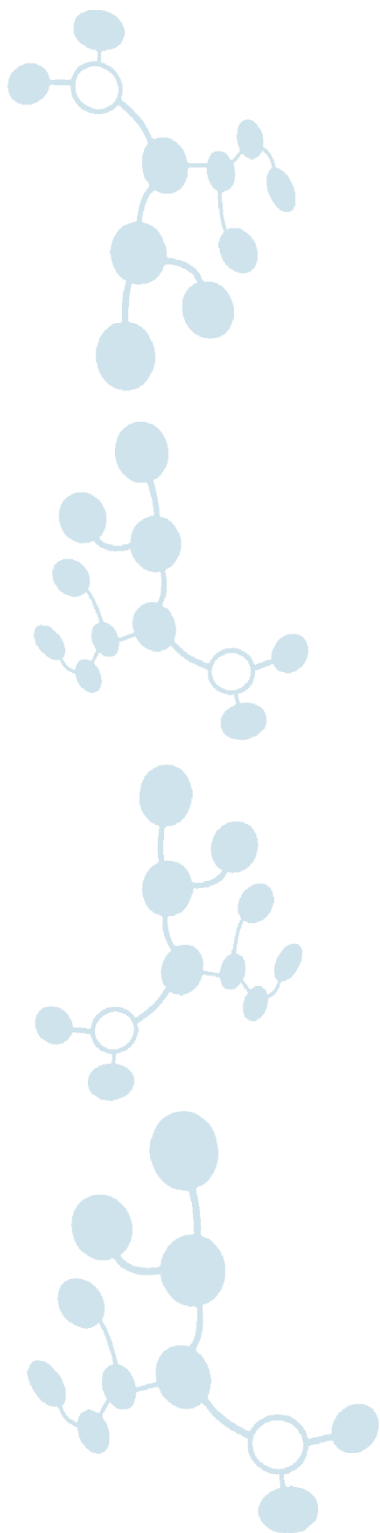
## 4. References

- Achard, P., Gong, F., Cheminant, S., Alioua, M., Hedden, P., and Genschika, P.** (2008). The cold-inducible CBF1 factor-dependent signaling pathway modulates the accumulation of the growth-repressing DELLA proteins via its effect on gibberellin metabolism. *Plant Cell*. **20**: 2117–2129.
- Alabadí, D. and Blázquez, M.A.** (2009). Molecular interactions between light and hormone signaling to control plant growth. *Plant Mol. Biol.* **69**: 409–417.
- Batada, N.N., Hurst, L.D., and Tyers, M.** (2006). Evolutionary and physiological importance of hub proteins. *PLoS Comput. Biol.* **2**: e88.
- Blázquez, M.A., Nelson, D.C., and Weijers, D.** (2020). Evolution of Plant Hormone Response Pathways. *Annu. Rev. Plant Biol.* **71**: annurev-arplant-050718-100309.
- Briones-Moreno, A., Hernández-García, J., Vargas-Chávez, C., Romero-Campero, F.J., Romero, J.M., Valverde, F., and Blázquez, M.A.** (2017). Evolutionary analysis of DELLA-associated transcriptional networks. *Front. Plant Sci.* **8**: 626.
- Catalá, R., Medina, J., and Salinas, J.** (2011). Integration of low temperature and light signaling during cold acclimation response in *Arabidopsis*. *Proc. Natl. Acad. Sci. U. S. A.* **108**: 16475–16480.
- Cerrudo, I., Caliri-Ortiz, M.E., Keller, M.M., Degano, M.E., Demkura, P. V., and Ballaré, C.L.** (2017). Exploring growth-defence trade-offs in *Arabidopsis*: phytochrome B inactivation requires JAZ10 to suppress plant immunity but not to trigger shade-avoidance responses. *Plant Cell Environ.* **40**: 635–644.
- Chico, J.M., Fernández-Barbero, G., Chini, A., Fernández-Calvo, P., Díez-Díaz, M., and Solano, R.** (2014). Repression of jasmonate-dependent defenses by shade involves differential regulation of protein stability of MYC transcription factors and their JAZ repressors in *Arabidopsis*. *Plant Cell*. **26**: 1967–1980.
- Claeys, H., De Bodt, S., and Inzé, D.** (2014). Gibberellins and DELLAs: Central nodes in growth regulatory networks. *Trends Plant Sci.* **19**: 231–239.
- Conti, L., Nelis, S., Zhang, C., Woodcock, A., Swarup, R., Galbiati, M., Tonelli, C., Napier, R., Hedden, P., Bennett, M., and Sadanandom, A.** (2014). Small Ubiquitin-like Modifier Protein SUMO Enables Plants to Control Growth Independently of the Phytohormone Gibberellin. *Dev. Cell*. **28**: 102–110.
- Deng, X.W., Xu, D., and Zhu, D.** (2016). The role of COP1 in repression of photoperiodic flowering. *F1000Research*. **5**: F1000 Faculty Rev–178.
- Galvão, V.C., Horrer, D., Küttner, F., and Schmid, M.** (2012). Spatial control of flowering by DELLA proteins in *Arabidopsis thaliana*. *Dev.* **139**: 4072–4082.
- Hernández-García, J., Briones-Moreno, A., Dumas, R., and Blázquez, M.A.** (2019). Origin of Gibberellin-Dependent Transcriptional Regulation by Molecular Exploitation of a Transactivation Domain in DELLA Proteins. *Mol. Biol. Evol.* **36**: 908–918.
- Jung, J.H. et al.** (2016). Phytochromes function as thermosensors in *Arabidopsis*. *Science*. **354**: 886–889.
- Kaya, C., Tuna, A.L., and Alves, A.A.C.** (2006). Gibberellic acid improves water deficit tolerance in maize plants. *Acta Physiol. Plant.* **28**: 331–337.
- Legris, M., Klose, C., Burgie, E.S., Rojas, C.C., Neme, M., Hiltbrunner, A., Wigge, P.A.,**

- Schäfer, E., Vierstra, R.D., and Casal, J.J.** (2016). Phytochrome B integrates light and temperature signals in Arabidopsis. *Science*. **354**: 897–900.
- Love, I.M. and Grossman, S.R.** (2012). It Takes 15 to Tango: Making Sense of the Many Ubiquitin Ligases of p53. *Genes and Cancer*. **3**: 249–263.
- Marín-de La Rosa, N., Sotillo, B., Miskolczi, P., Gibbs, D.J., Vicente, J., Carbonero, P., Oñate-Sánchez, L., Holdsworth, M.J., Bhalerao, R., Alabadi, D., and Blázquez, M.A.** (2014). Large-scale identification of gibberellin-related transcription factors defines group VII ETHYLENE RESPONSE FACTORS as functional DELLA partners. *Plant Physiol*. **166**: 1022–1032.
- Miyazaki, S., Hara, M., Ito, S., Tanaka, K., Asami, T., Hayashi, K. ichiro, Kawaide, H., and Nakajima, M.** (2018). An Ancestral Gibberellin in a Moss *Physcomitrella patens*. *Mol. Plant*. **11**: 1097–1100.
- Park, J., Oh, D.H., Dassanayake, M., Nguyen, K.T., Ogas, J., Choi, G., and Sun, T.P.** (2017a). Gibberellin signaling requires chromatin remodeler PICKLE to promote vegetative growth and phase transitions. *Plant Physiol*. **173**: 1463–1474.
- Park, Y.J., Lee, H.J., Ha, J.H., Kim, J.Y., and Park, C.M.** (2017b). COP1 conveys warm temperature information to hypocotyl thermomorphogenesis. *New Phytol*. **215**: 269–280.
- Peng, J. et al.** (1999). “Green revolution” genes encode mutant gibberellin response modulators. *Nature*. **400**: 256–261.
- Sarnowska, E.A. et al.** (2013). DELLA-interacting SWI3C core subunit of switch/sucrose nonfermenting chromatin remodeling complex modulates gibberellin responses and hormonal cross talk in Arabidopsis. *Plant Physiol*. **163**: 305–317.
- Sassi, M. et al.** (2012). COP1 mediates the coordination of root and shoot growth by light through modulation of PIN1- and PIN2-dependent auxin transport in Arabidopsis. *Dev*. **139**: 3402–3412.
- Sun, T.P.** (2011). The molecular mechanism and evolution of the GA-GID1-DELLA signaling module in plants. *Curr. Biol*. **21**: R338–R345.
- Tyler, L., Thomas, S.G., Hu, J., Dill, A., Alonso, J.M., Ecker, J.R., and Sun, T.P.** (2004). DELLA proteins and gibberellin-regulated seed germination and floral development in Arabidopsis. *Plant Physiol*. **135**: 1008–1019.
- Ubeda-Tomás, S., Swarup, R., Coates, J., Swarup, K., Laplaze, L., Beemster, G.T.S., Hedden, P., Bhalerao, R., and Bennett, M.J.** (2008). Root growth in Arabidopsis requires gibberellin/DELLA signalling in the endodermis. *Nat. Cell Biol*. **10**: 625–628.
- Weller, J.L., Hecht, V., Schoor, J.K.V., Davidson, S.E., and Ross, J.J.** (2009). Light regulation of gibberellin biosynthesis in pea is mediated through the COP1/HY5 pathway. *Plant Cell*. **21**: 800–813.
- Yoshida, H. et al.** (2018). Evolution and diversification of the plant gibberellin receptor GID1. *Proc. Natl. Acad. Sci. U. S. A.* **115**: E7844–E7853.
- Yu, Y., Wang, J., Shi, H., Gu, J., Dong, J., Deng, X.W., and Huang, R.** (2016). Salt stress and ethylene antagonistically regulate nucleocytoplasmic partitioning of COP1 to control seed germination. *Plant Physiol*. **170**: 2340–2350.
- Zhang, D., Jing, Y., Jiang, Z., and Lin, R.** (2014). The chromatin-remodeling factor PICKLE integrates brassinosteroid and gibberellin signaling during skotomorphogenic growth in Arabidopsis. *Plant Cell*. **26**: 2472–2485.

**Zhang, L., Luo, Z., Cui, S., Xie, L., Yu, J., Tang, D., Ma, X., and Mou, Y.** (2019). Residue of Paclobutrazol and Its Regulatory Effects on the Secondary Metabolites of *Ophiopogon japonicas*. *Molecules*. **24**: 3504.

D



# Conclusions





In this work, we have unveiled **two new mechanisms**: one for the regulation of DELLA levels in response to the environment, and one for the regulation of gene expression by DELLAs:

1. The E3 ubiquitin ligase COP1 mediates DELLA degradation both in a GA-dependent and -independent manner.
2. Direct regulation of DELLA polyubiquitination by COP1 is particularly relevant during the response to higher temperatures and to shade.
3. DELLA proteins regulate RNAPII-mediated transcriptional elongation through the interaction with Paf1c, probably by allowing its recruitment to the chromatin through a yet unknown mechanism.









